PETROLOGY, DEPOSITIONAL ENVIRONMENT AND DIAGENESIS OF MIDDLE PENNSYLVANIAN (DESMOINESIAN) 'LAGONDA INTERVAL' CHEROKEE GROUP IN EAST-CENTRAL KANSAS

by

James Edward Lardner

A thesis submitted in partial fulfillment
of the requirements for the degree of
Master of Science in Geology
in the Graduate College of
The University of Iowa

May, 1984

Thesis supervisor: Professor Robert L. Brenner

PETROLOGY, DEPOSITIONAL ENVIRONMENT AND DIAGENESIS OF MIDDLE PENNSYLVANIAN (DESMOINESIAN) 'LAGONDA INTERVAL' CHEROKEE GROUP IN EAST-CENTRAL KANSAS

by

James Edward Lardner

A thesis submitted in partial fulfillment
of the requirements for the degree of
Master of Science in Geology
in the Graduate College of
The University of Iowa

May, 1984

Thesis supervisor: Professor Robert L. Brenner

Graduate College
The University of Iowa
Iowa City, Iowa

CERTIFICATE OF APPROVAL

MASTER'S THESIS

This is to certify that the Master's thesis of

James Edward Lardner

has been approved by the Examining Committee for the thesis requirement for the Master of Science degree in Geology at the May, 1984 graduation.

Thesis committee: _____
Thesis Supervisor

_____
Member

_____
Member

ACKNOWLEDGMENTS

I would like to thank my committee chairman, Dr. Robert L. Brenner, for suggesting this topic, and for his guidence and encouragement during the research and writing of this manuscript, as well as Dr. P. H. Heckel and Dr. Keene Swett for serving as committee members and for their assistance and constructive criticism of this thesis. I would like to express my gratitude to Lynn Watney and the Kansas Geological Survey for supplying the cores and well-logs used in this study, and for financial assistance for field work.

Thanks are also due to Ken Kern for his assistance in thin-section preparation, Steve Denesen, who contributed time and information during various phases of the research and writing of this thesis, Umran Dogan for his assistance in SEM investigations and to the rest of the graduate students in the Geology Department, especially Kevin Putney and Murray Nelson, who have made the last two years worth coming back for.

Most of all, a special thanks to my parents, Dr. and Mrs. E. D. Lardner for their financial support and endless encouagement, and to Trish Horan for her understanding and patience over the past two years.

ABSTRACT

During Middle Pennsylvanian time, sedimentation in east-cental Kansas was influenced by deltaic progradation of siliciclastic materials and shoreline fluxuations caused by eustatic sea level changes. During periods of regression, rapid detrital influx from a northerly source area prompted a period of active delta progradation southward across the Cherokee platform. Transgression is recorded by carbonate and black shale deposition during periods of low sediment input.

Subsurface stratigraphic correlation of the "Lagonda" interval in east-central Kansas revealed two laterally discontinuous sandstone bodies. Although not continuous over large areas, the "Upper" and "Lower Squirrel" sandstone lenses occupy specific stratigraphic horizons within the "Lagonda" interval. Approximately 175 geophysical well-logs were used as control points to determine sandstone distribution and construct cross-sections across the study area. Environmental interpetations of geophysical well-log signatures and sandstone geometries suggest that the shales, sandstones, and coals of the "Lagonda" interval record the active progradation and abandonment of a fluvially-dominated

delta system. The "Lower Squirrel" sandstone and associated facies represent a variety of delta plain deposits, including distributary channel and mouth-bar, overbank and interdistributary bay deposits. Abandonment and subsidence of the delta complex resulted in the formation of a thin transgressive marine sandstone caprock overlying the inactive distributary channel and associated overbank deposits. The "Upper Squirrel" sandstone in east-central Kansas represents the deposition of siliciclastic materials within the distal delta-front or delta slope environment.

Diagenesis extensively altered the original mineralogy of the "Lower Squirrel" distributary channel and mouth-bar sandstone. During or immediately after deposition, pyrite formed as replacement of decomposed organic matter. Poorly developed clay rims on detrital grains are followed by extensive precipitation of silica cement as overgrowths on quartz grains. Extensive feldspar dissolution provided Si and Al ions and created the pore space necessary to allow for the formation of authigenic booklets of kaolinite. Fe-calcite cement formed in low oxygen, reducing conditions which permitted sufficient Fe^{++} in solution to form blocky, equant Fe-calcite spar. The overcompacted, fossiliferous, Fe-calcite cemented, transgressive marine sandstone suggests that diagenesis occurred in the deeper-burial connate environment.

TABLE OF CONTENTS

LIST OF TABLES

LIST OF FIGURES

INTRODUCTION

The Middle Pennsylvanian (Desmoinesian) Cherokee Group of eastern Kansas consists primarily of mudrocks with numerous sandstone lenses, thin limestones, black shales and coals. The upper Cherokee "Lagonda" interval contains at least two laterally discontinuous sandstone horizons. The elongate lenticular "squirrel" sandstones were named by drillers for the discontinuous nature of their subsurface occurrences and have long been the target of drillers in search of hydrocarbons. In 1903, oil was discovered in a "Lagonda" sandstone at a depth of 965 feet on the Crotts farm, southeast of LeRoy, Kansas (Jewett, 1954). The upper Cherokee "Lagonda" interval sandstones are the main focus of this study.

Location

The areal extent of this study includes Coffey County, northern Greenwood and Woodson counties and southern Lyon County in east-central Kansas, encompassing Township 19S through Township 24S and Range 10E through Range 17E (Figure 1). The lateral extent of this area was determined by the amount of well-log data available to provide reasonable well

control density in order to make depositional environment interpretations. Figure 2 is an index map of the area, showing the location of well-logs and cores used to correlate the "Lagonda" interval in the subsurface and determine sandstone distribution in the Cherokee basin.

Objectives

The objectives of this investigation are: 1) to determine the geometry, trends and lateral facies relationships between the "Lagonda" sandstone bodies of east-central Kansas; 2) to determine the depositional environment and source area of the siliciclastic material; 3) to determine the diagenetic history of the sandstones and the effects of diagenetic alterations upon sandstone reservoir properties; 4) to compare these results with previous investigations of adjacent areas (i.e. Reinholtz, 1982; Aden, 1982).

Previous Investigations

The Cherokee Group (Desmoinesian) was first described by Haworth and Kirk in 1894 from deposits in Cherokee County, Kansas (Jordan, 1957). The stratigraphy of Cherokee strata in eastern Kansas has been studied by Moore (1936), Lee (1943), Searight and others (1953), Howe (1956), Zeller (1968) and Wells and Anderson (1968).

Figure 1. Location of study area in east-central Kansas. Co=Coffey County; Ly=Lyon County; Gr=Greenwood County; Wo=Woodson County

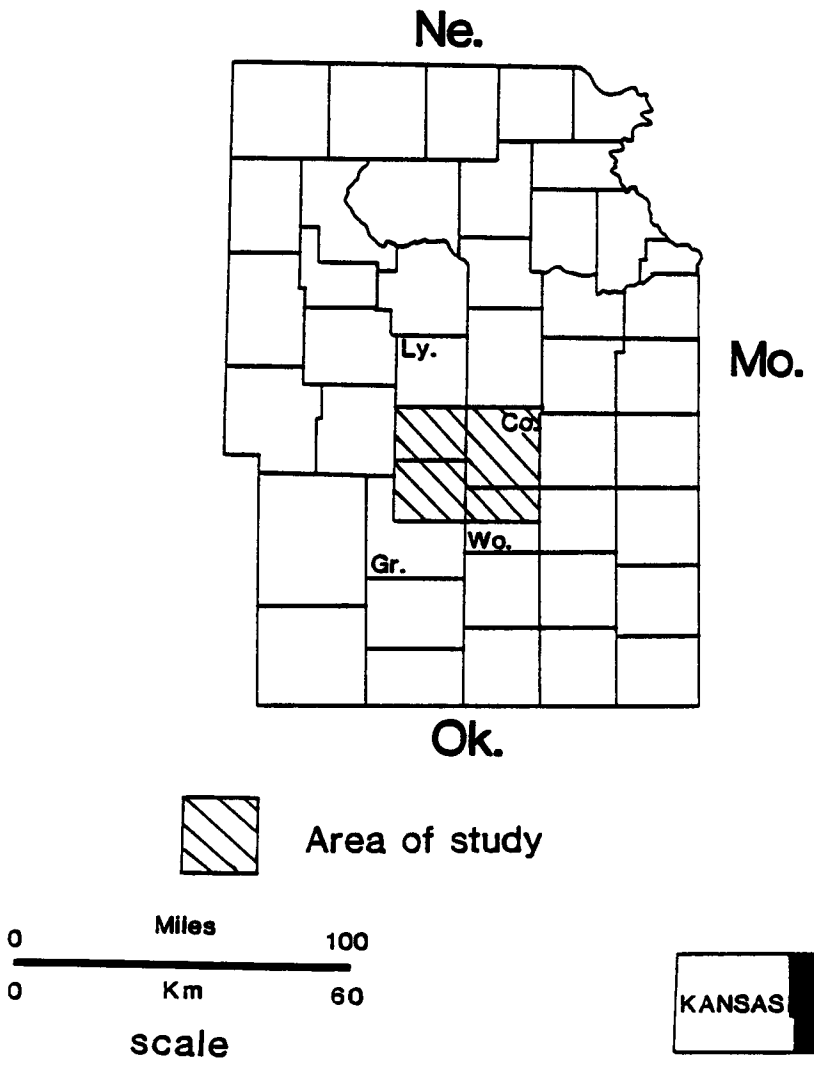
Ne.
Mo.
Ly.
Co.
Wo.
Gr.
Ok.
Area of study
0
Miles
100
0
Km
60
scale
KANSAS

Figure 2. Location map showing the distribution of well-logs and cores. Dots correspond to well-log locations. Circled dots correspond to well-logs with cores.

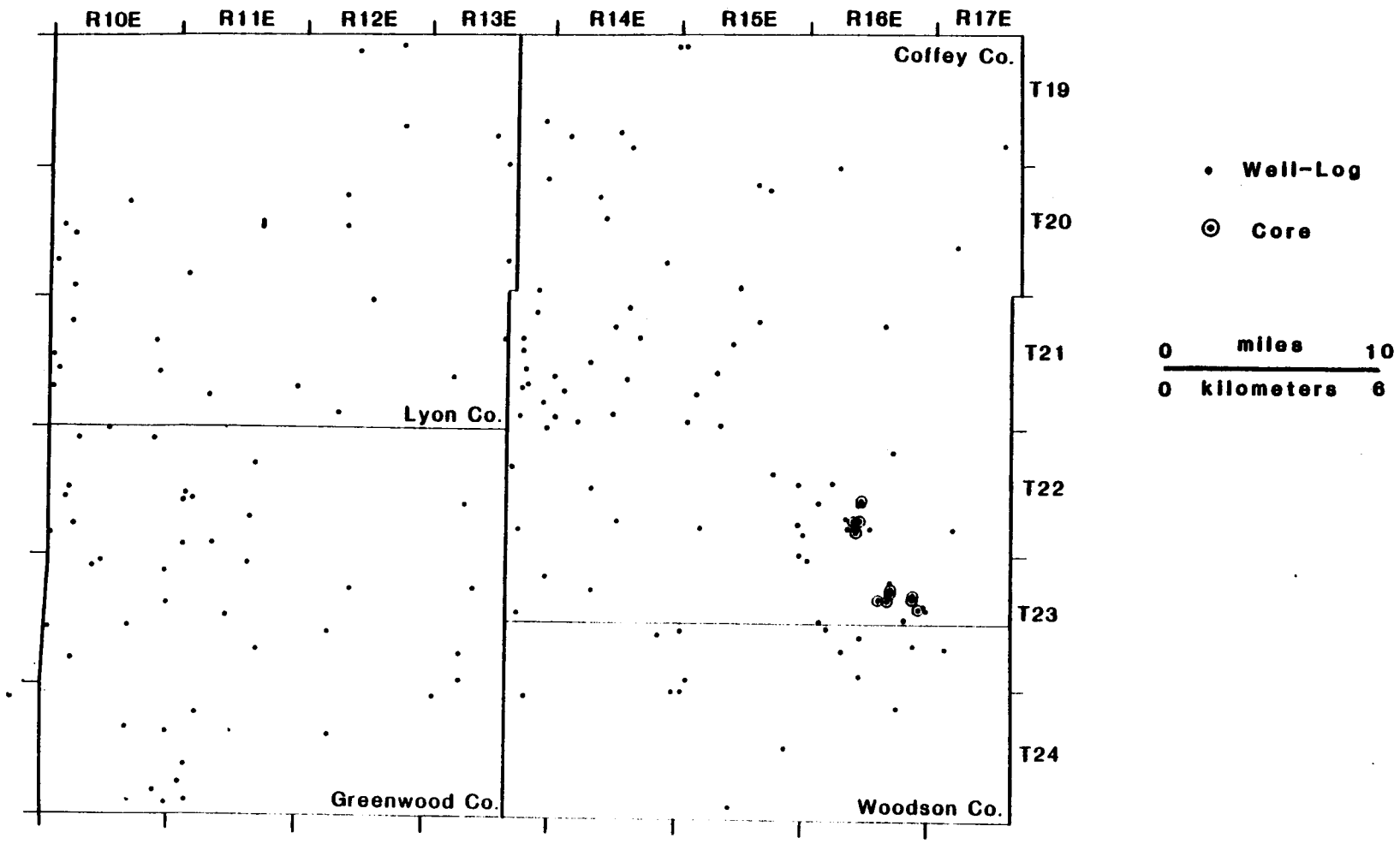
R10E
R11E
R12E
R13E
R14E
R15E
R16E
R17E
T19
T20
T21
T22
T23
T24
Coffey Co.
Lyon Co.
Greenwood Co.
Woodson Co.
Well-Log
Core
0 miles 10
0 kilometers 6

Howe (1956) recognized 18 formations bounded by laterally discontinuous coals, carbonates and shales within the Cherokee Group in southeastern Kansas. However, many of these boundaries cannot be traced into the subsurface (Zeller,1968). Ebanks and others (1977) found 6 units and Hulse (1979) found 9 stratigraphic intervals that are traceable in the subsurface throughout the basin. Ebanks and others (1977) investigated occurrences of heavy-oil in lower Cherokee sandstones in Bourbon, Crawford and Cherokee counties, in Kansas. Woody (1983) examined selected Cherokee sandstones in southeast Kansas and found diagenetic alterations similar to those in Pennsylvanian sandstones in north-central Texas and Tertiary sandstones of the Gulf Coast.

There are no known published studies of the "Lagonda" sandstones west of Anderson County, Kansas. In Anderson County, Charles (1927, 1941) and Rich (1926) discussed general characteristics and trends of important petroleum producing sands of the "Lagonda" interval. Bass (1936) investigated the shoestring sandstones that occur below the "Lagonda" sandstones in Greenwood and Butler counties in Kansas. More recently, Reinholtz (1982) discussed the distribution, petrology and diagenesis of the "Bush City Shoestring Sandstone" and the "Centerville Lagonda Sandstone" in Anderson County. Aden (1982) discussed the

depositional environment of the shales of the Lagonda Formation in Kansas and adjacent states.

Method of Study

Well-Log Analysis

Geophysical well-logs and core materials were obtained to delineate subsurface lithologic boundaries of the upper Cherokee "Lagonda" interval of east-central Kansas. Well-to-well log correlations of the "Lagonda" interval permit accurate subsurface mapping of lithologic units and assist in stratigraphic and depositional environment interpretations. Methods include the construction of structure, isopach and isolith maps and cross-sections that are used to identify specific depositional environments within the "Lagonda" interval.

Sandstone distribution maps were based on 175 gamma-ray-neutron logs and cores from eleven locations obtained from the Kansas Geological Survey (Figure 2). Cross-sections were constructed across the study area to illustrate stratigraphic relations and varying well-log signatures. Well-log density is approximately one every few square miles, but control often becomes sparse in regions where little or no sandstone was encountered and wells were not logged. Interpretations of the depositional environments within the "Lagonda" interval were based on

sandstone geometries and distributions, and on lateral facies relationships as determined from well-logs and cored sections.

Core Analyses

Eleven cores from the "Lower Squirrel" sandstone were available for sedimentologic and petrographic analyses. Gamma-ray logs and drillers logs were used to determine the stratigraphic position of the cores within the "Lagonda" interval. Lithologic sequences, textures and sedimentary structures within the vertically slabbed cores were examined, described and photographed.

Petrographic Analysis

Cored sections were sampled at regular intervals and where distinct lithologic and structural changes occurred. The sandstone chips cut from cores that were heavily oil-stained were cleaned using a soxhlet extractor and a heavy-oil solvent, decahydra-naphthalene. The solvent was flushed through the sandstone chip to remove hydrocarbon residue and allow easier identification of grains and grain relationships. Sandstone chips were impregnated with blue-dye epoxy to aid in recognition of porosity, interconnected pore space and dissolved grains. Selected thin-sections were stained with alizarin red-"S" and potassium ferricyanide to identify carbonate cements. The

petrographic microscope was used to examine 75 thin-sections to determine the composition of the "Lower Squirrel" sandstone. Modal analyses of 14 thin-sections from 7 cores was conducted, using 225 grid points per thin-section and classified according to Folk's classification scheme (1974) (Figure 3). Diagenetic history was determined using the petrographic microscope and Scanning Electron Microscope (SEM). The petrogrophic microscope was used to determine grain-to-grain, grain-to-cement and cement-to-cement relationships as well as to identify sand-sized grains in thin-section. The SEM was used identify authigenic clays and to observe diagenetic alterations and their effects upon pore-geometries. The cathodoluminoscope and X-ray diffraction analysis were used to determine compositional differences between carbonate cements and to support petrographic observations.

Geologic Setting

In Late Mississippian to Early Pennsylvanian time, the Mid-Continent east of the Ancestral Rocky Mountains was subject to rapid and intense deformation (Kluth and Coney, 1981). During Morrowan and Atokan time, all or most of eastern Kansas was exposed as a low-lying positive feature that consisted of Mississippian and older Paleozoic units.

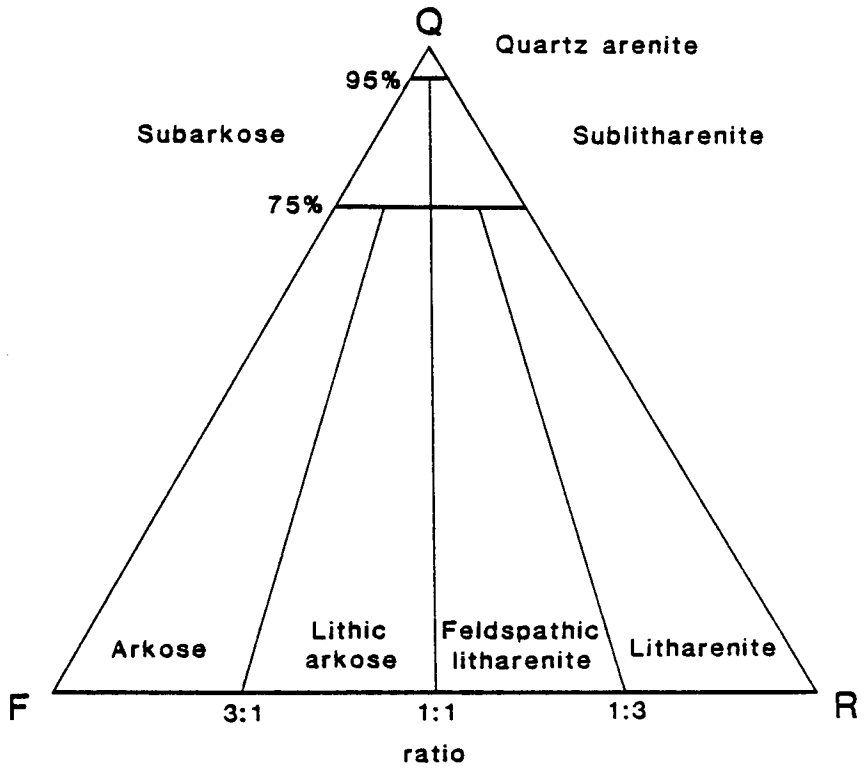

Figure 3. Sandstone classification scheme used in petrographic analysis of thin-sections (after Folk, 1974.).

By early Atokan time, the major Pennsylvanian tectonic features of the Mid-Continent had developed and influenced sedimentation in the Arkoma and Anadarko Basins in Oklahoma (Moore, 1979) (Figure 4). Deformation in eastern Kansas, possibly in response to the collision between the North American and South American-African plates, produced the Nemaha uplift, a major structural feature that extends from Nemaha County south through Sumner County (Kluth and Coney, 1981). This pre-Desmoinesian, post-Mississippian feature divided the Salina and Sedgwick basins to the west from the Forest City and Cherokee basins to the east. The Forest City and Cherokee basins are separated by the Bourbon arch, a low, positive feature that trends southeast from Lyon, through Coffey, Anderson and Bourbon counties and continues east into Missouri (Lee, 1943). The Cherokee shelf is a shallow northward extension of the Arkoma basin of Oklahoma and formed contemporaneously with the Forest City basin on the older Chautauqua arch (Merriam, 1963).

During Early Desmoinesian time, the Mid-Continent was intermittently inundated by marine waters during times of trangression events, and deltaic advances occurred during times of regression. The deltaic sediments prograded southward across the Cherokee shelf into the basins to the south. By Late Desmoinesian time, longer periods of marine advancement submerged the prograding deltaic sediments, and the Mid-Continent became a broad marine shelf (Moore, 1979).

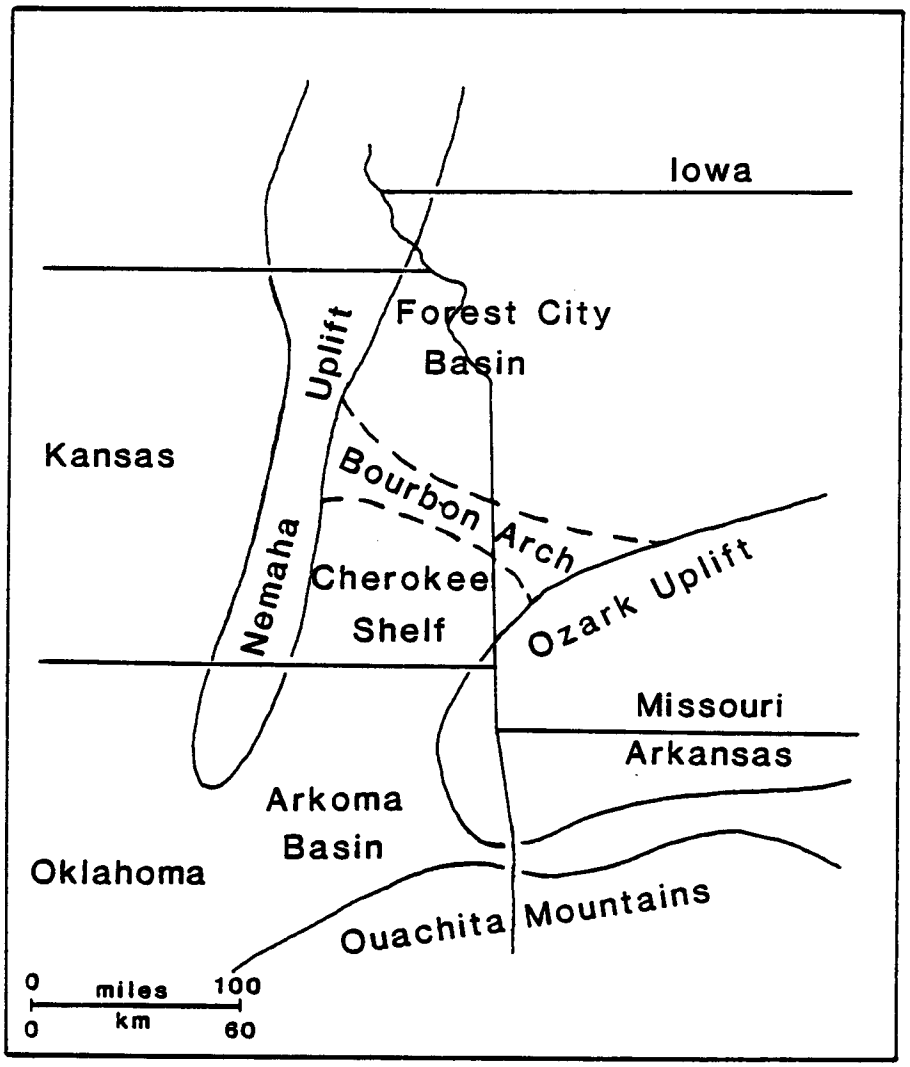

Figure 4. Middle Pennsylvanian structural features of eastern Kansas (modified from Moore, 1979).

During times of transgression, the Cherokee Sea advanced northward from Oklahoma, reworking sediments derived from newly uplifted source areas. Periodically, the Nemaha uplift and Bourbon arch exerted a major influence on sediment deposition in Kansas during portions of this period (Merriam, 1963). The Bourbon arch is thought to have frequently separated north-south transport of sediments between the Forest City basin and the Cherokee shelf during Mid- to Late Pennsylvanian time. The breaching of the Bourbon arch apparently occurred before the deposition of the Lagonda Formation (Lee, 1943). Once the sediments had covered the structurally high areas, the two basins may be considered a single large structural province (Jewett, 1954).

Cherokee Group

In eastern Kansas, the Cherokee Group marks the lowest major division of the Desmoinesian Stage and consists of all Pennsylvanian beds between the base of the Fort Scott Limestone and the top of the Mississippian (Merriam, 1963). The thickness of the Cherokee Group in southeastern Kansas ranges from 300 (100 m) to 400 (130 m) feet (Jewett, 1954) and is divided into the Krebs and Cabaniss formations, which are not easily recognizable in the subsurface. Howe (1956) suggested that the top of the Bluejacket sandstone may be

regarded as the upper boundary of the Krebs Formation (Zeller, 1968). Ebanks and others (1977) subdivided the Cherokee Group in southeastern Kansas into sandstone-bearing horizons on the basis of key marker-beds that are traceable into the subsurface and identifiable on geophysical well-logs.

STRATIGRAPHY

Geophysical well-log signatures are direct physical responses to variations in lithologic characteristics and interstitial fluid chemistry and can be used to delineate lithologic boundaries of subsurface units when rock samples are not available. Well-to-well log correlations of the "Lagonda" interval permit accurate subsurface mapping of lithologic units and when used in conjunction with core descriptions, are quantitative aids in stratigraphic and depositional environment interpretations.

In order to trace lithologies laterally between wells, lithic logs must respond to a rock property that remains consistent from well to well. The laterally continuous black shales of the Cherokee Group contain high concentrations of radioactive materials such as potassium-40 and uranium that are easily recognized on gamma-ray profiles. The gamma-ray response to the radioactive black shale is an abrupt deflection to the high end of the log scale, consistently going off scale. The black shales bounding the "Lagonda" interval are traceable throughout the Cherokee basin and therefore constitute key marker beds for correlation. Ebanks and others (1977), Visher and others

(1971) and Reinholtz (1982) used black shales as datum beds from which stratigraphic cross-sections were hung. This produced the framework to correlate the sandstone-bearing horizons within the Cherokee Group of eastern Kansas. Dense well control is necessary because of the discontinuous nature of the sandstones in the Cherokee Group. The thickness of laterally persistent limestones in the Cherokee Group are commonly below well-log resolution (approximately 2 feet) and are not detectable in many wells in eastern Kansas.

In the subsurface, the "Lagonda" interval comprises the sandstone-bearing mudrock horizon between the top of the black shale below the Verdigris Limestone and the base of the Excello Shale underlying the Fort Scott Limestone. Both of these boundaries are easily recognized by abrupt, high gamma responses of the gamma-ray curve, corresponding to the occurrence of the black Little Osage and Excello shales at the top of the interval, and the black shale underlying the Verdigris Limestone at the interval base (Figure 5). Surface workers have used the Verdigris Limestone as the interval base, but the thickness of this unit often drops below well-log resolution.

Several isopach maps were constructed to illustrate the distribution, trends and geometries of the sandstone bodies. Cross-sections were constructed to give a representative

Figure 5. "Type" gamma-ray and neutron signatures of "Lagonda" interval. Note black shales bounding "Lagonda" interval are recognized in subsurface by an abrupt, high gamma-ray deflection.

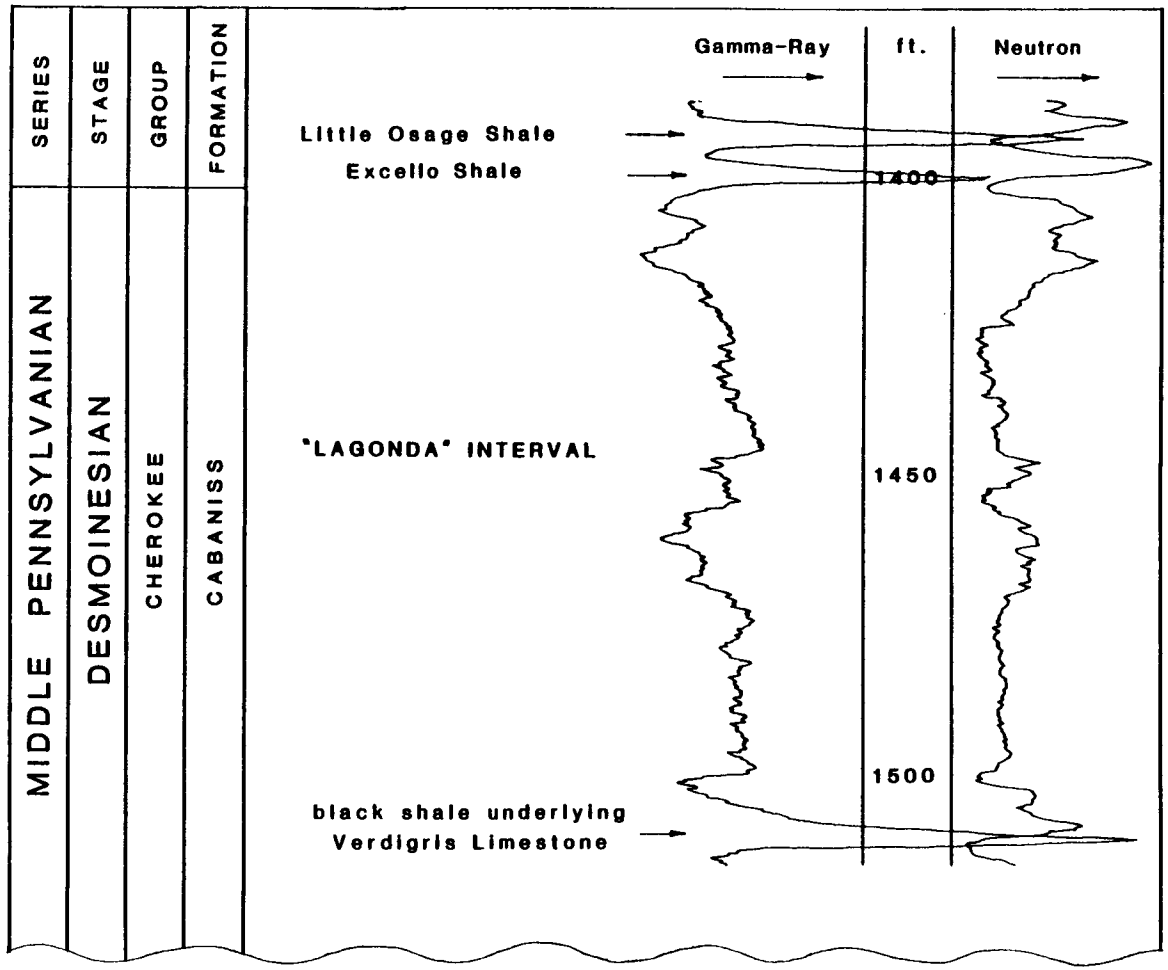
SERIES
STAGE
GROUP
FORMATION
MIDDLE PENNSYLVANIAN
DESMOINESIAN
CHEROKEE
CABANISS
Gamma-Ray
ft.
Neutron
Little Osage Shale
Excello Shale
1400
"LAGONDA" INTERVAL
1450
1500
black shale underlying
Verdigris Limestone

view of the "Lagonda" interval, transecting and bisecting trends of individual sandstone bodies and to illustrate the lateral persistence of the black shale marker beds. Two laterally discontinuous sandstone bodies were recognized on the basis of well-log signatures. Although not continuous over large areas, the "Upper" and "Lower Squirrel" sandstone lenses occupy specific stratigraphic horizons within the "Lagonda" interval (Figure 6). The top of the Excello Shale is the stratigraphic horizon used as a datum line.

Well-Log - Core Lithology Relationships

All geophysical well-logs, including gamma-ray-neutron logs, should be used in conjunction with geological rock data. Eleven cores from Coffey County were described and compared to their corresponding geophysical gamma-ray and neutron log curves (Figure 7).

In the Kanaco-Badger 1 well (Figure 8), a strong correlation exists between the gamma-ray log response and the lithologic characteristics in the cored lithology. However, the precise petrographic nature of lithologies and contacts between units (e.g., erosional, abruptly gradational) and types of sedimentary structures must be obtained directly from core observations. The base of the cored section shows an abrupt basal contact between the underlying silty shale and overlying very fine-grained,

Figure 6. Stratigraphic positions of the "Upper" and "Lower Squirrel" sandstones within the "Lagonda" interval.

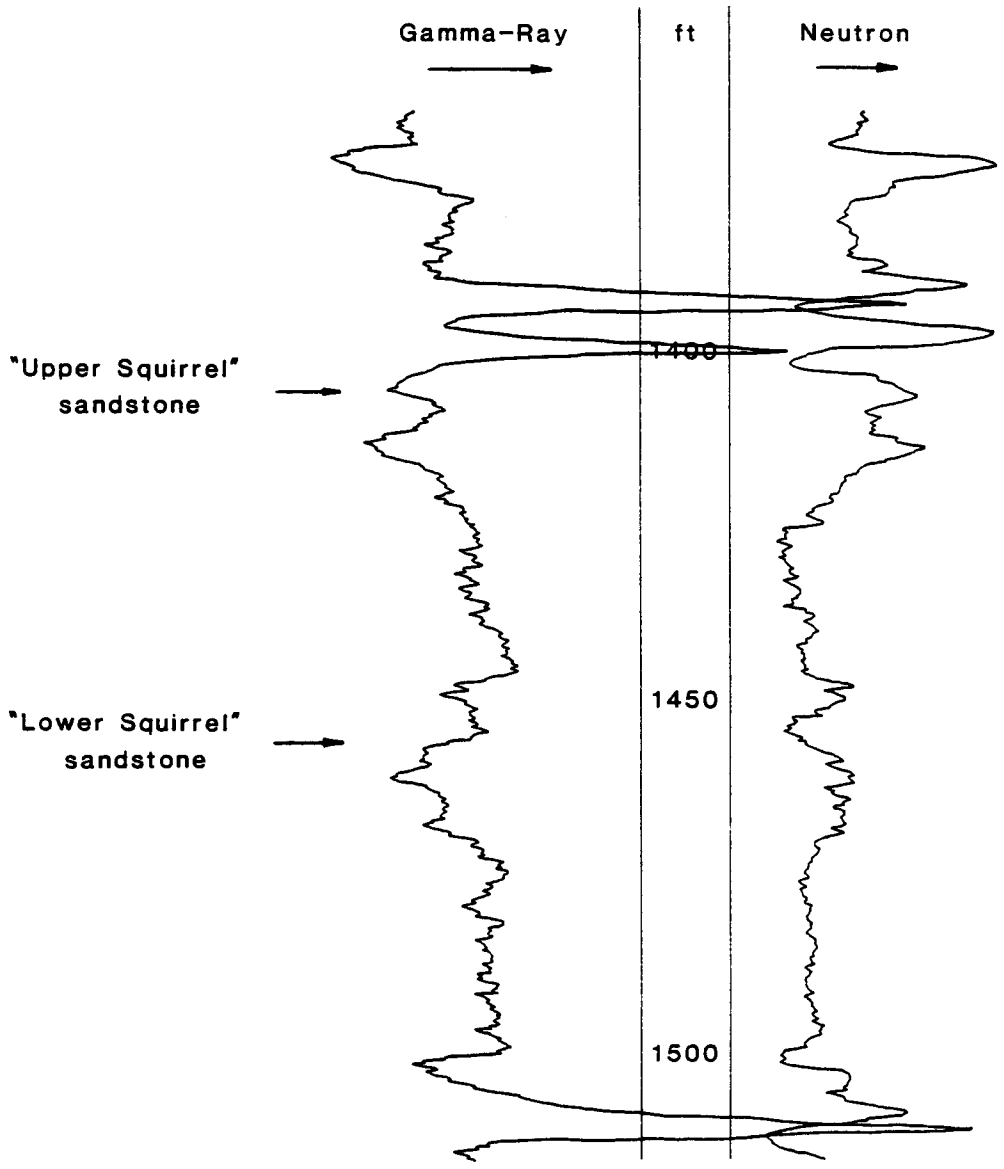
Gamma-Ray
ft
Neutron
"Upper Squirrel" sandstone
"Lower Squirrel" sandstone
1400
1450
1500

Figure 7. Gamma-ray well log with corresponding core description of "Lower Squirrel" sandstone. Slabbed core Bedwell-3, located in Sec. 11-23S-16E.

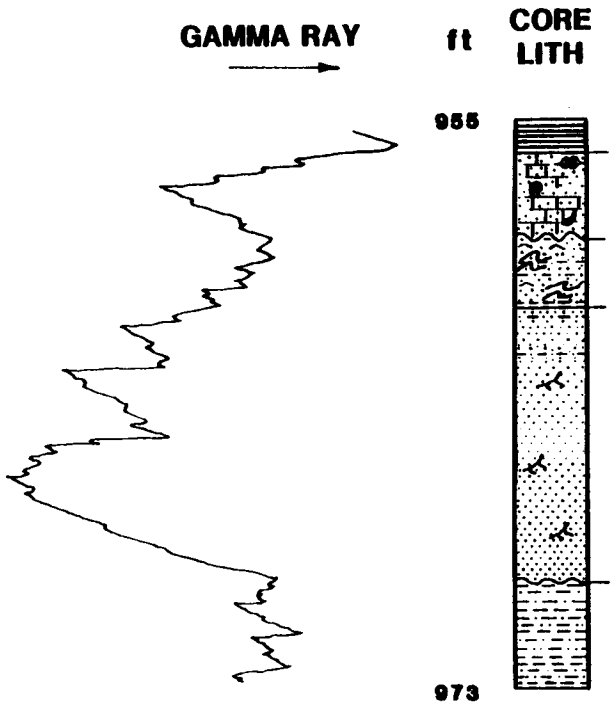

CORE DESCRIPTION

DARK GREY FOSSILIFEROUS CLAY-SHALE

FOSSILIFEROUS
CALCITE-CEMENTED SANDSTONE

CONVOLUTED SANDSTONE, SILTSTONE AND SHALE

RIPPLE-LAMINATED
FINE-GRAINED SANDSTONE

INTERSTRATIFIED SILTSTONE AND SHALE

ripple-laminated sandstone. The contact is recorded by the gamma-ray profile as a sharp deflection to the left (low gamma count), indicating a rapid change in lithology from the underlying higher gamma-count strata. The gamma-ray profile accurately records the thickness of the sandstone. More importantly, the well-log signature records the gradational, fining-upward sequence as a serrated, increasing gamma count curve, due to the increasing quantities of radioactive minerals that are contained in clay materials. Near the top of the core, a fossiliferous, calcite-cemented sandstone is present, and is characterized by a low gamma count with little or no porosity. This unit may be mistakenly interpreted to be limestone by well-log analysts lacking core data.

Although there are many variations in gamma-ray log signatures of the sandstones, they can be grouped into four generalized types based on the nature of contacts, similarities of fining- or coarsening-upward profiles and distances between well locations (Figure 9). Type A is characterized by an abrupt basal contact, serrated fining-upward profile and gradational upper contacts, corresponding to a "bell" or "cylinder" shape. Type B serrated curves are characterized by irregular, interbedded sequences of sandstone and shale. Type C curves are smooth and thin, with a very low gamma count, and a high neutron

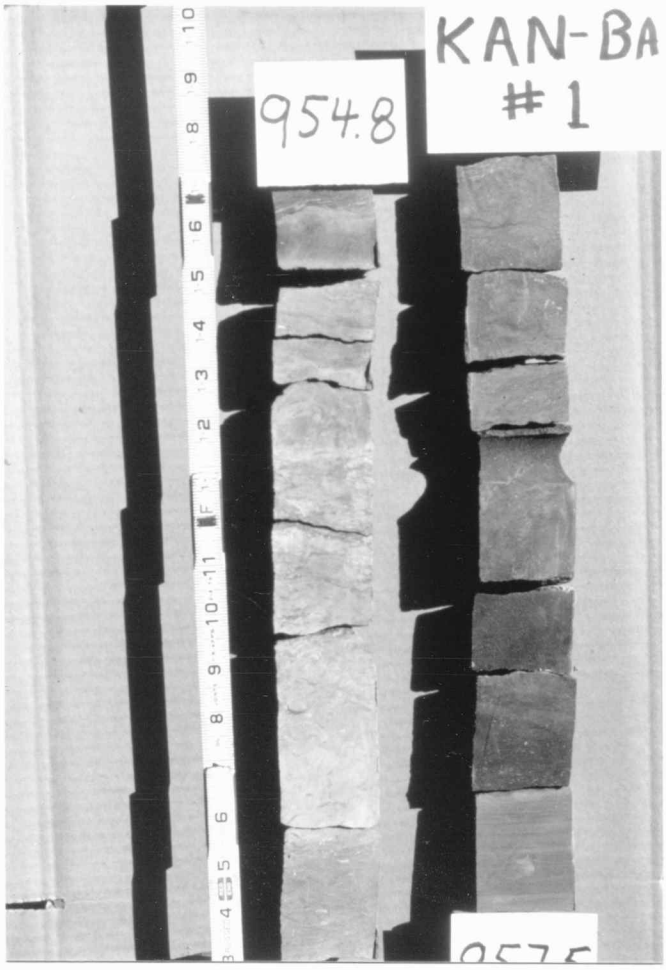

Figure 8. Photograph of cored section penetrating "Lower Squirrel" sandstone. Slabbed core Badger-1, located in Sec. 11-23S-16E.

log response indicating little or no porosity. Type D curves are "funnel-shaped", and in signature, have serrated gradational lower contacts and serrated, abrupt upper contacts.

Sandstone Distribution Map

Sandstone isolith maps were generated for the "Upper" and "Lower Squirrel" sandstones. A shale base line was constructed at gamma-ray values that relate to normal shales (as opposed to radioactive black shales). Similarly, a clean sandstone line was constructed, roughly coincident with the lowest gamma-ray readings that occur in clean sandstone units of the "Lagonda" interval (Figure 10). A 50% sand line bisects the region between the shale base line and the clean sand line. Thicknesses of sandstone units along this line were recorded and used to construct sandstone isolith maps.

The sandstone map of the "Lower Squirrel" indicates a radiating, lobate nature of sand distribution with the highest concentrations occurring where the sandstone bodies bifurcate (Figure 11). The variation of gamma-ray curve shapes indicates that the sandstone bodies are highly lenticular and laterally discontinuous.

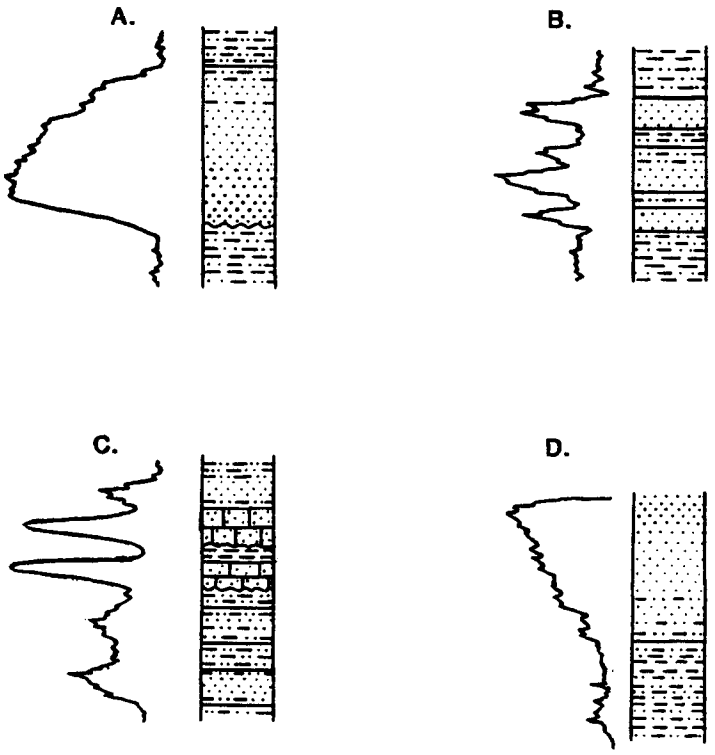

Figure 9. Four characteristic gamma-ray log patterns of "Lagonda" interval rocks in east-central Kansas. A) upward-fining sand/shale sequence with an abrupt base; B) thinly-bedded sand and shale; C) thin, calcite-cemented sandstone; D) upward-coarsening sand/shale sequence with an abrupt upper contact.

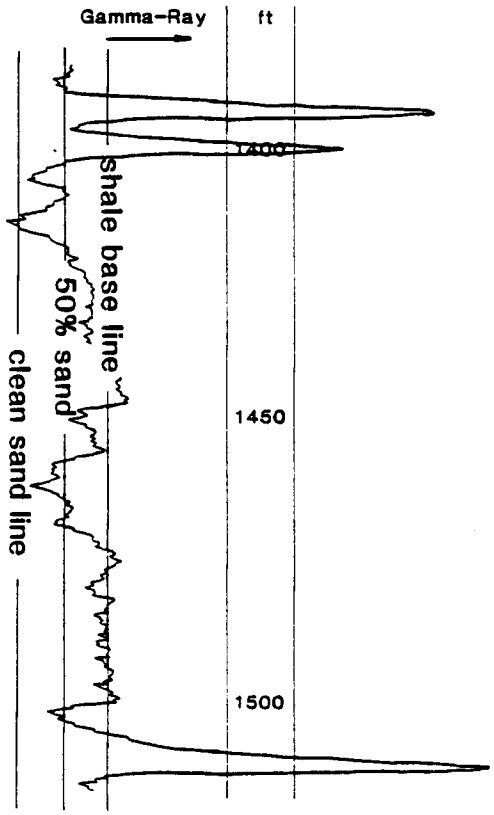

Figure 10. Method used to determine thicknesses of individual sandstone horizons within "Lagonda" interval. Normal shale, clean sand, and 50% sand lines were constructed for each well log. Thicknesses were recorded along 50% line for sandstone distribution maps.

Figure 11. Isolith Map of "Lower Squirrel" Sandstone. Contour interval equals 5 feet.

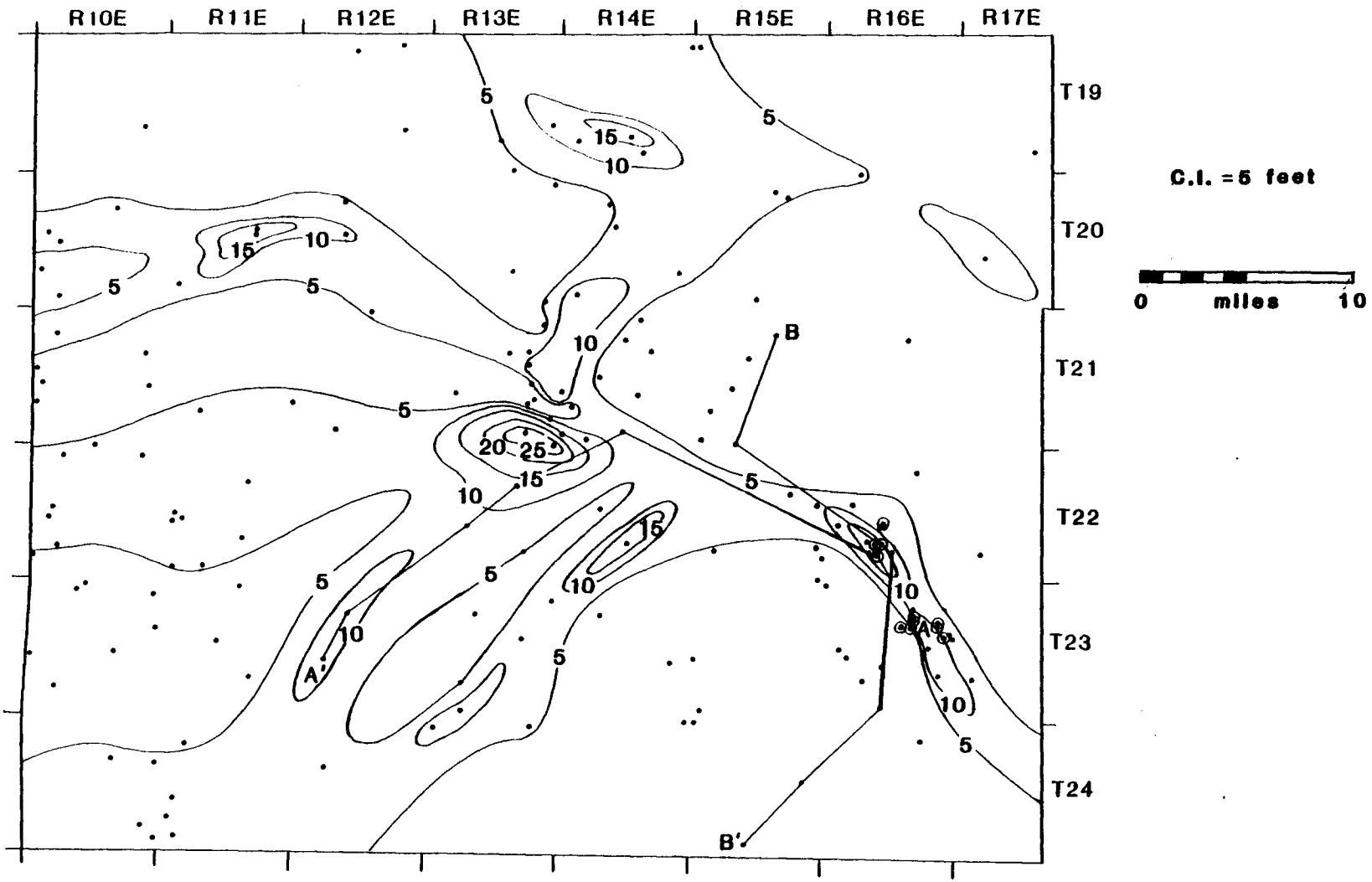
R10E
R11E
R12E
R13E
R14E
R15E
R16E
R17E
T19
T20
T21
T22
T23
T24
C.I. = 5 feet
0
miles
10
A
A'
B
B'
5
10
15
20
25

Stratigraphic Cross-Sections

Cross-section A-A_9 is an east-west cross-section that cuts longitudinally through a lobe of the lenticular "Lower Squirrel" sandstone (Figure 11). All the well-logs used in cross-sections clearly show the two radioactive black shales used as datum lines, although the black shale marking the lower boundary is not shown because the logged interval in these wells did not penetrate the black shale underlying the Verdigris Limestone.

The gamma-ray profiles are characterized by sharp basal contacts, serrated fining-upward profiles with gradational upper contacts (Type A log; Figure 12). Cored sections of this interval show an abrupt, often erosional basal contact between sandstones and the underlying shale and siltstones. Sandstone units grade from fine-grained, low-angle, ripple-laminated sandstone at the base, to an intercalated very fine-grained sandstone, siltstone and shale at the top of the unit.

Cross-section B-B' is a north-south cross-section that cuts perpendicular to the trend of an individual sandstone lobe. The cross-section consists of six well-logs from different locations within the study area. In this cross-section, well 19-22-16E records the thick, fining-upward profile characteristic of cross-section A-A' (Figure 13). Immediately to the north and south of well

Figure 12. Cross-section A-A along sandstone trend showing consistent well log response of "Lower Squirrel" sandstone. Gamma-ray sandstone profiles are characterized by sharp basal contacts, serrated fining-upward sequences with gradational upper contacts (dots).

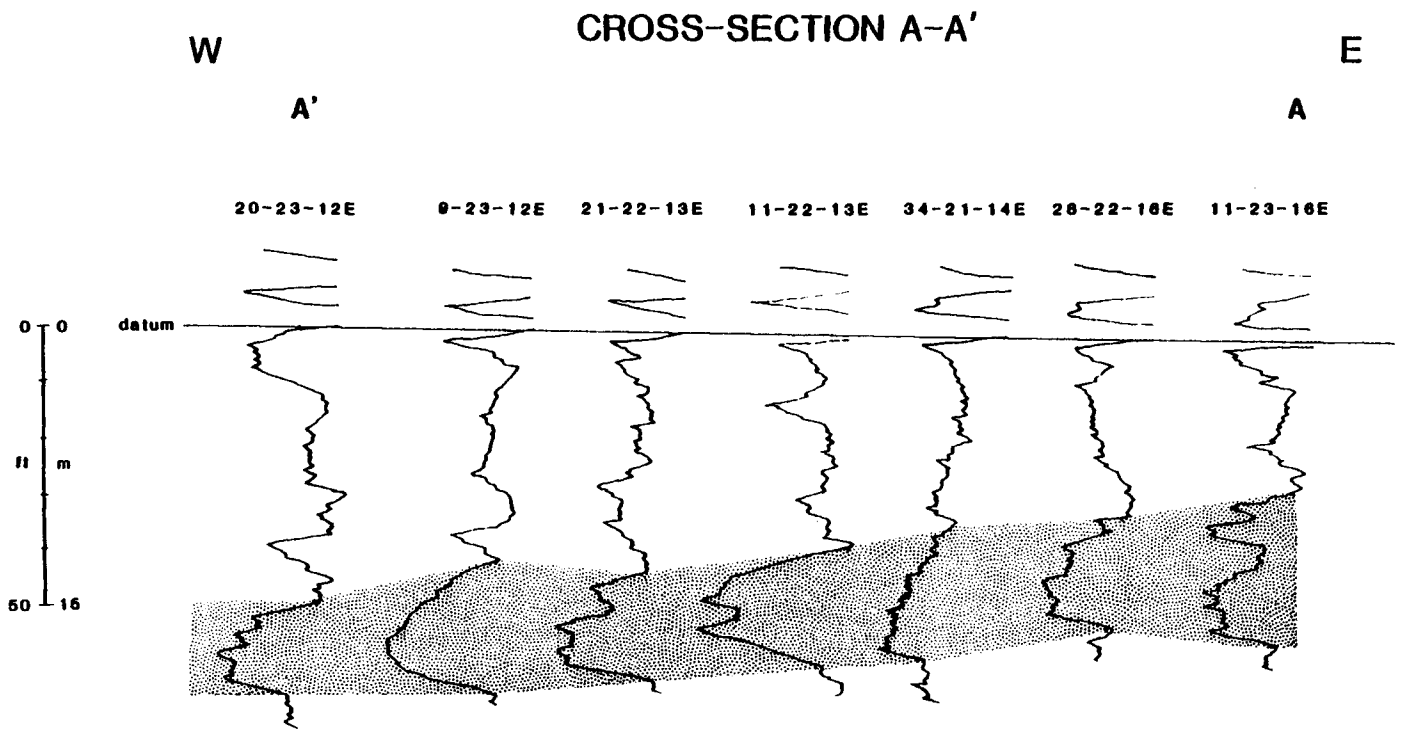
CROSS-SECTION A-A'
W
E
A'
A
20-23-12E
9-23-12E
21-22-13E
11-22-13E
34-21-14E
26-22-16E
11-23-16E
datum
0
0
ft
m
50
15

19-22-16E, well-logs 33-22-16E and 13-24-15E record an abrupt thinning of the sandstone body. The irregular and variable log patterns suggest that the sediments within this interval consist of interbedded sandstone, siltstone and shale (Type B log). Toward the ends of the cross-sections, the well-logs record a consistent, serrated pattern of relatively high gamma radiation, suggesting a thick sequence of shaley sediments.

Figure 13. Cross-section B-B across sandstone trend showing laterally discontinuous and lenticular nature of "Lower Squirrel" sandstone (shaded).

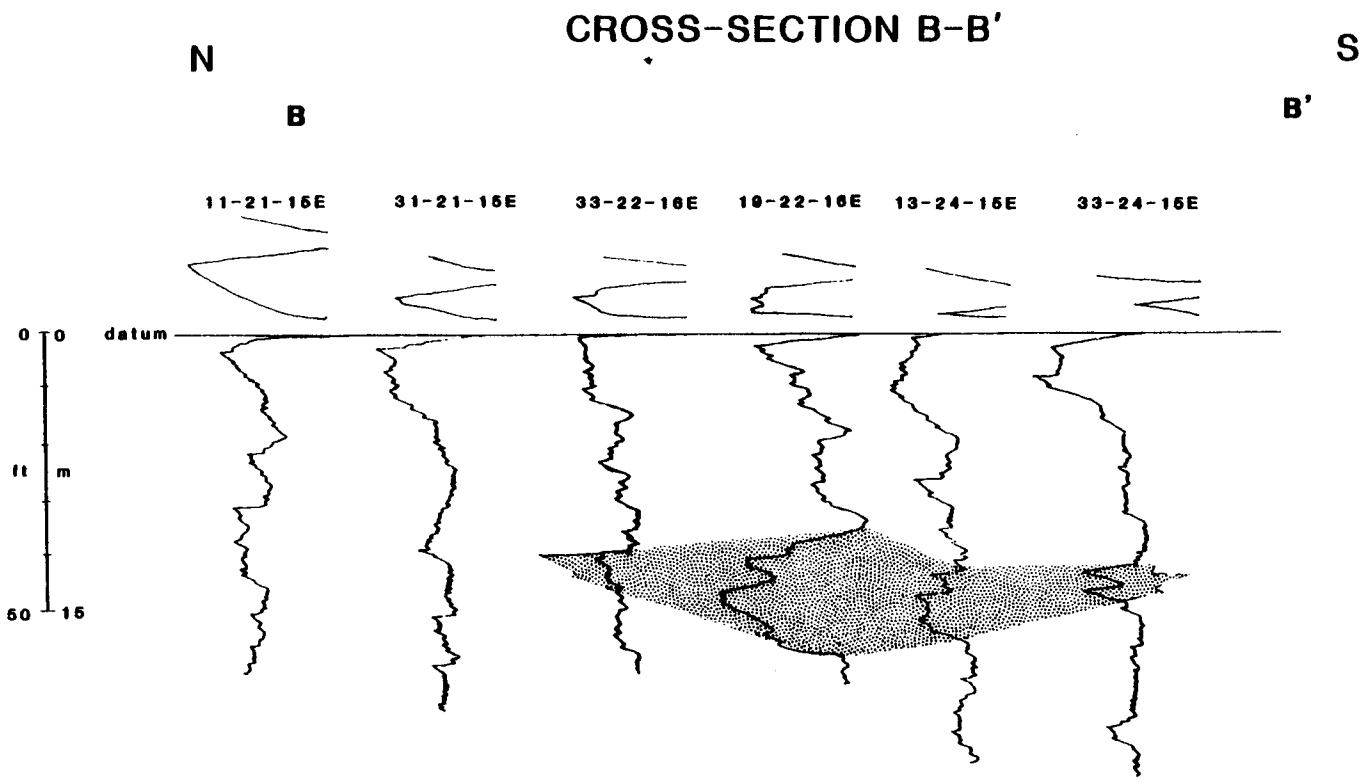
CROSS-SECTION B-B'
N
S
B
B'
11-21-15E
31-21-15E
33-22-16E
10-22-16E
13-24-15E
33-24-15E
datum
0
0
ft
m
50
15

DEFINITION OF LITHOFACIES

Sedimentalogic analysis of the "Lagonda" interval was based on subsurface core material. Eleven cores were described in detail and subdivided into units based on grain size, bedding characteristics, sedimentary structures and depositional sequence. Lithologies were described and used to aid in stratigraphic, sedimentologic and depositional interpretations. Lengths of cored sections that penetrate the "Lower Squirrel" sandstone range from six to twenty-four feet (2 to 6 meters). The sandstone thicknesses range from one to ten feet (0.3 to 3 meters), although some sandstone core samples were removed by drillers for core analyses. The color of clay-free (clean), sandstone varies fron tan to black, depending on the extent of oil staining. The sandstones are moderately sorted, fine-grained and composed of quartz (about 40%) with somewhat subordinate amounts of feldspar (25%), and micas (Table 1). Cements include authigenic clays, Fe-calcite and silica.

Five lithofacies were recognized in the cored intervals: a) interlaminated siltstone and shale; b) ripple-laminated to low-angle cross-bedded sandstone with basal conglomerate; c) interstratified contorted and

convoluted sandstone, siltstone and shale; d) calcite-cemented fossiliferous sandstone; e) thinly laminated, dark grey clay-shale with abundant marine fossils and macerated plant fragments (Figure 14).

Lithofacies A

Lithofacies A consists of intercalated dark grey shale and siltstone and sandstone with abundant carbonaceous debris. The dark grey shale consists of thin laminated sets ranging from 0.2 cm to 3.0 cm thick. The siltstone and sandstone layers are usually 1.0 cm to 2.0 cm thick with occasional load structures and slight oil stains. Petrographical analyses show that lithofacies A consists of very fine-grained sand-sized quartz, feldspars and micas interstratified with thin laminae of muscovite. The mica layers form continuous layers along bedding planes. Authigenic clays and lesser amounts of silica overgrowths cement most of this unit.

Lithofacies B

Fine-grained, ripple-laminated sandstones constitute the major components of lithofacies B. The sandstones are dominated by small-scale sedimentary structures, including low-angle crossbeds, climbing-bedform ripples and ripple stratification laminae. The sandstones are interstratified with lesser amounts of silt and clay near the top of the

Figure 14. Idealized fining-upward sandstone sequence and corresponding gamma-ray log signature of "Lower Squirrel" sandstone. Five lithofacies recognized include: A) interlaminated siltstone and shale; B) ripple-laminated to low-angle cross-bedded sandstone; C) interstratified sandstone, siltstone amd shale D)calcite-cemented fossiliferous sandstone; E) dark grey shale with organic debris and marine fossils. Slabbed core Bedwell-3.

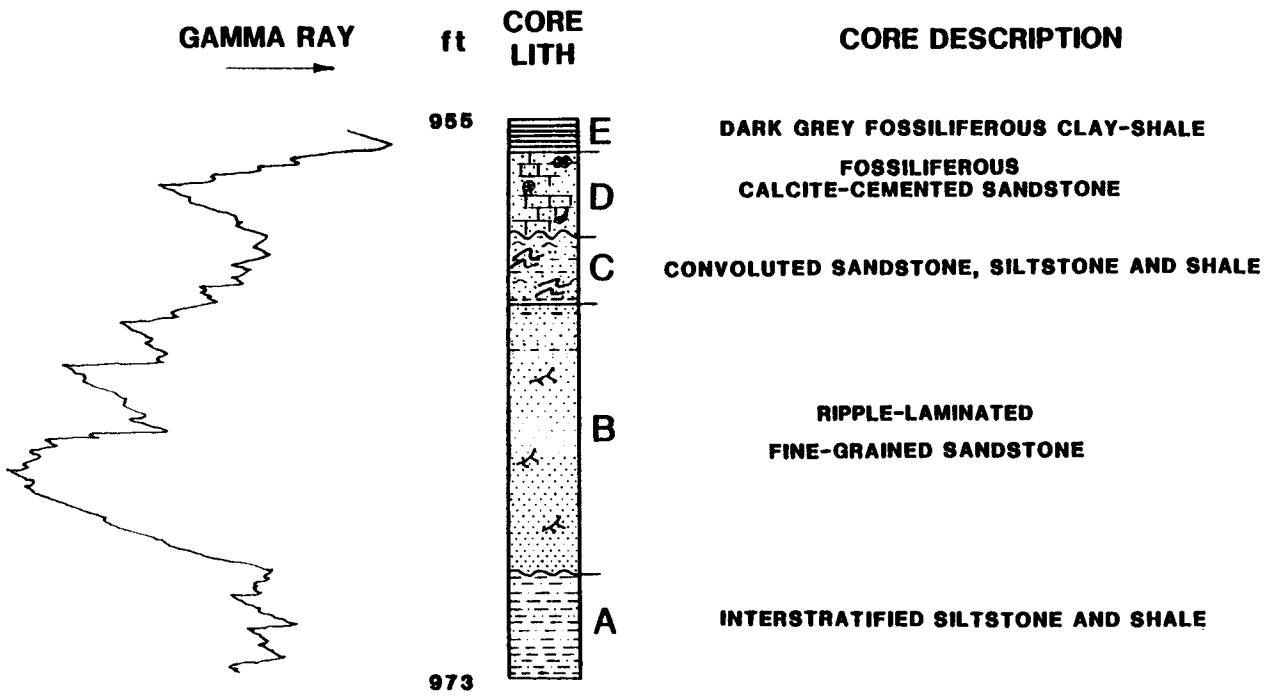
GAMMA RAY
ft
CORE LITH
CORE DESCRIPTION
955
973
E
D
C
B
A
DARK GREY FOSSILIFEROUS CLAY-SHALE
FOSSILIFEROUS CALCITE-CEMENTED SANDSTONE
CONVOLUTED SANDSTONE, SILTSTONE AND SHALE
RIPPLE-LAMINATED FINE-GRAINED SANDSTONE
INTERSTRATIFIED SILTSTONE AND SHALE

unit, forming a fining-upward sequence. Sandstones are usually black due to heavy oil stains.

Petrographically, lithofacies B consists of a fine-grained, moderately well sorted, angular to subangular sandstone composed primarily of monocrystalline quartz (36-44%) with lesser amounts of feldspar (10-18%), rock fragments (1-2%) and micas (4-15%). Numerous quartz overgrowths exist, although much porosity and interconnected pore-space persists (13-21%) (Figure 15). Quartz overgrowths, authigenic clays, and lesser amounts of calcite cement the siliciclastics of this unit.

Lithofacies C

Lithofacies C consists of convoluted and contorted beds of intercalated sandstone, siltstone and shale (Figure 16). Structural features include slumping , contorted bedding and flow rolls, possibly resulting from rapid infilling and extremely high porewater content of silt and clay material. Silt-filled burrows (Figure 17), carbonaceous plant material and pyrite are common. Micaceous partings are commonly observed on bedding planes.

Petrographically, lithofacies C consists primarily of monocrystalline quartz (45-55%), feldspar (12-15%) and micas (14-26%). Authigenic clays and silica constitute most of the cement and occlude many pore spaces and pore throats.

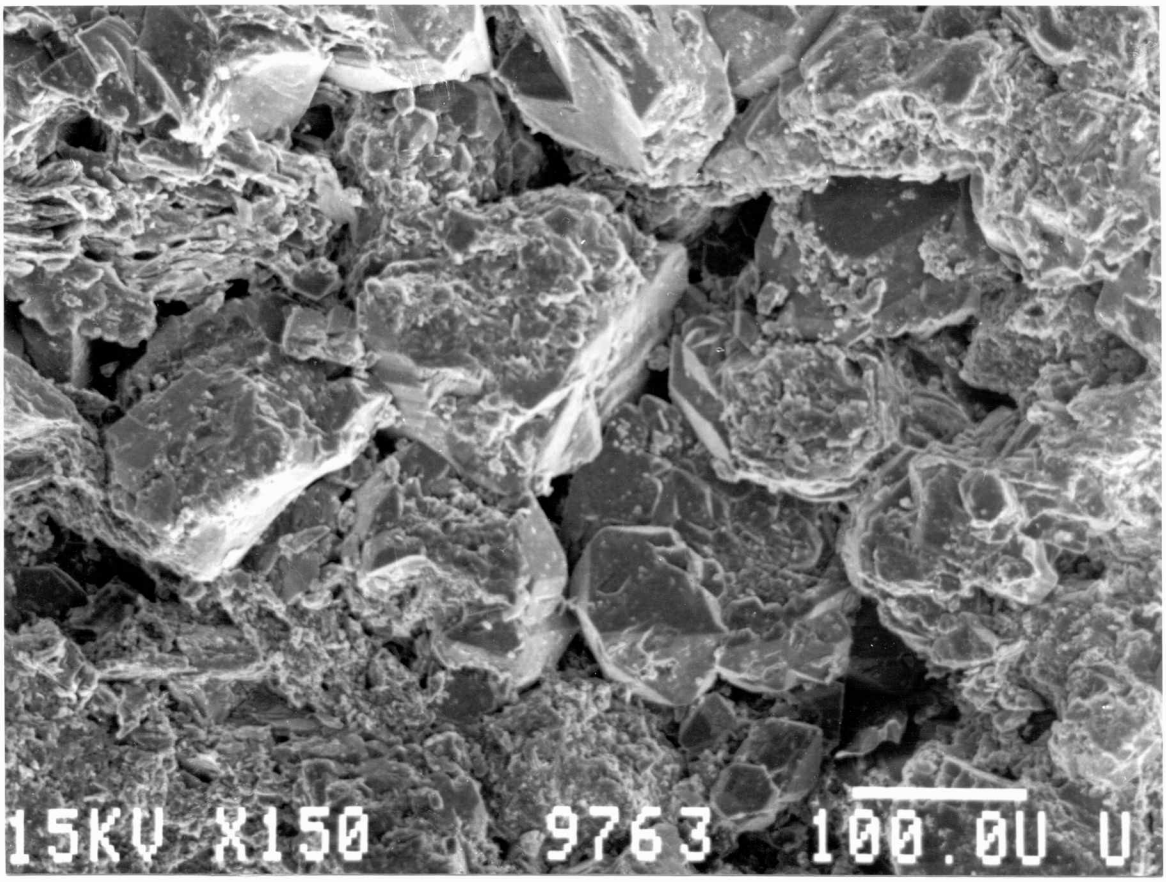

Figure 15. Scanning electron micrograph showing numerous pore spaces and interconnected pore throats in lithofacies B. Sample KB-1-976.3. Bar scale equals 10 microns.

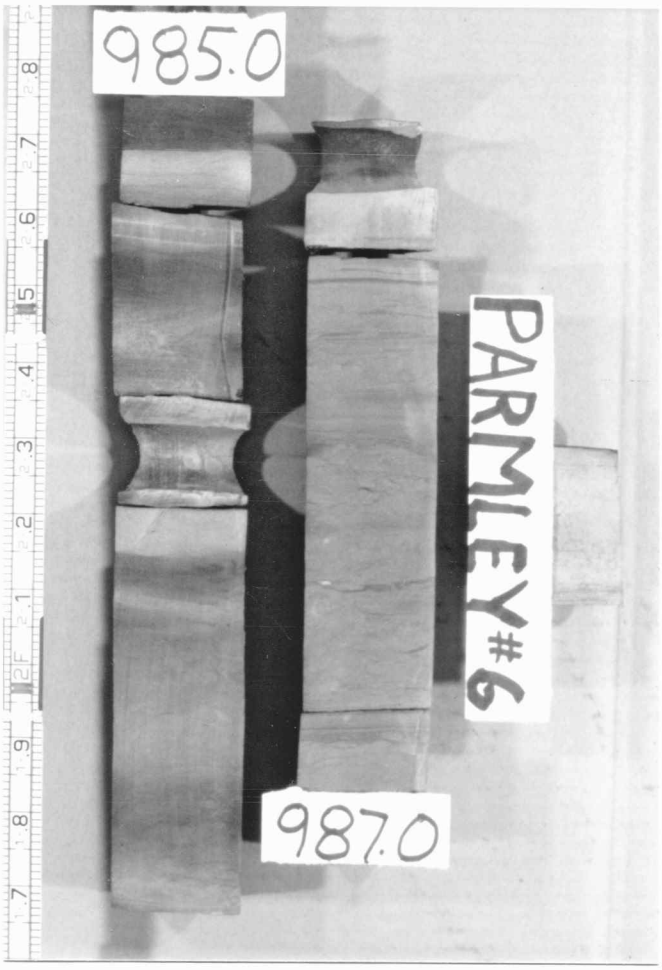

Figure 16. Photograph of convoluted and contorted sandstone, siltstone and shale in Lithofacies C. Slabbed core Parmely-6, located in Sec. 29-22S-17E.

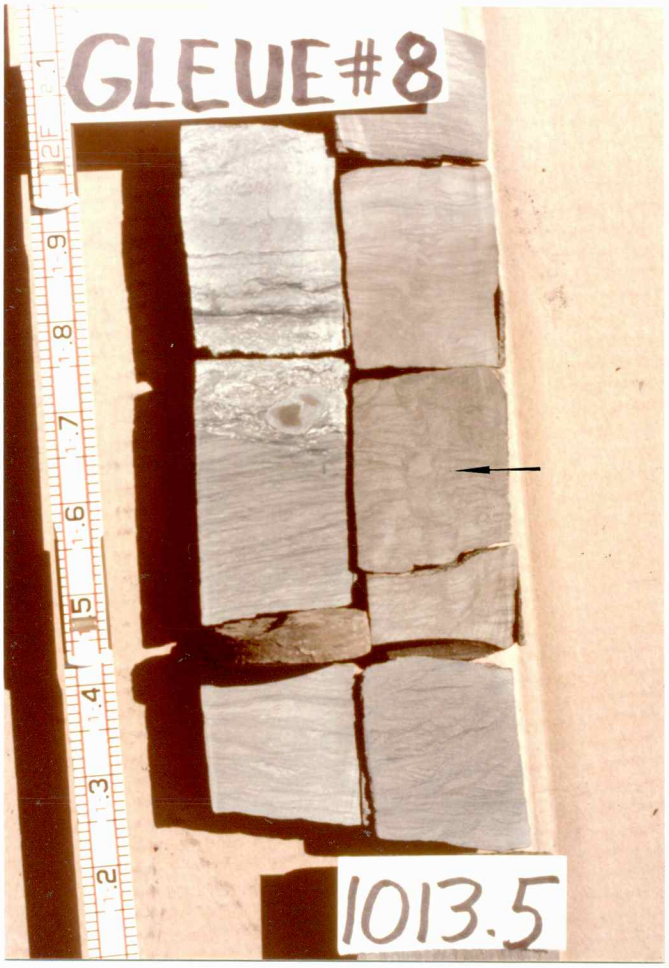

Figure 17. Photograph of silt-filled burrow within Lithofacies C. (arrow) Slabbed core Gleue-8, located in Sec. 22-22S-16E.

Minor amounts of poikilotopic calcite cement portions of the unit.

Lithofacies D

Lithofacies D consists of fossiliferous, calcite-cemented, sandstone varying from white to tan in cored sections depending on the proportion of carbonate cement and oil stain. The fossils are predominantly broken and disarticulated shell fragments that may reach 1 cm in maximum diameter (Figure 18). The siliciclastics are moderately well sorted and dominated by quartz (20-45%) with lesser amounts of feldspar and muscovite. Small scale sedimentary structures include ripple-laminae and scoured basal contacts, forming an erosional contact with lithofacies C (Figure 17).

Petrographically, lithofacies D shows abundant marine fossil fragments, including brachiopods, echinoderms and foraminifers (3-47%). Medium to fine-grained monocrystalline quartz, feldspars and micas often appear "floating" in poikilotopic calcite cement. Calcite cement constitutes much of the unit (5-34%), filling most of the intergranular pore space.

Lithofacies E

Lithofacies E consists of dark grey fossiliferous clay-shale with abundant carbonaceous plant fragments.

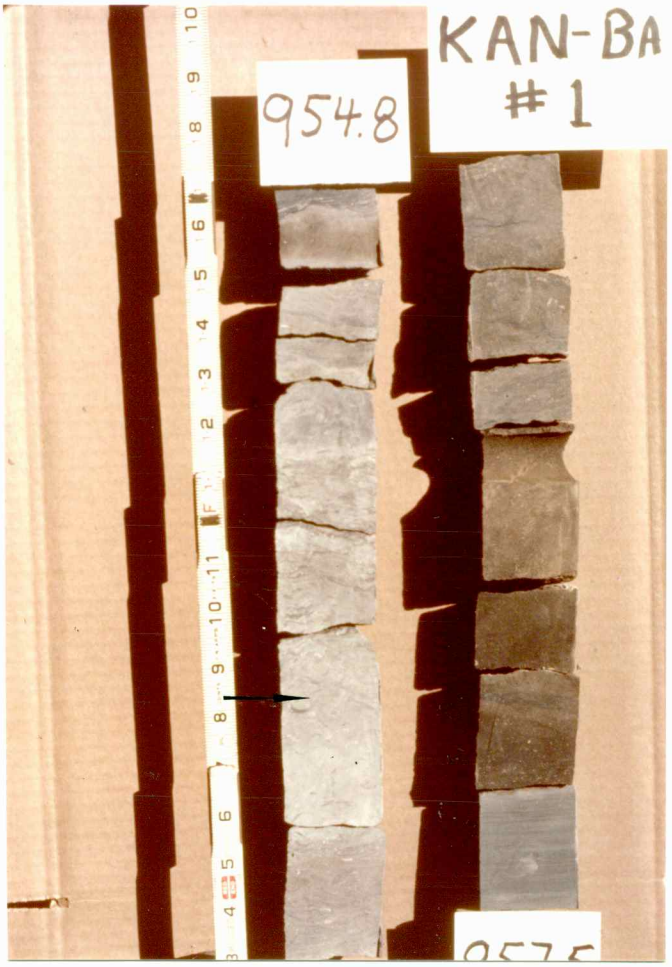

Figure 18. Photograph of cored section showing numerous fossil fragments within Lithofacies D. Cored sample Kanaco-Badger 1.

Pyrite is common, replacing plant fragments and whole shells. Soft sediment deformation structures are common. The basal contact is abruptly gradational with lithofacies D. Lithofacies E probably represents suspension deposition under very low energy conditions as evidenced by undisturbed clay laminae and whole shells.

SANDSTONE PETROLOGY

Sandstones from two different lithofacies of the "Lower Squirrel" Lagonda sandstone were distinguished on the basis of stratigraphic sequence, fossil content, sedimentary structures and degree and type of cementation (Figure 19).

The sandstone from lithofacies B consists of fine-grained monocrystaline quartz with lesser amounts of feldspar, muscovite, and rock fragments. Cements include silica, kaolinite and Fe-calcite. Porosity ranges from 13 to 21 percent. Lithofacies D consists of a medium- to fine-grained sandstone composed primarily of monocrystalline quartz grains with lesser amounts of potassium feldspar, and abundant, often broken and disarticulated marine fossil fragments, including brachiopods, echinoderms and foraminifers. Siliciclastic grains often appear "floating" in poikilotopic Fe-calcite cement.

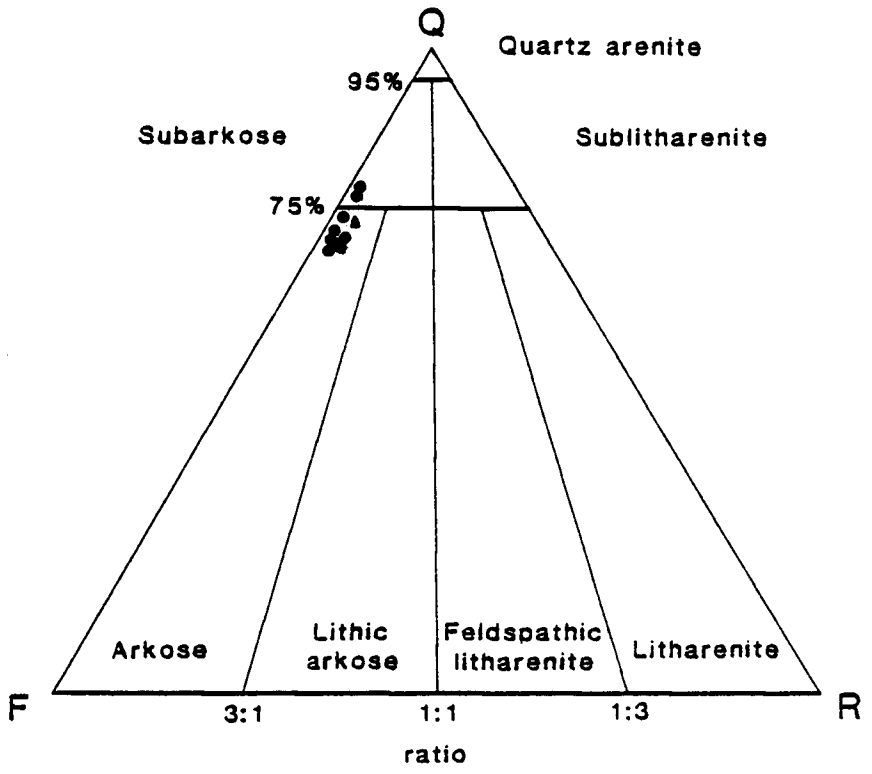

Figure 19. Triangular diagram plot of detrital sand-sized grains. Q=monocrystalline and polycrystalline quartz; F=feldspars; R=sedimentary rock fragments and chert. Triangle subdivisions are from Folk (1974). Dots=less than 10% clay matrix; triangles=greater than 10% clay matrix. Data summarized in tables 1 and 2.

"Clean" Sandstone - Lithofacies B

Detrital Minerals

Monocrystalline Quartz

Monocrystalline quartz is the most abundant detrital mineral in the "Lower Squirrel" sandstone, ranging from 36 to 44 percent of the bulk rock (Table 1). Quartz grains are very fine- to medium-grained, ranging from 0.6 to 0.27 mm in maximum diameter in thin-section. Very fine-grained quartz sand grains are angular to subangular with low sphericity, and the fine to medium-grained quartz sand is subangular to subrounded with moderate sphericity. Most quartz grains show slightly undulose extinction (1 to 10 degrees) and a few display strong (greater than 10 degrees) undulose extinction. Numerous overgrowths on quartz grains obscure the original grain shape, forming subhedral to euhedral shaped grains and/or an interlocking quartzite-like mosaic of grains. Subhedral to euhedral silica overgrowths are typical of the coarser-grained sandstones (Figure 20). Finer-grained sandstones are characterized by patchy, subhedral to anhedral, interlocking silica cement (Figure 21). Occasional early clay coatings or "dust" rims are present on the quartz grains between individual detrital grain cores and the overgrowths (Figure 22). Quartz grains are occasionally etched and replaced by Fe-calcite. Microlite inclusions in monocrystalline quartz grains

include tourmaline, rutile and rare vermicular booklets of chlorite.

Polycrystalline Quartz

Polycrystalline quartz grains are highly variable with respect to the number of subcrystals and suture patterns. Most polycrystalline quartz consists of elongate grains with straight and sutured borders between interlocking, equant quartz subcrystals and occasional muscovite inclusions. The polycrystalline quartz grains are subangular to subrounded and moderately spherical, ranging in grain size from 0.13 to 0.22 mm in maximum diameter.

Potassium Feldspar

Potassium feldspar is the most abundant feldspar of the "Lower Squirrel" Lagonda sandstone, ranging from 9 to 16 percent of the bulk rock. Feldspars are recognized on the basis of optical properties including presence of cleavage, Carlsbad twinning, sericitization along cleavage traces and presence of relict honey-combed and doughnut-shaped grains (Figure 23). Potassium feldspar grains are generally fine- to medium-grained, subangular to subrounded, ranging from 0.12 to 0.22 mm in maximum diameter.

Table 1

Modal analyses of selected thin-sections from lithofacies B sandstone based on counts of 225 points.

Well Name	Lincoln Bedwell 3			
Sample No.	LB-3 959.5	LB-3 961.1	LB-3 966.8	LB-3 967.8
DETRITAL				
Quartz				
Monocrystalline	(91) 40%	(98) 44%	(101) 45%	(94) 42%
Polycrystalline	(3) 1%	(5) 2%	(3) 1%	(9) 4%
Feldspar				
Potassium	(20) 9%	(32) 14%	(27) 13%	(36) 16%
Plagioclase	(7) 3%	(6) 3%	(3) 1%	(6) 3%
Mica				
Muscovite	(20) 9%	(15) 7%	(11) 5%	(9) 4%
Biotite	(6) 3%	(3) 1%	(4) 2%	0
Rock Fragments				
Shale	(2) 1%	(3) 1%	0	0
Quartz-Mica	0	(1) Tr	(1) Tr	(2) 1%
Fossils				
Brachiopods	0	0	0	0
Echinoderms	0	0	0	0
Foraminifers	0	0	0	0
Organic Material	(2) 1%	(1) Tr	(2) 1%	(1) 1%
Authigenic				
Carbonate				
Fe-calcite	(1) Tr	(4) 2%	(6) 3%	(12) 6%
Clays				
Kaolinite	(6) 3%	(8) 4%	(16) 7%	(12) 5%
Sericite	(14) 7%	(12) 5%	(12) 6%	(8) 4%
Chlorite	1	0	0	0
Silica	(7) 3%	(5) 2%	(7) 3%	(4) 2%
Pyrite	(2) 1%	(2) 1%	(2) 1%	(1) Tr
Fe-oxide	(3) 1%	(2) 1%	(3) 1%	(1) Tr
POROSITY				
Primary	(22) 10%	(10) 5%	(16) 8%	(11) 5%
Secondary	(18) 8%	(18) 8%	(10) 5%	(18) 8%
TOTAL	(225) 100%	(225) 100%	(225) 100%	(225) 100%

Table 1--continued

Well Name	Lincoln Meats 8		Kanaco Badger 1	
Sample No.	IM-8 948.9	IM-8 949.9	KB-1 967.0	KB-1 973.2
DETRITAL				
Quartz				
Monocrystalline	(84) 37%	(82) 36%	(85) 38%	(93) 42%
Polycrystalline	(3) 1%	(6) 3%	(4) 2%	(4) 2%
Feldspar				
Potassium	(32) 14%	(35) 16%	(33) 15%	(30) 13%
Plagioclase	(7) 3%	(5) 2%	(4) 2%	(9) 4%
Mica				
Muscovite	(13) 6%	(10) 9%	(20) 9%	(24) 11%
Biotite	(1) Tr	(2) 1%	(5) 2%	(5) 2%
Rock Fragments				
Shale	0	0	0	(1) Tr
Quartz-Mica	0	0	(1) Tr	0
Fossils				
Brachiopods	0	0	0	0
Echinoderms	0	0	0	0
Foraminifers	0	0	0	0
Organic Material	(3) 1%	(2) 1%	(1) Tr	0
AUTHIGENIC				
Carbonate				
Fe-calcite	(4) 2%	(3) 1%	0	0
Clays				
Kaolinite	(4) 2%	(4) 2%	(3) 1%	(6) 3%
Sericite	(12) 6%	(6) 3%	(14) 7%	(15) 7%
Chlorite	0	0	0	0
Silica	(6) 3%	(7) 3%	(3) 1%	(6) 3%
Pyrite	(5) 2%	(9) 4%	(2) 1%	(2) 1%
Fe-oxide	(2) 1%	(2) 1%	(2) 1%	(3) 1%
POROSITY				
Primary	(15) 7%	(17) 8%	(13) 6%	(7) 3%
Secondary	(34) 15%	(35) 15%	(35) 15%	(17) 8%
TOTAL	(225) 100%	(225) 100%	(225) 100%	(225) 100%

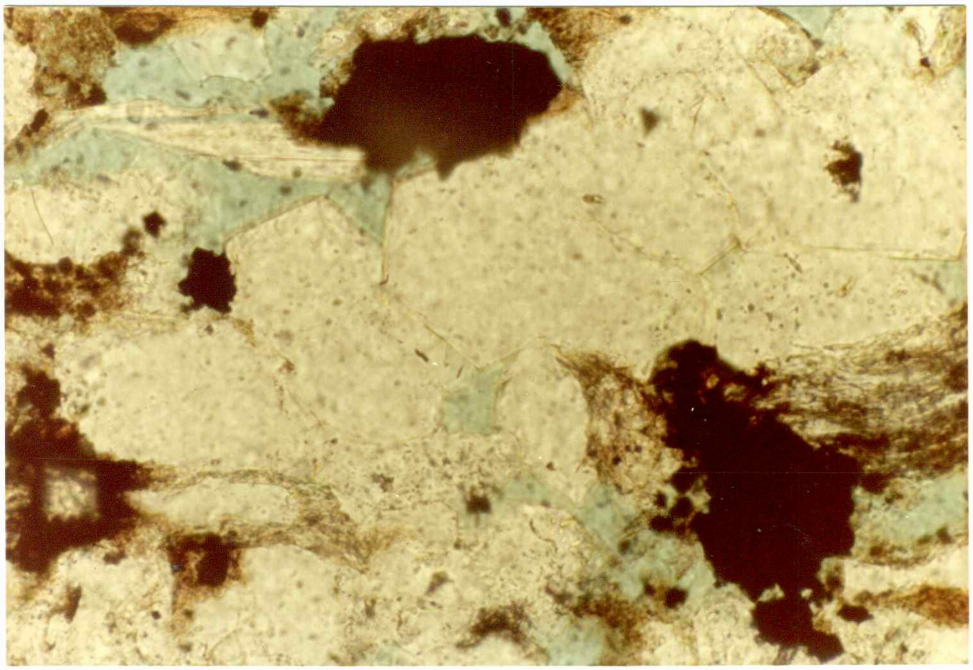

Figure 20. Photomicrograph of quartz grains with well-developed euhedral quartz overgrowths. Plane light. Sample LM-8-949.9. Bar scale equals 0.1 mm.

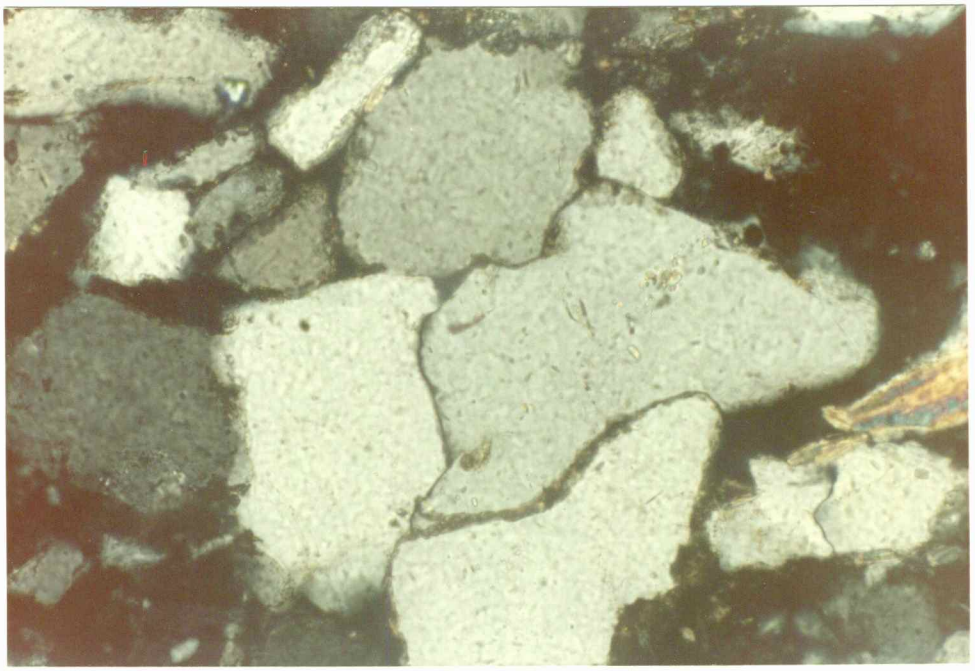

Figure 21. Photomicrograph of interlocking mozaic of silica cement characteristic of finer-grained sandstone units. Cross-polarized light. Sample LM-8-945.2. Bar scale equals 0.1 mm.

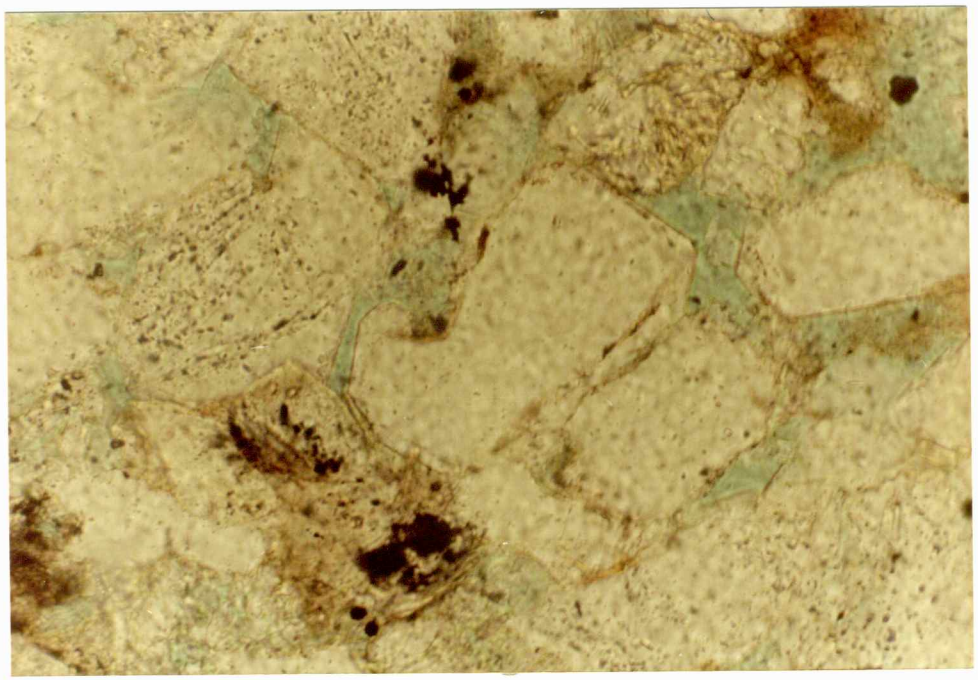

Figure 22. Photomicrograph of early clay rim on detrital quartz grain. Plane light. Sample LM-8-949.9. Bar scale equals 0.1mm.

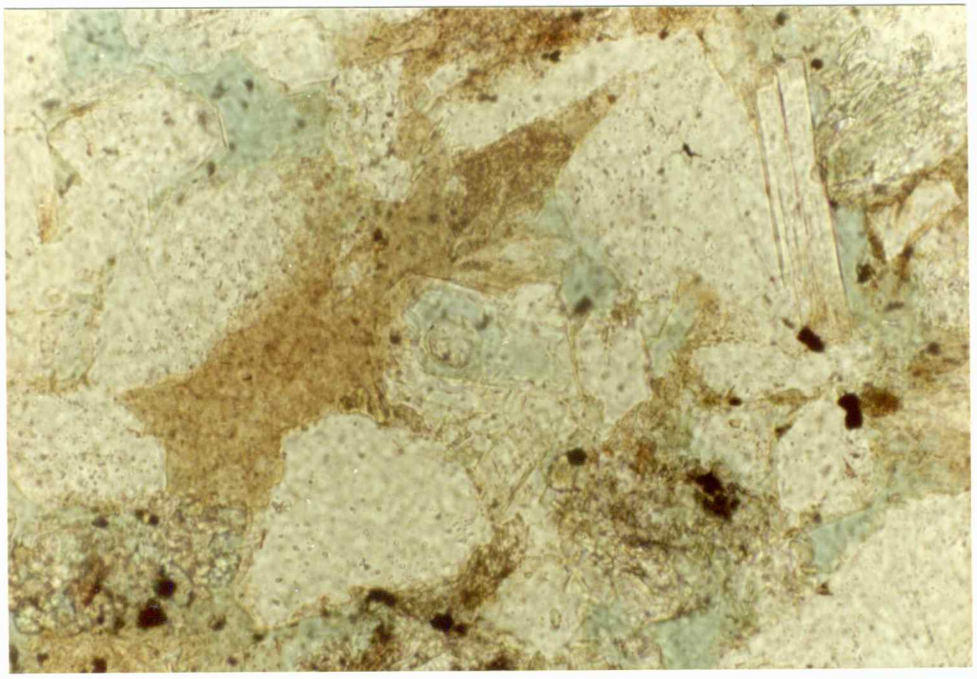

Figure 23. Photomicrograph showing partially dissolved feldspar grains, forming honey-combed grain shape in lithofacies B. Plane light. Sample KB-1 967.0. Bar scale equals 0.1mm.

Plagioclase Feldspar

Plagioclase feldspar grains were recognized by the presence of multiple, albite twinning. The maximum extinction angles between adjacent laminae (Michael-Levy Method) varies from 14 to 21 degrees, suggesting that the plagioclase grains are of albite composition. Reinholtz (1982) also determined an albite composition for plagioclase feldspars from the "Lagonda" sandstones from Anderson County, Kansas just east of the study area. Plagioclase grains are generally fine-grained, ranging from 0.15 to 0.25 mm in maximum diameter and are subangular to subrounded with low sphericity. Alteration of plagioclase grains consists of aligned sericite along cleavage traces and partial dissolution leaving relict honey-combed grains.

Extensive dissolution of potassium and plagioclase feldspar grains contributes up to 70% of the total porosity in the sandstone (Figure 24). Feldspar dissolution has been recognized as a possible contributor to secondary porosity in sandstone reservoirs (Heald and Larese,1973; Land and Milliken, 1981). In Cherokee Group sandstones, secondary porosity due to feldspar dissolution contributes to effective, interconnected, pore space (Woody, 1983).

Compositional differences within individual feldspar grains are indicated by doughnut-shaped grains formed by dissolution of the central core (Heald and Larese, 1973) and

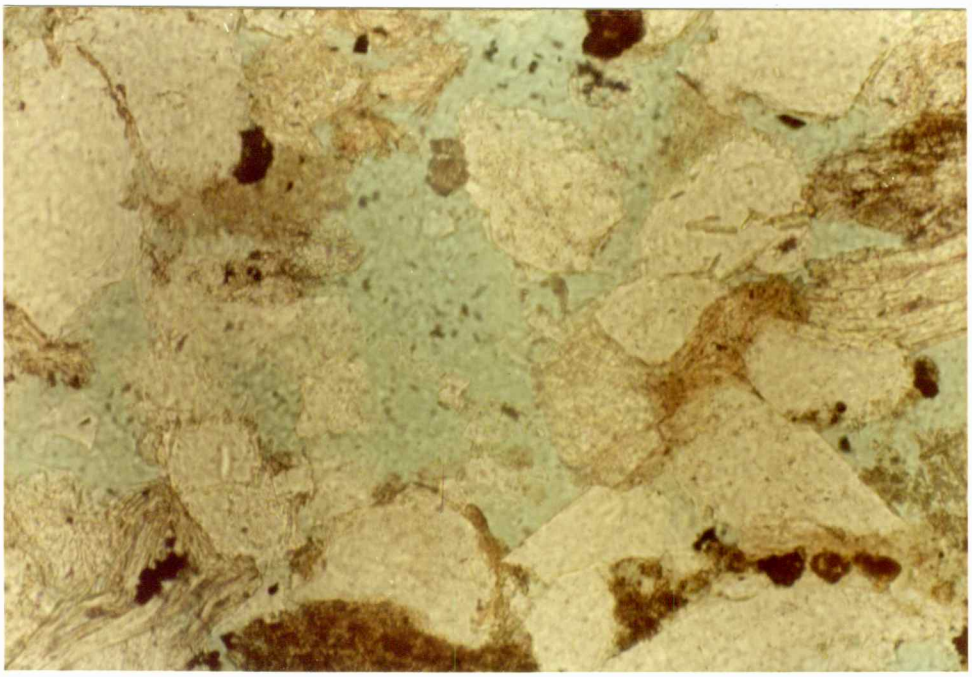

Figure 24. Photomicrograph showing extensive dissolution of former feldspar grains, creating effective secondary porosity. Plane light. Sample KB-1 967.0. Bar scale equals 0.1mm.

by highly irregular boundaries between the void and the remaining grain. Plagioclase feldspar grains are occasionally fractured and often split by carbonate cement along the twinned laminae.

Petrographic evidence suggests that kaolinite is a common alteration product of feldspar.

Rock Fragments

Rock fragments compose a small percentage of the detrital components of the "Lower Squirrel" Lagonda sandstone. Rock fragments include argillaceous siltstone-shale clasts, chert and foliated quartz-mica fragments.

Argillaceous rock fragments occur as deformed, reddish-brown, fine-grained siltstone-shale clasts and are easily recognized as patchy, larger than normal clay-filled "pore fillings" (Figure 25). The clasts, composed of silt-sized grains of quartz, feldspar and micas in a clay matrix, are deformed around more resistant siliciclastic grains, often occluding porosity by clogging adjacent pore throats.

Rare detrital chert consists of subrounded grains ranging from 0.17 to 0.22 mm in diameter, and shows little alteration.

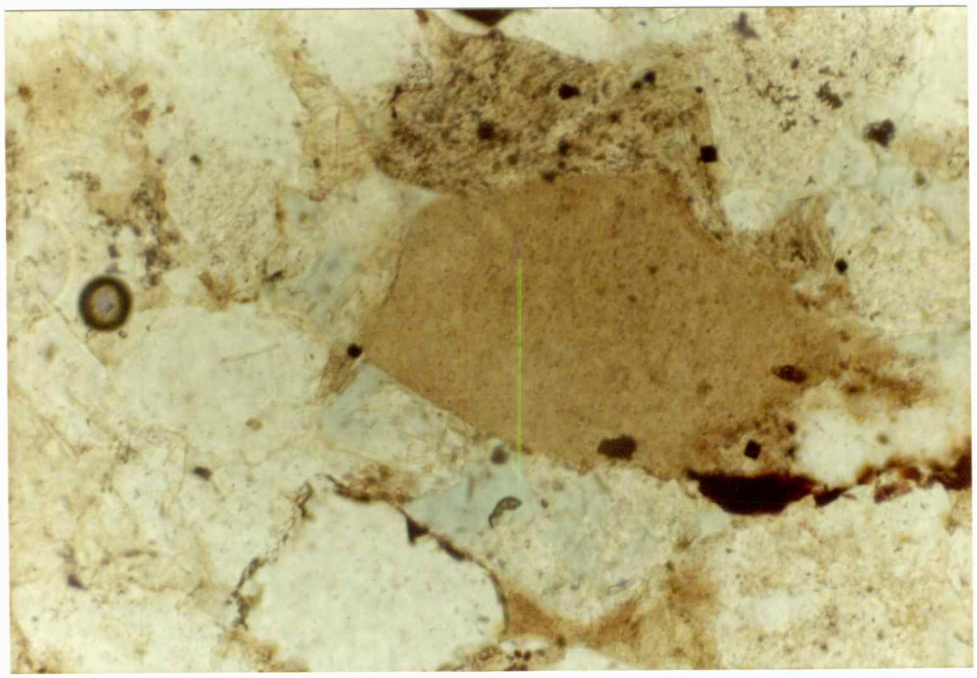

Figure 25. Photomicrograph showing compactional effects on argillaceous rock fragment. Plane light. Sample LB-3-961.1. Bar scale equals 0.1mm.

Foliated quartz-mica fragments consist of elongate quartz subcrystals interlayered with muscovite and biotite. The size of the fragments varies from 0.16 to 0.23 mm in diameter. Alteration of the mica flakes to chlorite is common.

Muscovite

Muscovite is a conspicuously abundant accessory mineral in the "Lower Squirrel" Lagonda sandstone, ranging from 4 to 15 percent of the bulk rock. Muscovite occurs as colorless euhedral laths ranging in size from 0.15 to 1.3 mm in maximum diameter. The grains are usually aligined parallel to stratification, forming numerous micaceous partings along bedding planes. In the coarser sandstones, deformation results in broken or bent muscovite grains around more resistant detrital grains (Figure 26). In intercalated sandstone and shale sequences, the micas show few compactional effects, probably due to their greater abundance, larger size and much finer-grained quartz and feldspar fragments. Crystallization of pyrite rhombs and carbonate cement occasionally split muscovite laths along prominant cleavage planes (Figure 27). Petrographic evidence suggests that kaolinite is a common alteration product of muscovite. Reinholtz (1982) and Woody (1983) also observed this relationship within the Cherokee Group sandstones.

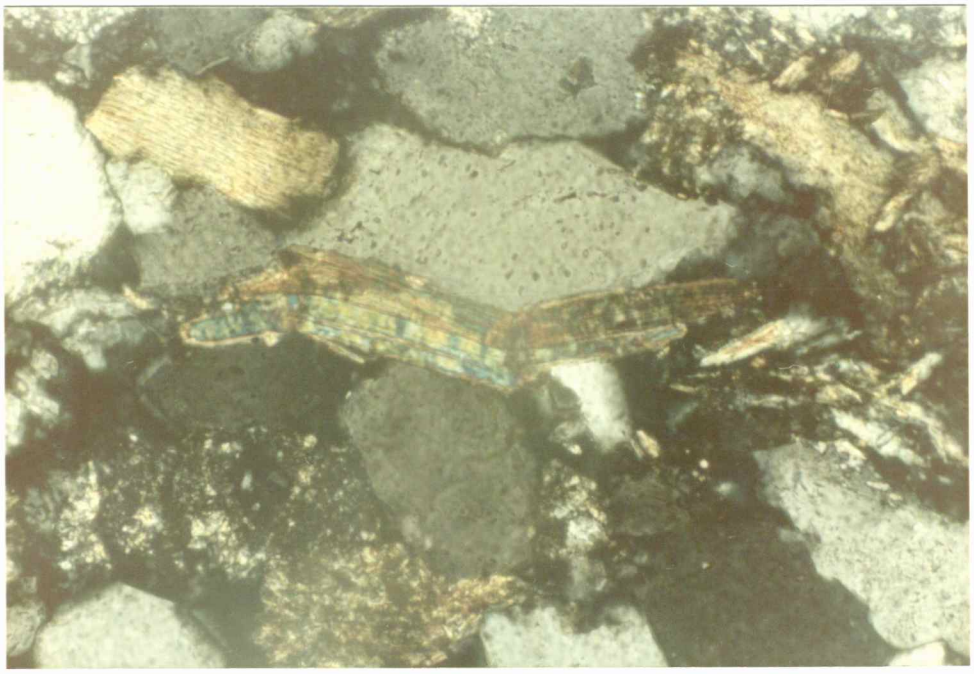

Figure 26. Photomicrograph of muscovite deformation in coarser-grained sandstone. Muscovite grain is bent and broken around more resistant detrital grains. Cross-polarized light. Sample LB-3 966.8. Bar scale equals 0.1mm.

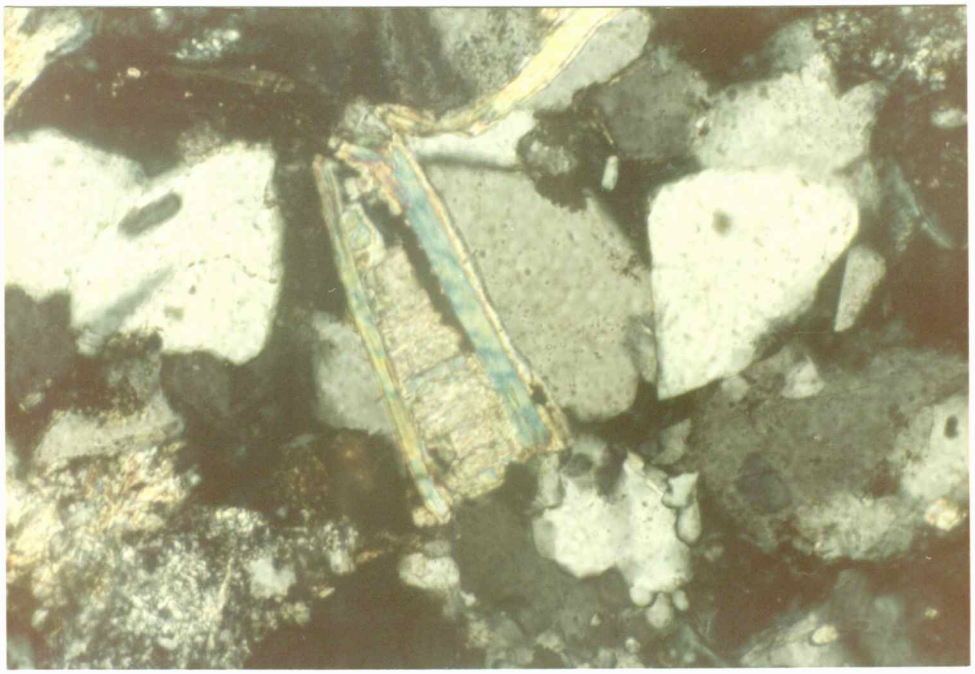

Figure 27. Photomicrograph of muscovite grain split by Fe-calcite cement. Cross-polarized light. Sample LM-8-948.9. Bar scale equals 0.1mm.

Biotite

Biotite occurs in trace amounts in the "Lower Squirrel" sandstone, and recognized as euhedral, strongly pleochroic green to reddish-brown laths 0.12 to 0.31 mm in diameter. Alteration to hematite resulting from the oxidation of iron in biotite is common.

Organic Matter

Organic matter occurs as dark reddish-brown to black material within pore spaces and along laminar planes (Figure 28). The organic matter probably represents resistant waxes and lignins left after decay of organic material that was deposited rapidly in the absence of bacteria (Folk, 1974). Samples that were not thoroughly cleaned using the soxhlet extraction process contain trapped hydrocarbons or "dead oil" that partially fill pore spaces. Pyrite and hematite are commonly associated with organic material.

Heavy Minerals

Trace amounts of heavy minerals, including zircon and tourmaline, were regularly encountered, ranging from .05 to .09 mm in maximum diameter. Burggraf et al (1981) described heavy minerals in Cherokee Group sandstones in Iowa, including magnetite, zircon, tourmaline, garnet, ilmenite, chloritoid, rutile, sphene, leucoxene and iron oxides.

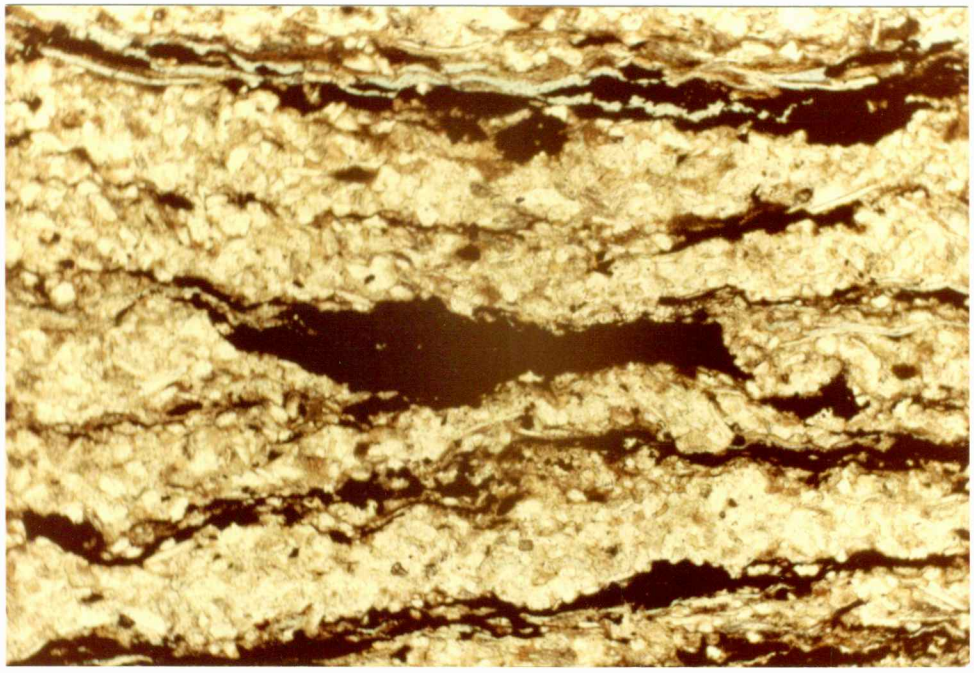

Figure 28. Photomicrograph of organic matter within pore space and along bedding planes. Plane light. Sample LB-3 968.5. Bar scale equals 0.1mm.

Authigenic Components

Quartz Overgrowths

Silica overgrowths on quartz grains are the most common and widespread cementing agent of the "Lower Squirrel" sandstone. Quartz overgrowths are easily recognized as euhedral crystal faces that extend into open pore spaces, and as interlocking crystals forming a quartzite-like mosaic (Figure 20). However, the amount of silica cement was difficult to determine because few early clay rims were visible, and the fine-grained nature of the sandstone prevented good resolution with the cathodoluminoscope. Irregular grain boundaries formed by interlocking quartz crystals are the result of two or more separate overgrowths precipitating in the same pore space. Euhedral overgrowths are typical of coarser-grained sandstones, and finer-grained sandstones are characterized by patchy, interlocking quartz overgrowths.

Clays

Authigenic kaolinite in the "Lower Squirrel" sandstone usually occurs as stacked pseudohexagonal booklets, contributing up to 7 percent of the bulk composition (Table 1). In thin-section, kaolinite is recognized as low-birefringent, pore-filling clusters of stacked booklets (Figure 29). SEM examinations reveal large vermicular

booklets of kaolinite within pore spaces (Figure 30). Individual crystal diameters range from 8 to 10 microns, creating secondary ineffective microporosity between individual platelets and stacked booklets.

Minor amounts of authigenic illite were observed using the SEM (Figure 31). Aden (1982) found detrital illite to be the most abundant clay within the shales of the "Lagonda" interval along the outcrop belt.

Sericite is a common alteration product of feldspar. Replacement by the impure, K-deficient mica usually occurs along cleavage planes and grain boundaries.

Fe-Calcite

Fe-calcite is a common but irregularly distributed cementing agent of the "Lower Squirrel" sandstone, occurring as poikilotopic cement surrounding one or more detrital grains and as patchy, irregular pore-filling cement (Figure 32). Feldspar grains are often partially or almost totally replaced by Fe-calcite. Quartz grain boundaries are occasionally etched, and muscovite laths are commonly split along prominant cleavage planes by Fe-calcite crystals (Figure 32).

Pyrite

Pyrite is the most common opaque mineral in the "Lower Squirrel" sandstone, occurring as small, irregular cubes and

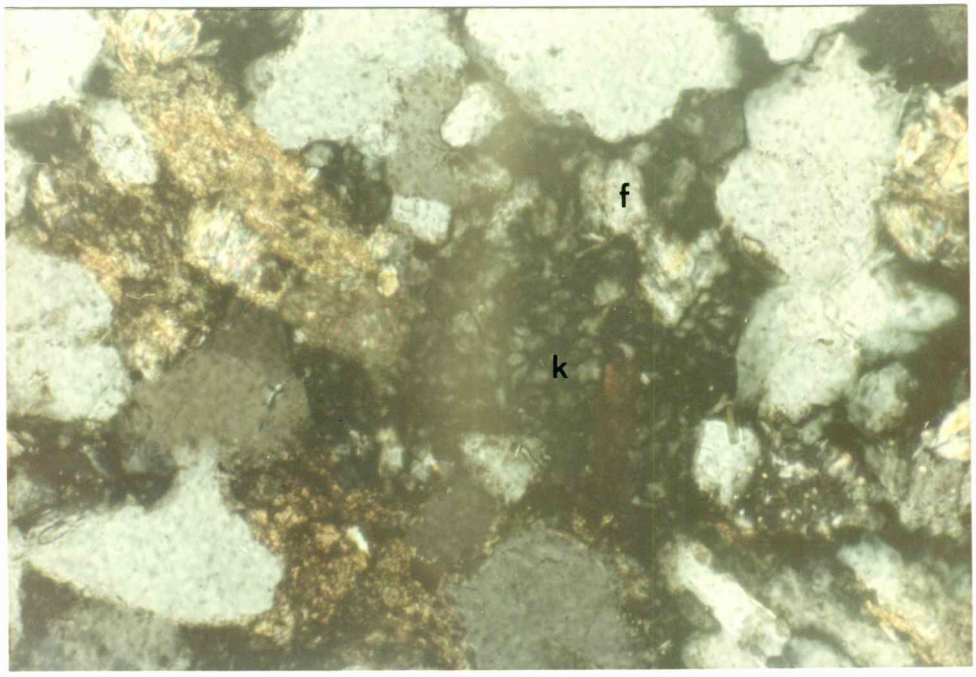

Figure 29. Photomicrograph of pore-filling authigenic kaolinite. Note extensively dissolved feldspar grains (f) in association with kaolinite clusters (k). Cross-polarized light. Sample LB-3 966.8. Bar scale equals 0.1mm.

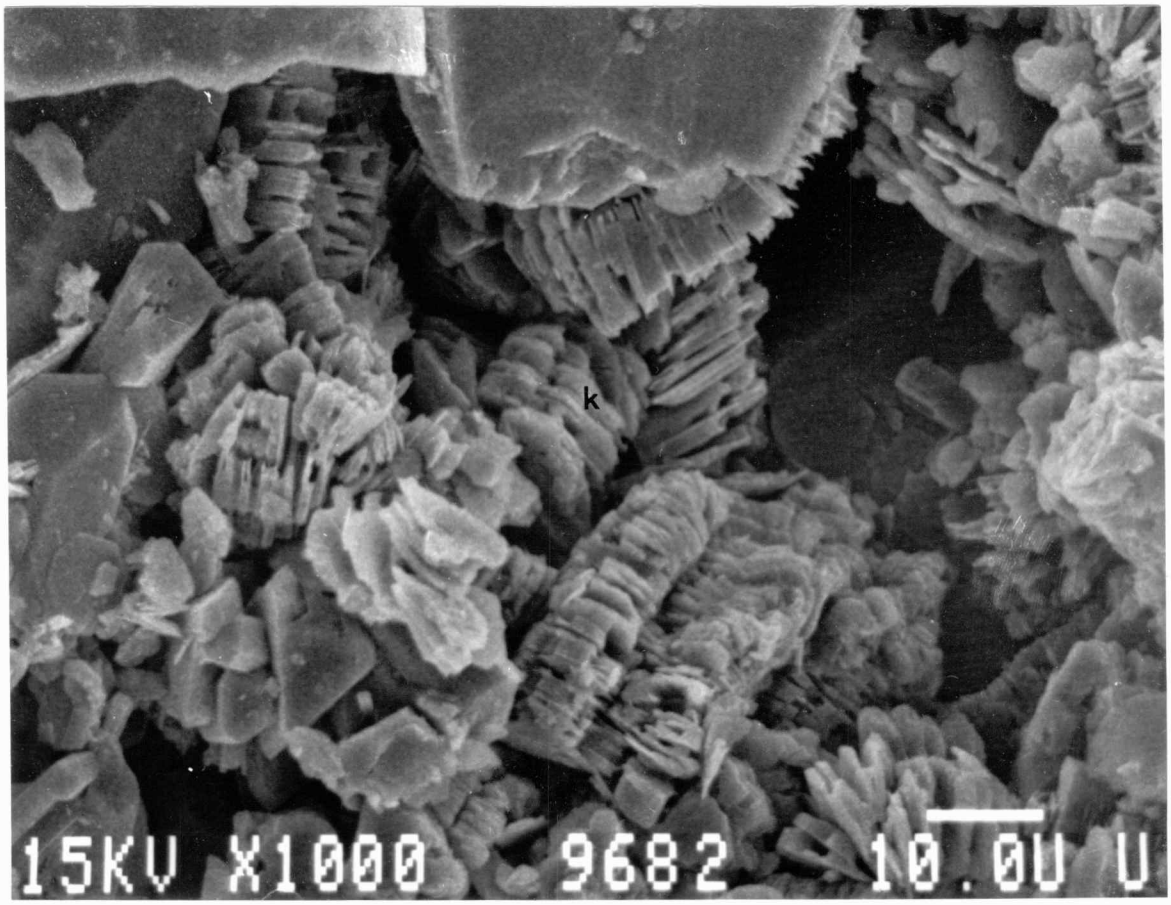

Figure 30. Scanning electron micrograph showing stacked vermicular booklets of authigenic kaolinite clogging pore spaces. Well-developed pseudohexagonal crystals of authigenic kaolinite are typically 10 microns in diameter. Sample KB-1-968.2. Bar scale equals 10 microns.

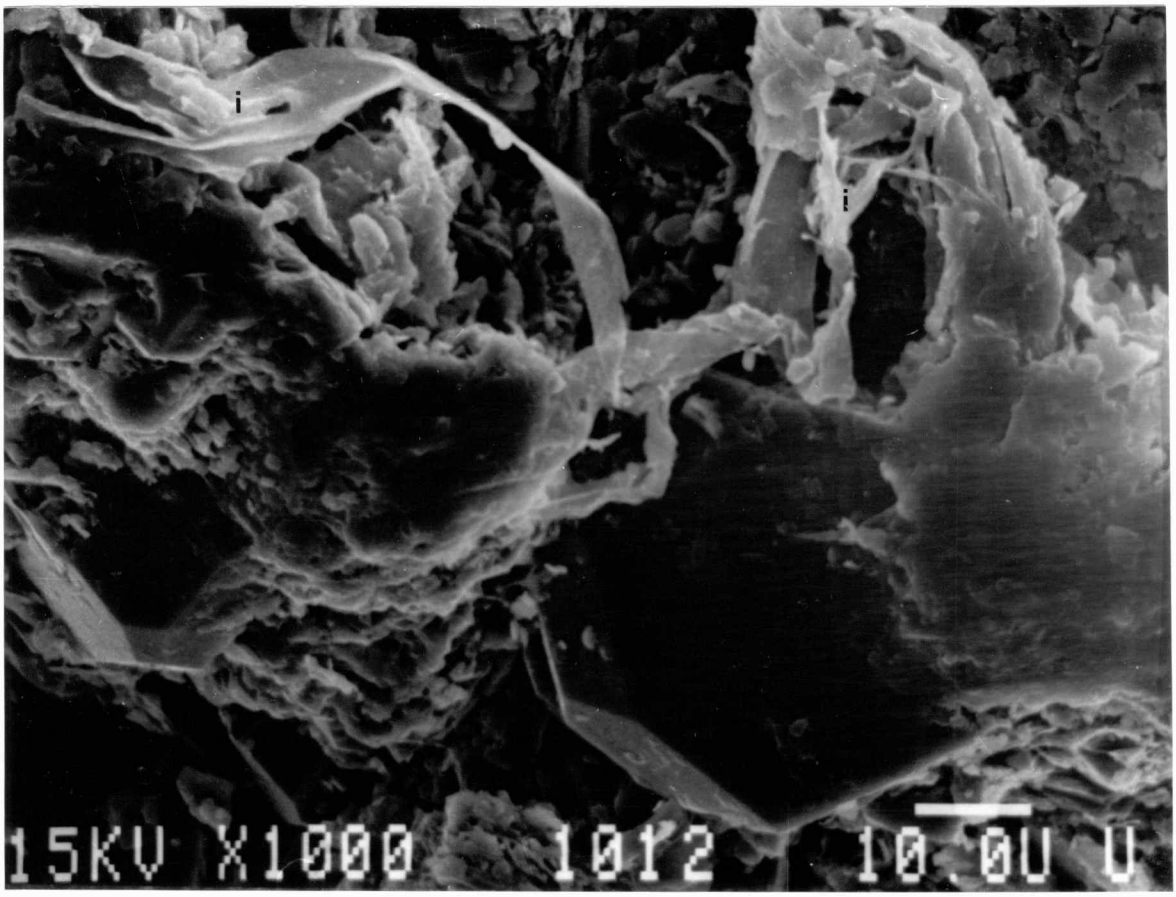

Figure 31. Scanning electron micrograph of authigenic illite. Note delicate crystal morphology. Sample LR-4-1012.7. Bar scale equals 10 microns.

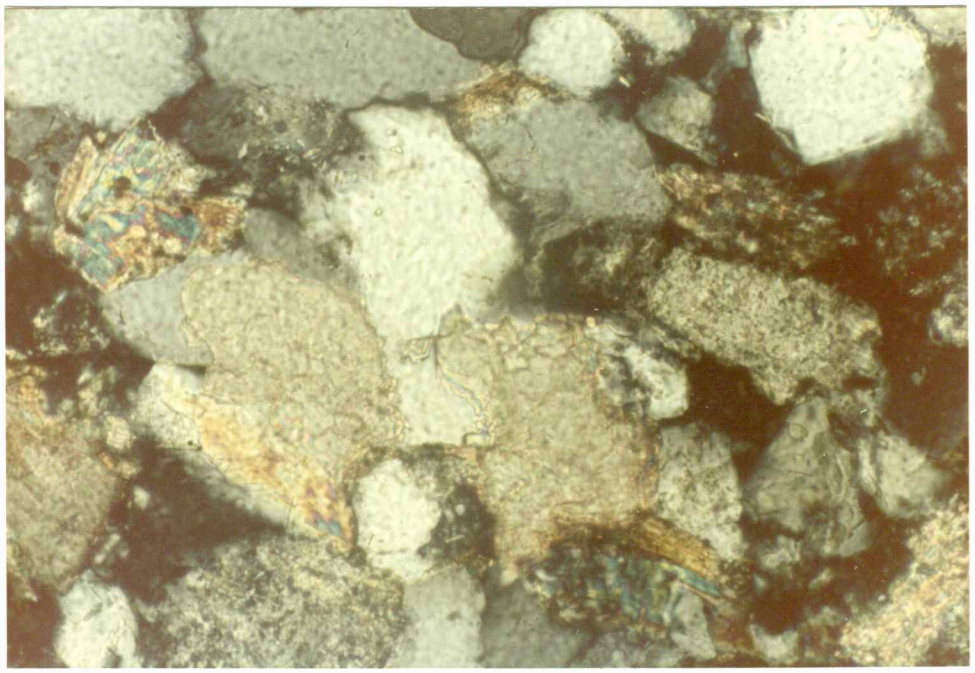

Figure 32. Photomicrograph of patchy, irregularly distributed Fe-calcite cement etching and replacing detrital grains. Cross-polarized light. Sample LB-3 967.8. Bar scale equals 0.1mm.

clusters of crystals within the clay matrix. When abundant, pyrite clusters appear to be aligned parallel to stratification (Figure 33), probably as replacement of organic fragments.

Fossiliferous Calcite-Cemented Sandstone

The sandstone of lithofacies D can be recognized macroscopically in cores as a thin (1 to 2 feet thick), white to grey, fossil-bearing, carbonate-cemented unit with an abrupt, erosional lower contact (Figure 34), and a gradational or abrupt upper contact. Where the sandstone is well developed, the unit consists of moderately well sorted, medium-grained quartz and feldspar grains and numerous broken and disarticulated marine fossil fragments, including brachiopods, echinoderms and foraminifers (Table 2) (Figure 35). The unit is pervasively cemented by Fe-calcite. A marked decrease in the amount of mica, carbonaceous plant detritus, and fine silt, and presence of marine fossil fragments suggests the unit is compositionally and sedimentologically different than previously described sandstone units (lithofacies B and C). Where lithofacies B sandstone is not well developed, the unit consists of a fossiliferous sandstone with numerous irregular dark grey shale laminae and silt (Figure 36). The gamma-ray-neutron log responses to this lithology have abrupt and thin curve

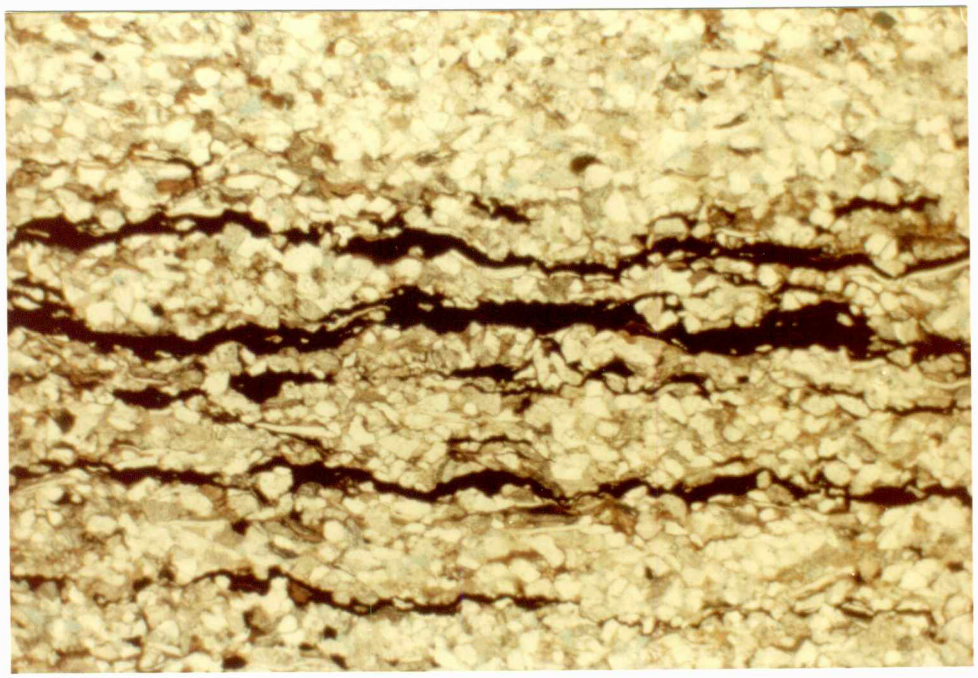

Figure 33. Photomicrograph showing pyrite rhombs and clusters aligned parallel to stratification. Pyrite probably occurs as replacement of organic matter. Plane light. Sample LB-3 958.3. Bar scale equals 0.1mm.

shapes, with a low gamma count and little or no neutron porosity (Type C log) (Figure 9).

Detrital Components

Monocrystalline Quartz

Monocrystalline quartz is the most common siliciclastic mineral in the sandstone, ranging from 19 to 42 percent of the bulk rock (Table 2). Quartz sand grains are medium- to fine-grained, subangular to subrounded with moderate sphericity, ranging from 0.1 mm to 0.34 mm in maximum diameter. Most quartz grains display slightly undulose extinction, but up to 7 percent of the monocrystalline quartz grains show strongly undulose extinction. Quartz grain surfaces are commonly etched and replaced by Fe-calcite cement.

Polycrystalline Quartz

Most polycrystalline quartz grains are characterized by straight and sutured borders between interlocking equant quartz subcrystals, and are subrounded and moderately spherical, ranging from 0.7 mm to 0.25 mm in maximum diameter. Alteration of polycrystalline quartz includes etching and replacement along individual subcrystal contacts and along grain boundaries by Fe-calcite cement.

Table 2

Modal analyses of selected thin-sections from lithofacies D sandstone based on counts of 225 points.

Well Name	Kanaco Badger 1			
Sample No.	KB-1 955.4	KB-1 955.9	KB-1 956.7	KB-1 957.3
DETRITAL				
Quartz				
Monocrystalline	(77) 34%	(84) 37%	(81) 36%	(84) 38%
Polycrystalline	(13) 6%	(10) 5%	(6) 3%	(5) 2%
Feldspar				
Potassium	(20) 9%	(15) 7%	(38) 18%	(24) 11%
Plagioclase	(6) 3%	(7) 3%	(4) 2%	(4) 2%
Mica				
Muscovite	(2) 1%	(1) Tr	(1) Tr	(4) 2%
Biotite	(1) Tr	0	0	(1) Tr
Rock Fragments				
Shale	0	0	0	0
Quartz-Mica	0	(2) 1%	0	(3) 2%
Fossils				
Brachiopods	(16) 7%	(18) 8%	(14) 6%	(24) 11%
Echinoderms	(12) 5%	(16) 7%	(6) 3%	(37) 17%
Foraminifers	(4) 2%	(3) 1%	0	
Organic Material	0	0	0	0
AUTHIGENIC				
Carbonate				
Fe-calcite	(71) 32%	(40) 19%	(19) 8%	(4) 2%
Clays				
Kaolinite	0	(4) 2%	(3) 1%	(1) Tr
Sericite	0	(2) 1%	(7) 3%	(11) 5%
Chlorite	0	(3) 1%	(2) 1%	(1) Tr
Silica	(1) Tr	(3) 1%	(3) 1%	(2) 1%
Pyrite	(1) Tr	(2) 1%	(1) Tr	(3) 1%
Gypsum	0	0	(9) 4%	0
Fe-oxide	(2) 1%	(3) 1%	(2) 1%	(2) 1%
POROSITY				
Primary	0	(3) 1%	(7) 3%	(2) 1%
Secondary	0	(8) 4%	(22) 10%	(11) 5%

Table 2--continued

Well Name	Lincoln Parmely 6	Lincoln Webb 4
Sample No.	LP-6 976.4	LWB-4 941.3
DETRITAL		
Quartz		
Monocrystalline	(40) 18%	(87) 39%
Polycrystalline	(3) 3%	(6) 3%
Feldspar		
Potassium	(7) 3%	(12) 5%
Plagioclase	0	(2) 1%
Mica		
Muscovite	0	(1) Tr
Biotite	0	0
Rock Fragments		
Shale	(5) 2%	(7) 3%
Quartz-Mica	0	0
Fossils		
Brachiopods	(63) 28%	(15) 7%
Echinoderms	(36) 16%	(23) 10%
Foraminifers	(2) 1%	0
Organic Material	0	0
AUTHIGENIC		
Carbonate		
Fe-calcite	(55) 24%	(49) 22%
Clays		
Kaolinite	(1) Tr	0
Sericite	(2) 1%	(4) 2%
Chlorite	0	(2) 1%
Silica	0	(1) Tr
Pyrite	(1) Tr	(6) 3%
Gypsum	(10) 5%	(7) 3%
Fe-oxide	0	(3) 1%
POROSITY		
Primary	0	0
Secondary	0	0
TOTAL	(225) 100%	(225) 100%

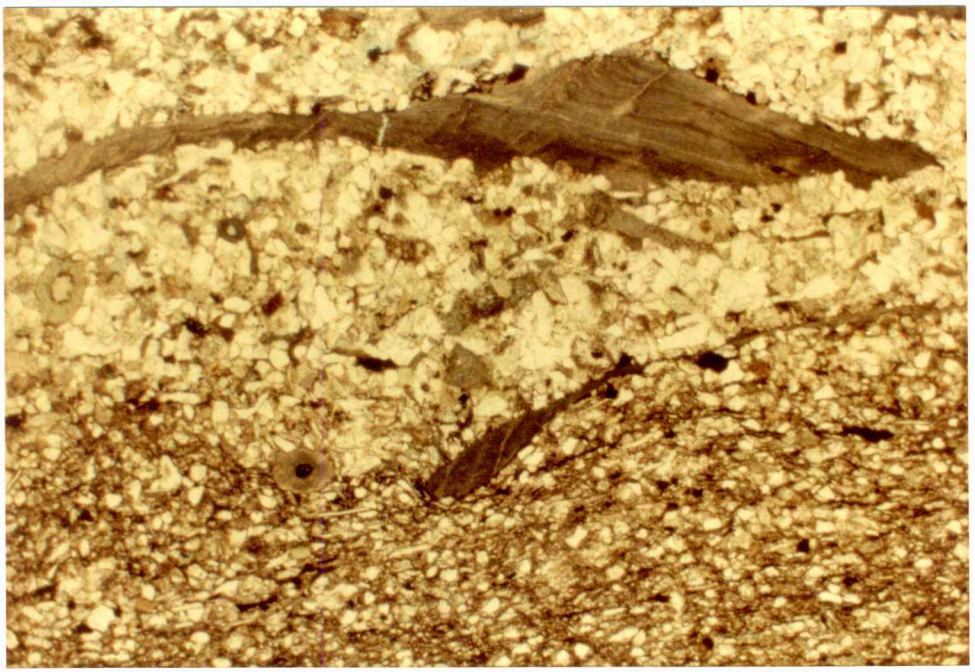

Figure 34. Photomicrograph of erosional lower contact between finer-grained lithofacies C (below), and coarser-grained lithofacies D (above). Plane light. Sample KB-1-957.4. Bar scale equals 1.0mm

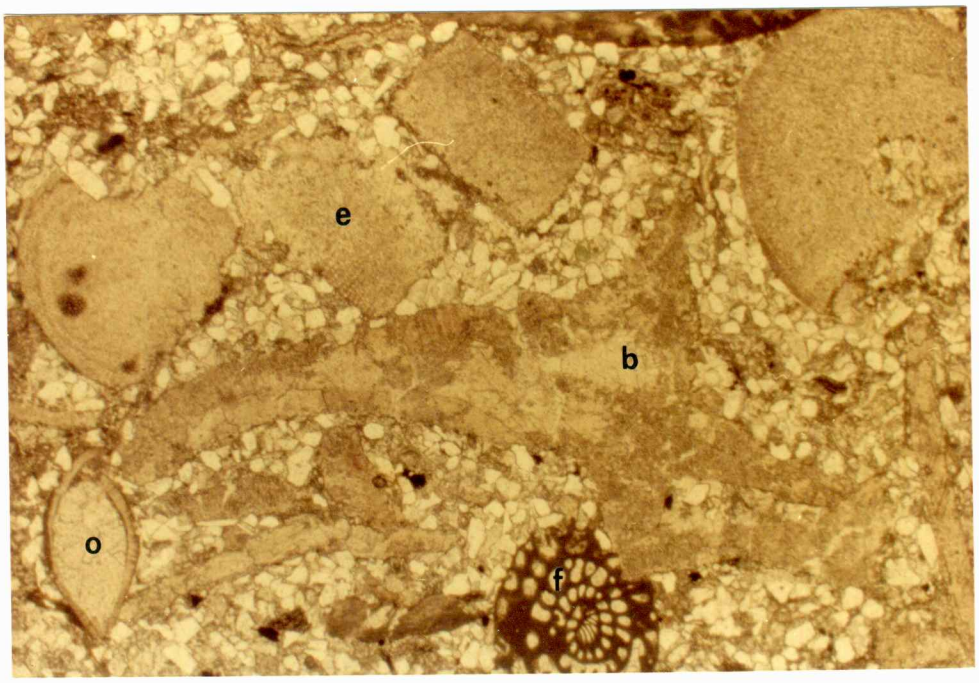

Figure 35. Photomicrograph of numerous broken and disarticulated marine fossils. Fossils include brachiopods (b), echinoderms (e), ostrocods (o),and foraminifers (f). Plane light. Sample LP-6-976.4. Bar scale equals 1.0mm.

Figure 36. Photograph of fossiliferous sandstone interstratified with dark-grey shale laminae. Sample LG-8-1101.7.

Feldspar

Potassium feldspar is the most abundant feldspar in fossiliferous, calcite-cemented sandstone units. Feldspar grains are generally medium- to fine-grained, subangular to subrounded, ranging from 0.17 to 0.26 mm in diameter, and make up from 1 to 21 percent of the bulk rock. Fe-calcite cement partially to extensively replaces feldspar grains along cleavage planes and grain boundaries (Figure 37). Partial feldspar dissolution creates minor amounts of secondary porosity (Figure 38). Plagioclase feldspar occurs in minor amounts.

Fossils

Abundant and diverse marine fossil fragments, including brachiopods (impunctate, pseudopunctate and Composita), echinoderms (crinoids), and foraminifers (fusulinids, encrusters, and Endothyra), characterize this sandstone, constituting up to 47 percent of the bulk rock (Table 2). Fossil fragments are generally broken and disarticulated, ranging from 0.1 mm to 1.3 cm in maximum diameter. Occasionally, partial dissolution of high-Mg calcite echinoderm fragments creates effective secondary macroporosity (Figure 39). Poikilotopic gypsum cement is often associated with fossil fragments, filling voids within brachiopod shells and enveloping siliciclastic grains. Rare

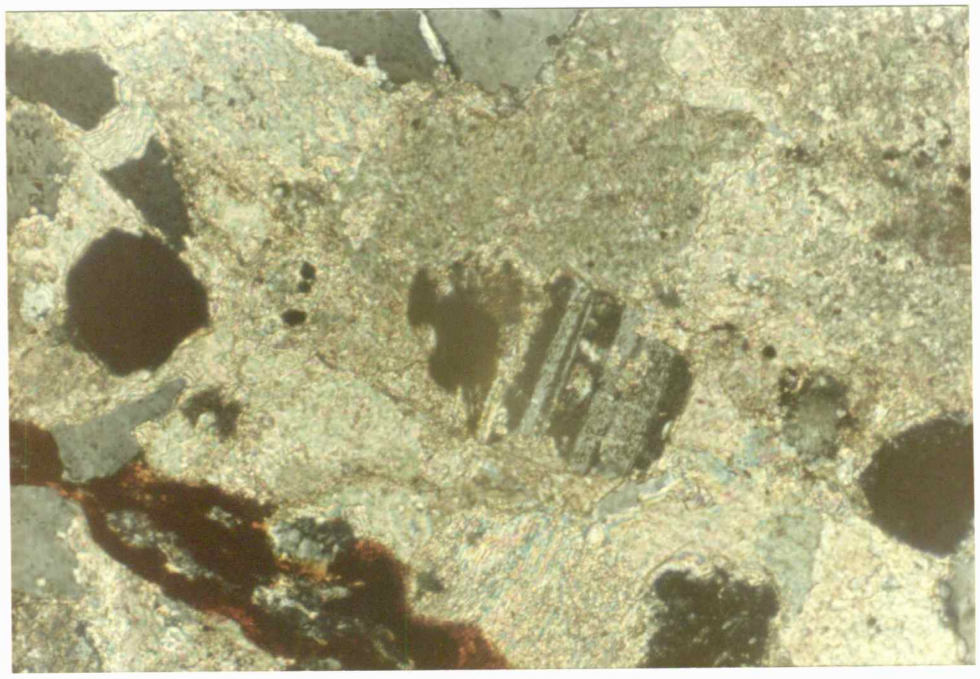

Figure 37. Photomicrograph of feldspar grain partially replaced by Fe-calcite. Cross-polarized light. Sample KB-1 955.9. Bar scale equals 0.1mm.

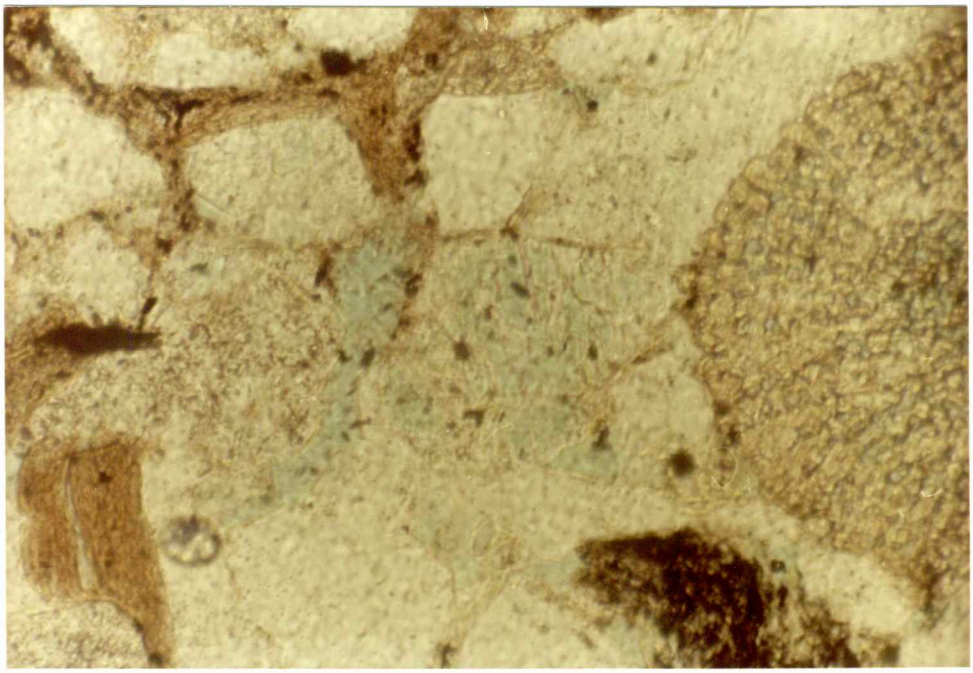

Figure 38. Photomicrograph of feldspar dissolution in Lithofacies D. Feldspar dissolution creates minor amounts of secondary porosity. Plane light. Sample KB-1 956.7. Bar scale equals 0.1mm.

phosphate nodules (Figure 40), phosphatized echinoderm fragments and pyritized shell fragments were observed. Hematite is a common alteration product of high-Mg calcite echinoderm fragments.

Muscovite

Muscovite is a minor detrital constituent of the fossiliferous, calcite-cemented sandstone, occurring in trace amounts to 2 percent of the bulk rock. Muscovite occurs as colorless euhedral to subhedral laths, ranging from 0.13 to 1.2 mm in maximum diameter. The mica laths show little or no alteration and are commonly bent or broken around more resistant siliciclastic grains. Fe-calcite cement occasionally splits muscovite laths along prominent cleavage planes.

Authigenic Components

Quartz Overgrowths

Silica overgrowths on detrital quartz grains are a consistant but minor cementing agent of lithofacies D sandstone. Quartz overgrowths are recognized as euhedral crystal faces that extend into the poikilotopic calcite cement. Occasionally, euhedral quartz crystal faces are etched and replaced by calcite cement.

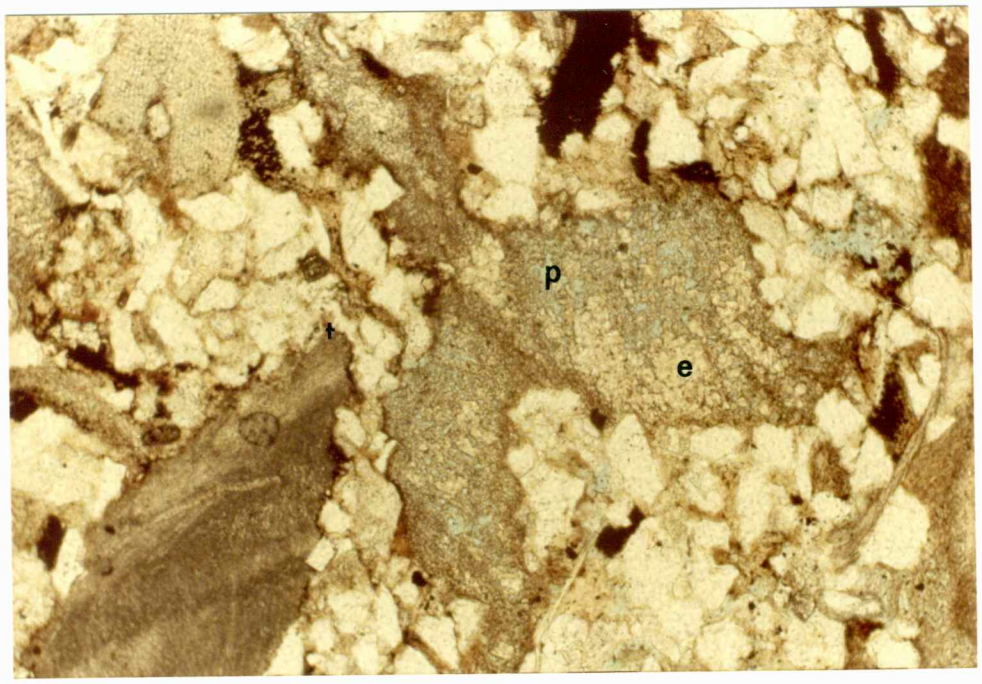

Figure 39. Photomicrograph showing partial dissolution of high-Mg calcite echinoderm fragments (e), creating secondary porosity (p). Note the unaltered low-Mg calcite brachiopod fragment (b). Plane light. Sample KB-1 957.3. Bar scale equals 0.1mm.

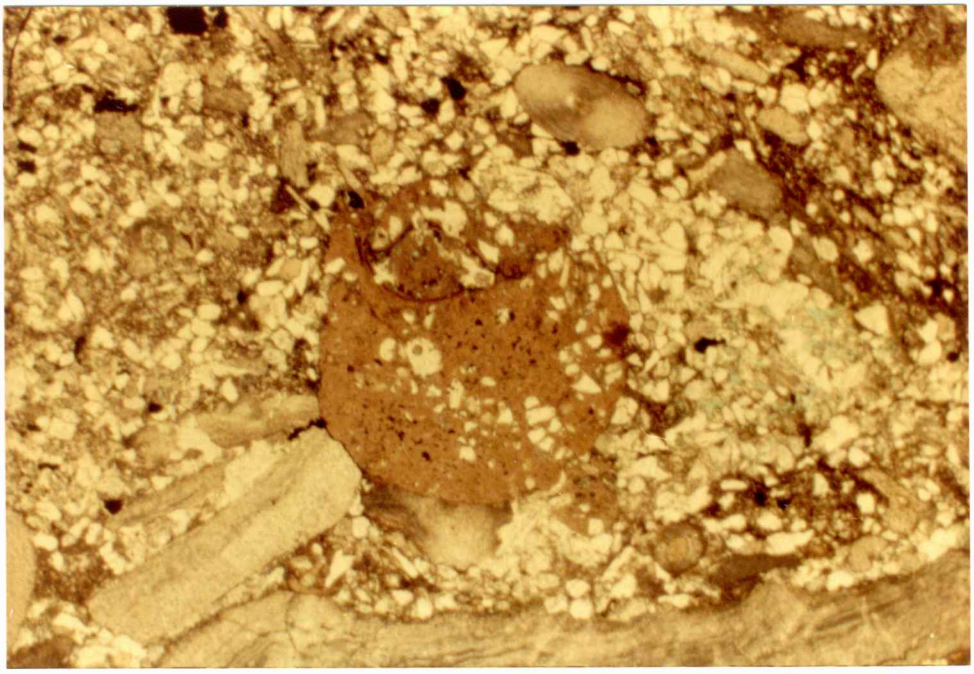

Figure 40. Photomicrograph of phosphate nodule. Note numerous siliciclastic grains and whole fossil incorporated within the nodule. Plane light. Sample LM-8-941.9. Bar scale equals 0.1mm.

Fe-Calcite

Fe-calcite is the principle cementing agent of the lithofacies D sandstone, occurring as poikilotopic, pore-filling spar cement surrounding one or more detrital grains (Figure 41) and forming up to 40 percent of the bulk rock (Table 2). Fe-calcite partially to extensively replaces feldspar grains and to a lesser extent, etches and replaces quartz grain surfaces. Siliciclastic grains often appear to be "floating" in poikilotopic Fe-calcite cement. Generally, Fe-calcite cement reduces primary porosity to only trace amounts.

Pyrite

Pyrite and hematite are ubiquitous minor constituents of the sandstone and are closely associated with organic material, particularly echinoderm fragments and macerated plant fragments. Pyrite typically occurs as small, isolated cubic crystals or clusters of crystals within the calcite cement.

Gypsum

Gypsum occurs as poikilotopic cement and is commonly associated with brachiopod and echinoderm fragments, filling interstitial pore space and voids within the fossils of lithofacies D (Figure 42). Gypsum also occurs as bladed, single cyrstal cement.

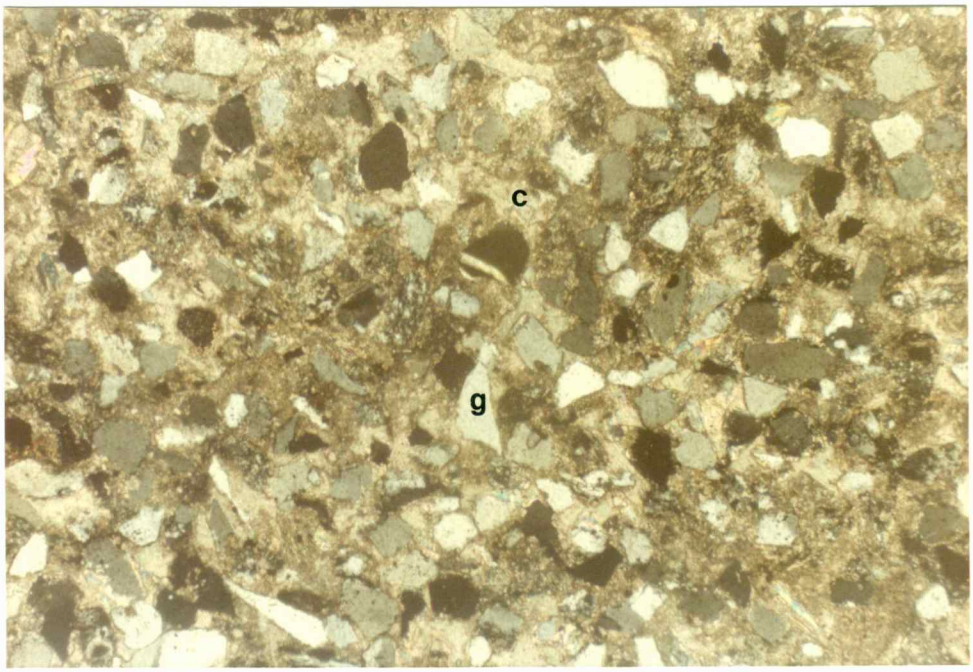

Figure 41. Photomicrograph of poikilotopic pore-filling Fe-calcite (c) surrounding detrital grains (g). Porosity and permeability are nearly eliminated by calcite cement. Detrital grains are partially etched and replaced by Fe-calcite. Cross-polarized light. Sample KB-1 955.4. Bar scale equals 0.1mm.

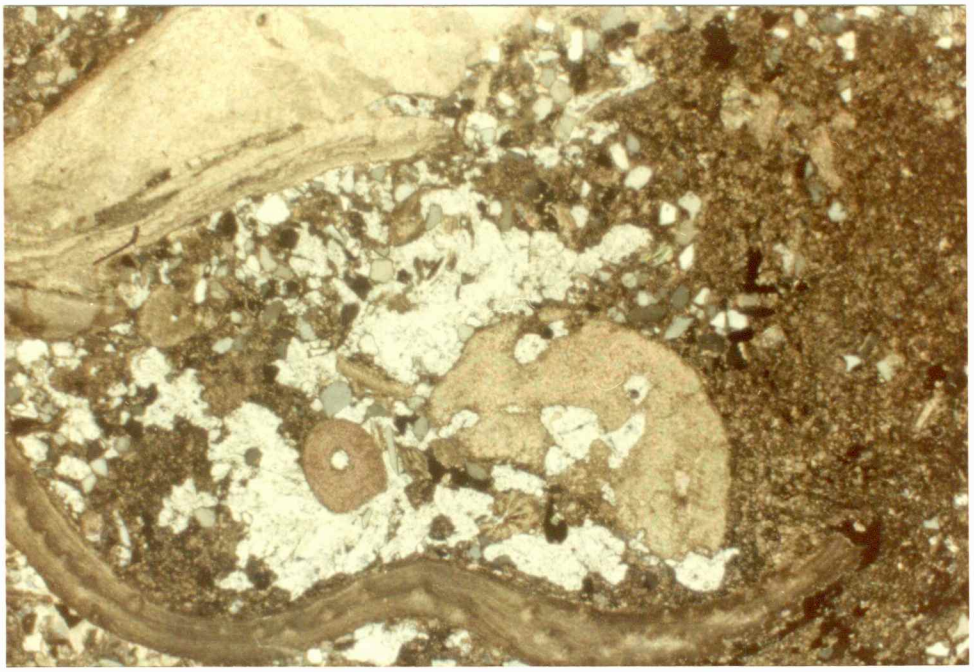

Figure 42. Photomicrograph of poikilotopic gypsum cement (g). Gypsum cement is commonly associated with fossil fragments. Gypsum fills large interstitial pore spaces and voids within fossils. Cross-polarized light. Sample LP-6 976.4. Bas scale equals 1.0mm.

Petrographic Distinction Between Lithofacies B and Lithofacies D

Significant compositional and textural differences between the previously described lithofacies B and D suggest different environmental regimes. Data summarized in tables 1 and 2 indicate that although lithofacies B and D contain similar percentages of detrital quartz and feldspar grains, lithofacies B contains a conspicuously large amount of detrital muscovite fragments (4-13%) that are often aligned parallel to stratification. Authigenic cements in lithofacies B consist primarily of authigenic clays (5-10%) and quartz overgrowths. Pyrite is a locally common authigenic cement, and when abundant, appear to be aligned parallel to bedding, probably as replacement of organic fragments. Significant amounts of primary (10%) and secondary (15%) porosity persist throughout the unit.

Lithofacies D, however, contains abundant and diverse marine fossil fragments (up to 45%), including brachiopods, echinoderms, foraminifers, and ostrocods, and is often pervasively cemented by Fe-calcite, reducing porosity to only trace amounts. Detrital muscovite grains are often absent in thin-section, and when present, do not appear to be aligned with stratification. Lithofacies D is also lower than lithofacies B in authigenic clay and silica cement.

DEPOSITIONAL ENVIRONMENT OF THE "LOWER SQUIRREL" SANDSTONE AND ASSOCIATED FACIES

Interpretation of the "Lower Squirrel" sandstone depositional environments of east-central Kansas was based on 1) sandstone geometry and distribution; 2) lithological interpretation of well-log signatures; and 3) composition, sedimentary structures and depositional sequence of lithofacies from core material.

The succession of lithofacies recognized in cores, and the environmental interpretation of geophysical well-log signatures suggests that the "Lower Squirrel" sandstone and associated facies represent an actively prograding deltaic complex that was abandoned and subsequently buried by thin, shallow marine deposits that were laid down during a period of marine transgression. Principal phases of deposition were 1) submarine progradation of prodelta and delta front sediments; 2) deposition of distributary channel-mouth-bar deposits and crevasse splays; 3) abandonment of the delta and marine destruction of the subsiding lobes, followed by 4) the deposition of thin marine bars composed of reworked broken shells and sand.

Distributary Channel-Mouth-Bar Deposits

The "Lower Squirrel" sandstone distribution map (Figure 11) indicates that the sandstone bodies are narrow and elongate, and laterally discontinuous. Some sandstone bodies bifurcate, with individual sand lobes extending to the west, south and east. The thickest concentration of sand deposits occurs at points where channels bifurcate.

Stratigraphic cross-sections B-B' illustrates the lateral and vertical geometry of the "Lower Squirrel" sandstone. An abrupt thinning of the sandstone occurs directly adjacent to the elongate sandstone bodies (Figure 13), while the sand thickens at the expense of the underlying shale. Stratigraphic cross-section A-A' along depositional strike of the sand body, illustrates the persistent and consistent low-gamma log response to the sandstone. An abrupt basal contact, and an increase in gamma radiation upward, forms a sequence with a characteristic upright bell-shaped curve (Type A log). Cores penetrating the sandstone body show coarser-grained sandstone concentrated near the base of the unit (lithofacies B), fining-upward into a sequence of intercalated, contorted sandstone, siltstone and shale layers containing abundant carbonaceous plant detritus (lithofacies C). In the type well-log (Figure 7), the abrupt, low-gamma deflection at the base of the sandstone

interval relates to a sharp, erosional contact between the underlying intercalated sandstone, siltstone and shale (lithofacies A) and the overlying coarser-grained sandstone (lithofacies B) in some cores from this interval.

In most modern deltas, distributary channels remain straight, as they do not accrete laterally like meandering channels. Distributary channels scour down and become entrenched in the underlying distributary mouth-bar deposits and marine clays (Coleman and Prior, 1982). Consequently, distributary channel-fill sandstone bodies are very narrow and display bifurcating or anastomosing patterns (Brown, 1979). According to Busch (1974), sand-thickening at the expense of the underlying shale is a fundamental criteria for a channel deposit.

Visher and others (1971) suggested that major distributary channels near the base of the Bluejacket delta in Oklahoma show considerable scouring into the underlying prodeltaic sandstone and shale. Coleman and Prior (1982) found that the only common attribute of distributary channel sand deposits is a tendency for any substantial amount of sand to concentrate near the base of the channel and at points where the channel bifurcates (lithofacies B).

The remainder of the channel-fill consists of erratically-bedded sandstone, carbonaceous siltstone and clay layers (lithofacies C), that resulted from rapid

infilling of the channel and extremely high porewater content of the sediments. Visher and others (1971) suggested that lower delta plain distributary channels are often interbedded with thin, commonly bioturbated siltstone and shales. In modern deltas, intercalated sands, silts and shales are often convoluted and burrowed (Coleman and Prior, 1982).

Gamma-ray logs have been shown to correlate directly with increasing or decreasing grain-size profiles of siliciclastic sequences due to variations in radioactive-clay contents (Galloway, 1968; Selley, 1976). Studies of modern depositional systems have shown that characteristic grain-size profiles reflect depositional patterns (Selley, 1976; Coleman and Prior, 1982). According to Selley, the presence or absence of carbonaceous detritus is dependent upon the amount of sediment reworked. In high energy, turbulent environments (i.e., shoals and beaches), plant material is abraded, oxidized and rarely preserved. However, in environments characterized by rapid deposition (i.e. deltas or submarine fans), carbonaceous detritus is often preserved due to the lack of reworking. Selley (1976) proposed four basic environmental interpretations based on gamma-ray log profile characteristics and the presence or absence of glauconite or carbonaceous detritus (Figure 43). The abundant carbonaceous plant fragments and numerous

muscovite fragments in lithofacies B suggests rapid deposition with little or no reworking.

The elongate and lenticular sandstone geometry, abrupt basal contact, fining-upward sequence indicated by the gamma-ray log profile and the presence of carbonaceous plant detritus suggests the "Lower Squirrel" sand bodies represent deltaic distributary channels and mouth-bar deposits.

Overbank and Bay-Fill Deposits

Between and adjacent to major distributaries, log patterns and cores show interbedded sandstone, siltstone and shale sequences. The type well-log for this facies illustrates the repetitive nature of the stacked sandstone-mudstone sequences (Figure 44). Cores penetrating this sequence show fine-grained, ripple-laminated sandstones with occasional small-scale cross beds grading abruptly into intercalated siltstone and shales that contain numerous macerated plant fragments. This sequence is capped by a fossiliferous, calcite-cemented sandstone with irregular thin laminae of dark grey shale.

Stratigraphic cross-section B-B' illustrates the serrated log pattern, indicating thinly interbedded sandstone, siltstone and shale, directly adjacent to the lenticular sandstone body (Figure 13 , well-log 33-24-15E).

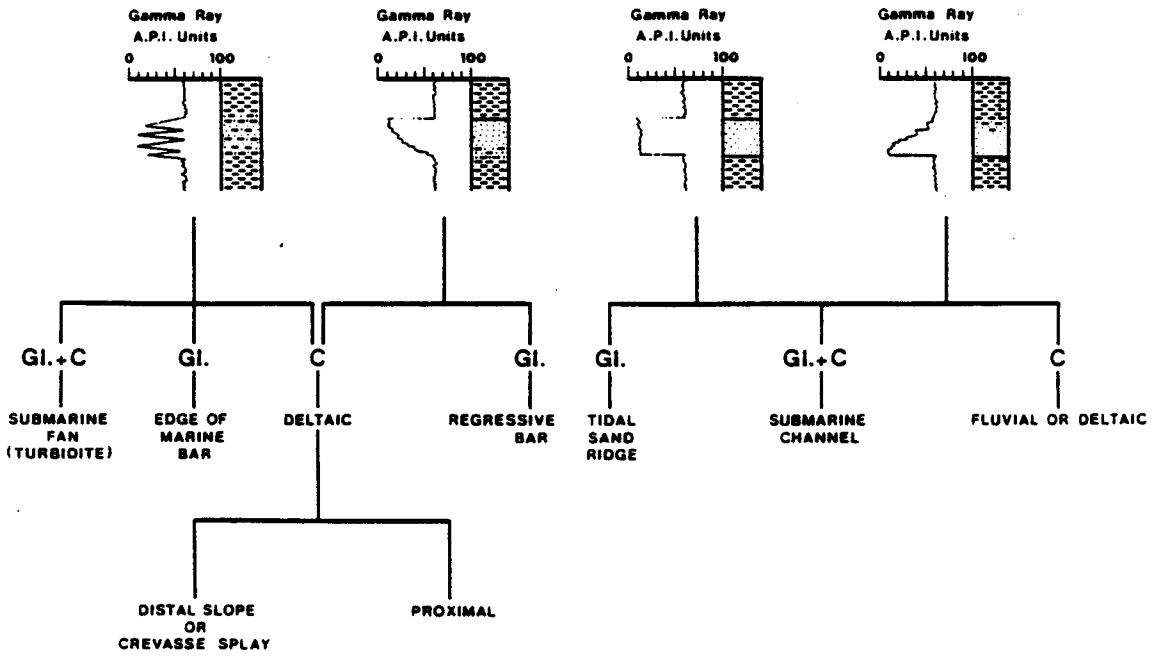

Figure 43. Four characteristic log patterns in clastic sedimentary rocks (after Selley, 1976).

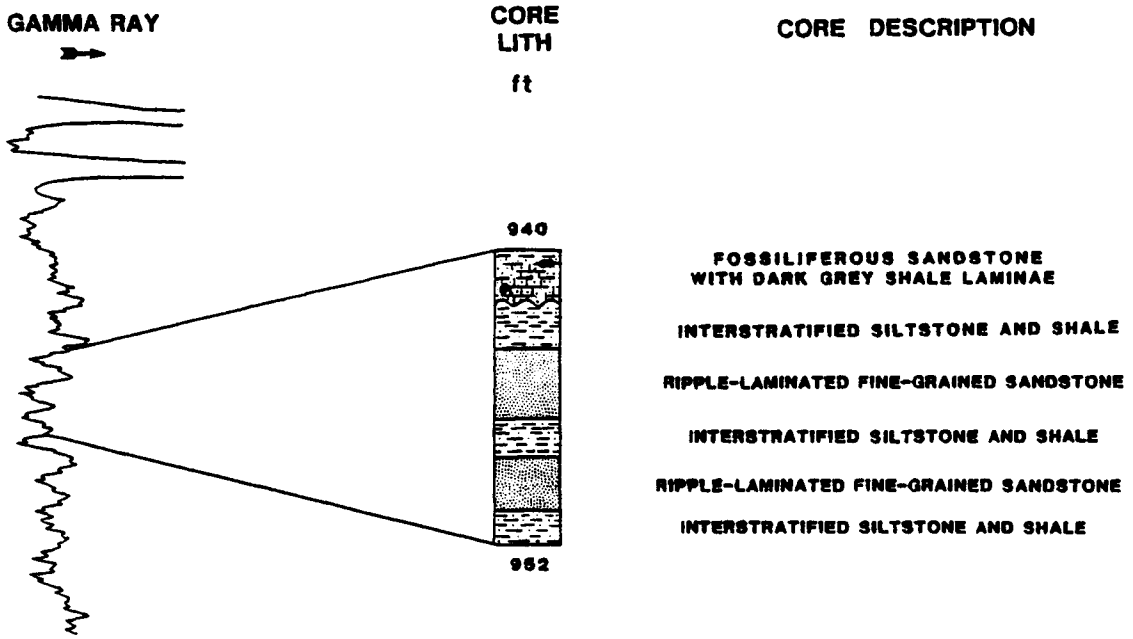

Figure 44. "Type" log pattern of overbank and bay-fill deposits. Sediments consist of interbedded sand and shale units.

Interbedded sandstone, siltstone and mudstones associated with channel sandstone units were identified in a variety of overbank environments in uppermost Pennsylvanian rocks of north-central Texas, including natural levees, floodplains and crevasse-splays (Allen, 1965). Overbank facies are characterized by interbedded finely laminated sandstone, siltstone and mudstone containing diverse types of preserved ripple and planar laminations (Galloway and Brown, 1973).

According to Coleman and Prior (1982), one of the major facies associated with modern deltas are bay-fills and crevasse splays that break through levees along main distributaries and infill the numerous bays within the lower delta-plain. Although individual fills are relatively thin, continued subsidence and repetition of similar processes result in stacking one bay-fill on top of another, eventually building a thick sequence of lower delta-plain deposits (Coleman and Prior, 1982).

The serrated log pattern, indicating interbedded sandstone, siltstone and shale, and the presence of carbonaceous plant detritus suggests deposition in a crevasse-splay environment (Figure 43). The interdistributary sequence is gradational into distributary type sequences. Variations in the thickness of the sandstones are related to the proximity to a distributary.

Transgressive Marine Deposits

A thin unit consisting of a fossiliferous, calcite-cemented marine sandstone is traceable over much of the study area (lithofacies D) (Figure 45), and overlies the distributary channel and associated overbank deposits of lithofacies C (Figure 46). This unit scours down into the underlying intercalated carbonaceous sandstone, siltstone and shale, forming an erosional contact between lithofacies C and lithofacies D (Figure 34). It grades upward into a dark grey fossiliferous shale that contains numerous plant fragments (lithofacies E).

The abundance of broken and disarticulated marine shells, absence of detrital muscovite and carbonaceous plant debris, and an erosional lower contact with underlying distributary channel and overbank deposits suggest deposition in a high-energy, turbulent marine environment. The unit is probably associated with marine transgression following the abandonment, subsidence and reworking of delta plain deposits, forming local shelly marine bars and berms above the underlying distributary channel and associated overbank deposits.

Similar Pennsylvanian sandstones in the Mid-Continent have been interpreted as marine shoals that were formed during the destruction of subsiding, inactive delta lobes. These shoals formed thin, shallow-water barrier-bars,

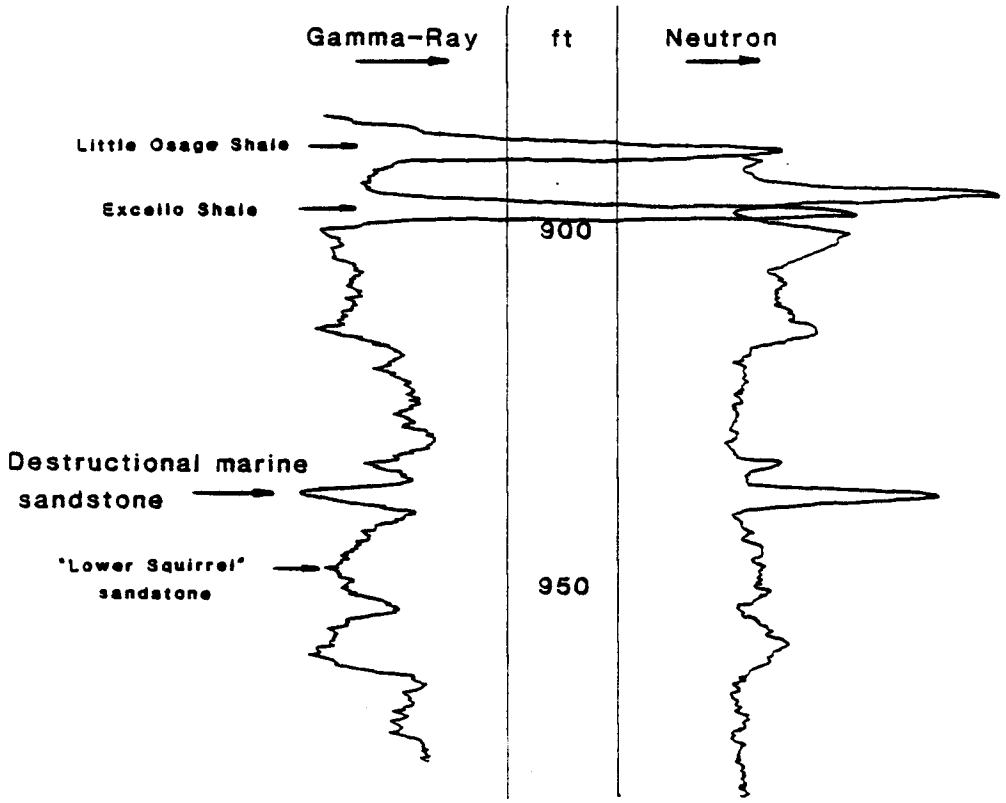

Figure 45. "Type well-log of transgressive marine sandstone unit (Lithofacies D) overlying "Lower Squirrel" sandstone. Neutron log indicates little or no porosity.

Figure 46. Sandstone distribution map of Lithofacies D. Contour interval equals 2 feet.

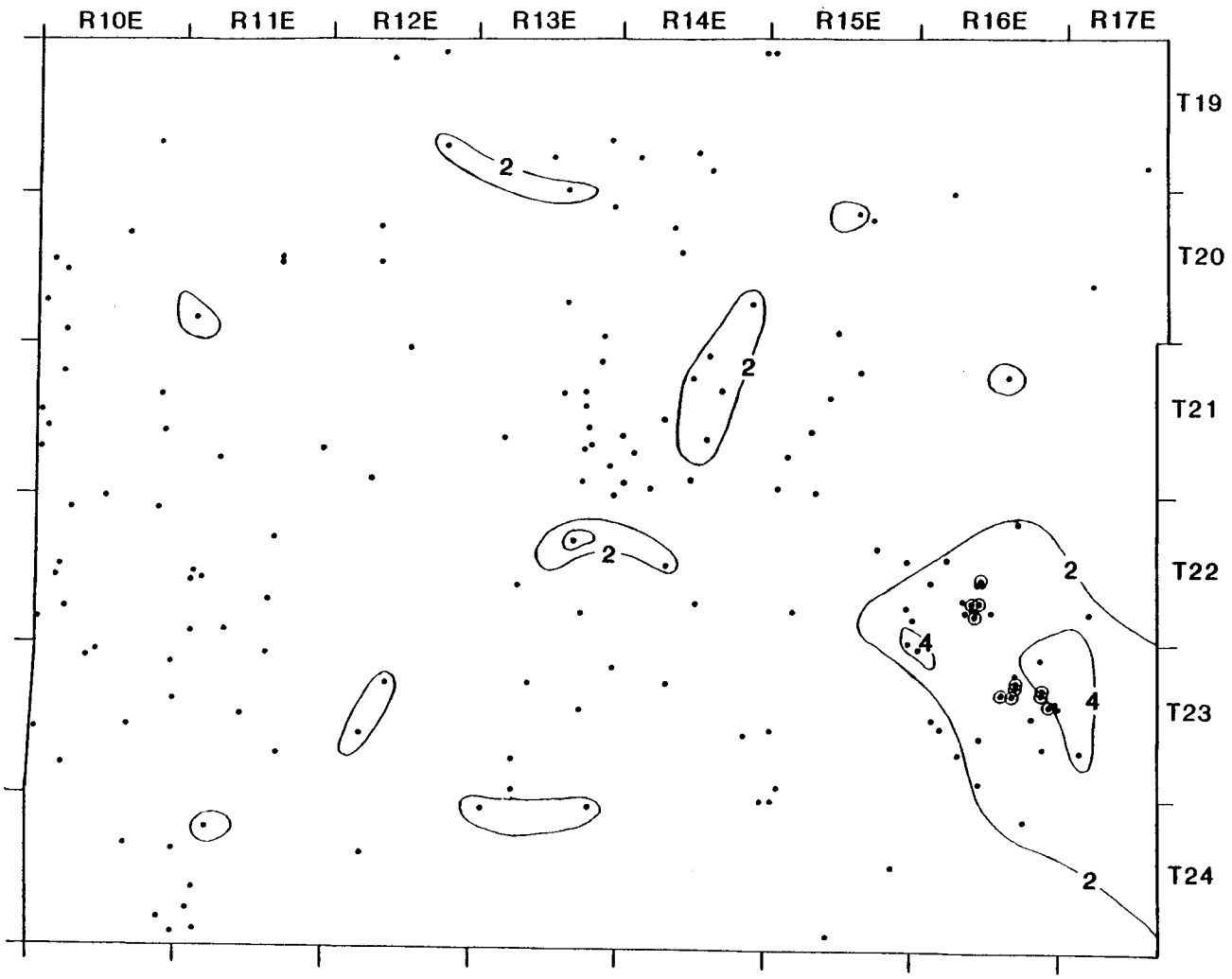
R10E
R11E
R12E
R13E
R14E
R15E
R16E
R17E
T19
T20
T21
T22
T23
T24
2
2
2
2
4
4

littoral sheet sandstones and shoal-water limestones, and generally consist of thin, coarsening-upward sequences with local lenses composed of broken marine shells (Brown, 1979). Visher and others (1971) observed that much of the Bluejacket delta complex in Oklahoma is covered by a transgressive marine sandstone and limestone unit. Locally, it formed a thicker marine-bar sandstone separated by shale from the lower, more massive sandstone unit. They suggested that the unit was formed by the reworking of natural levee deposits after the abandonment and subsidence of the inactive delta complex.

Inner Shelf-Interdistributary Bay Deposits

The top of the cored sequence consists of dark grey, fossiliferous mudstone with occasional pyritized shells and carbonaceous debris (lithofacies E). The calcareous mudstone has a gradational lower contact with the underlying calcite-cemented sandstone of lithofacies D (Figure 36).

The unit probably represents gradual marine incursion over the subsiding, abandoned deltaic complex, with deposition of bay and shallow-marine muds over the shoal sands. A similar sequence was observed by Shannon and Dahl (1971) in Pennsylvanian (Strawn Group) sandstones in Texas. They concluded that upon abandonment and subsidence of the

deltaic complex, the area was inundated by marine waters that deposited brackish-water bay sediments. Cleaves (1975) interpreted fossiliferous mudstones overlying destructional-reworked delta plain deposits (Strawn Group) to be the result of continued marine transgression and deposition of inner-shelf sediments. Visher and others (1971) noted that marine shales commonly overlie transgressive marine sandstone and limestone units at the top of Bluejacket deltaic sequences in Oklahoma.

Paleogeographic Reconstruction

The presence of thin coals overlying the Verdigris Limestone suggest that peat deposits formed within lowland marshes and swamps along a vegetated coastline of the sea that withdrew after widespread Verdigris deposition. Transgression of the Lagonda Sea resulted in an east to north-east shift of the coastline, inundating the region with marine and transitional deposits. After sea level rise slowed or stopped, delta progradation of sediments formed interbeds of very fine-grained sands, silts and clays in distal delta-front environments and interlobe areas (lithofacies A).

Rapid detrital influx from the source area prompted a period of more active delta progradation. This period is recorded by a marked increase in siliciclastic material from the north to northeast, forming a variety of delta plain

deposits that include distributary channel and mouth-bar, overbank, and interdistributary bay deposits. These facies prodraded southwestward across the study area (Figure 47). The active progradation caused incisement by the "Lower Squirrel" distributary channels into the previously deposited distal delta-front materials. The elongate geometry of the sandstone suggests a low marine-energy, fluvially-dominated delta complex.

Abandonment and subsidence of the delta complex resulted in the formation of local sand highs, possibly produced by differential compaction of sand and mud associated with channel and overbank deposits (Figure 48). Marine transgression and reworking of the local sand highs formed a thin transgressive marine sandstone caprock over the inactive distributary channels and associated overbank deposits.

Further transgression is recorded by suspension deposition of dark grey fossiliferous shale in inner shelf and interdistributary bay environments.

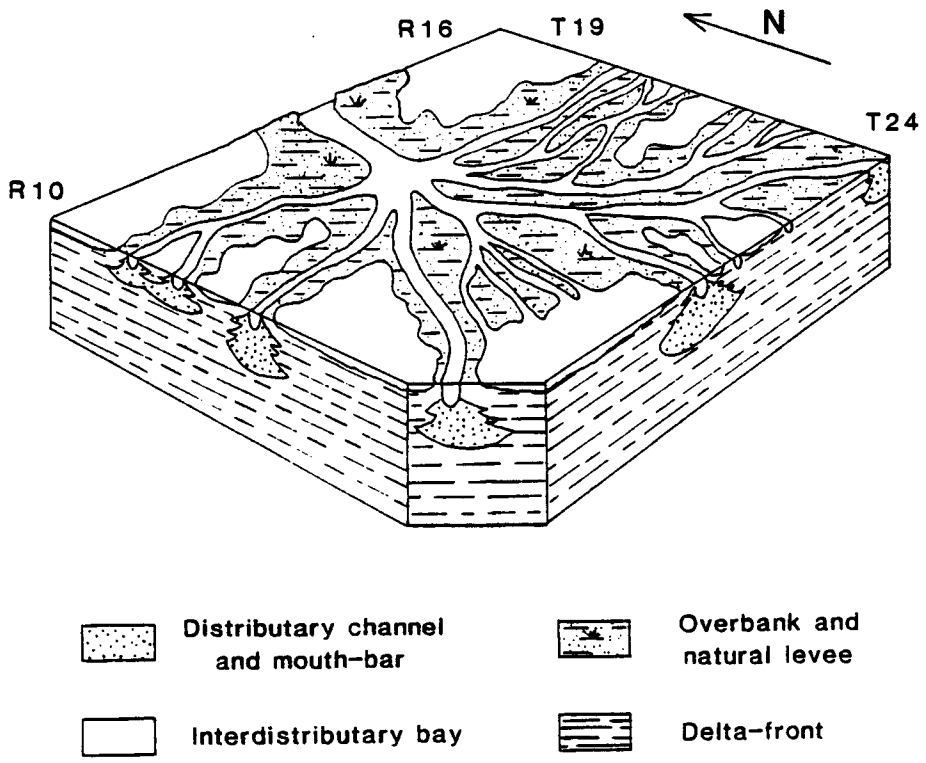

Figure 47. Paleogeographic reconstruction illustrating deposition of the "Lower Squirrel" sandstone. Progradation of detlaic lobes resulted in incisement of distributary channels into previously deposited delta-front materials.

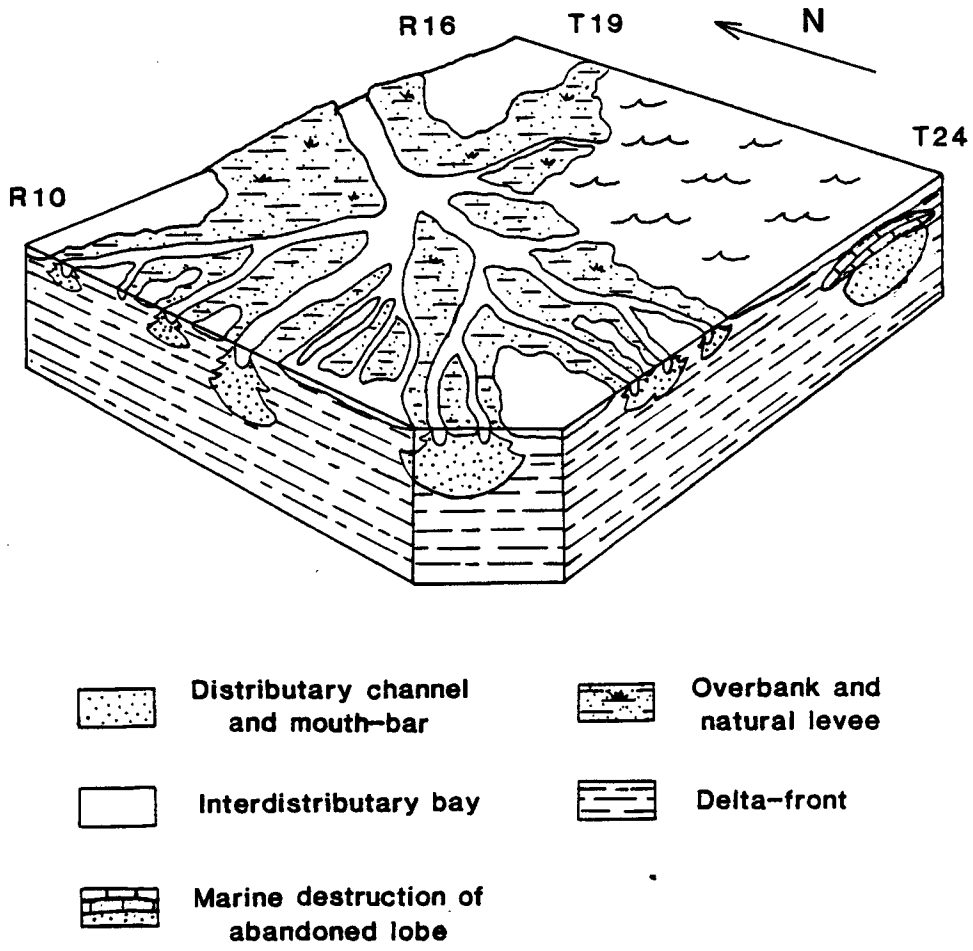

Figure 48. Paleogeographic reconstruction illustrating marine transgression and reworking of local sand highs after delta lobe abandonment in southeastern part of the study area.

DEPOSITIONAL ENVIRONMENT OF THE "UPPER SQUIRREL" SANDSTONE

Interpretation of the "Upper Squirrel" sandstone depositional environment in east-central Kansas was based on: 1) sandstone geometry and distribution; 2) lithological interpretations of well-log signatures; 3) preliminary investigations of the "Lagonda" interval sandstones in northeast Kansas, and southeast Kansas and northeast Oklahoma.

Although cores penetrating the "Upper Squirrel" sandstone were not availiable from the study area, gamma-ray log signatures were used to determine sand thicknesses, and increasing or decreasing grain-size profiles within the siliciclastic sequence. The isolith map of the "Upper Squirrel" sandstone indicates that a thin, widespread sandstone is present at the top of the "Lagonda" interval (Figure 49).

The gamma-ray log profiles of the "Upper Squirrel" sandstone indicate a coarsening-upward sand and shale sequence with a gradational lower contact with the underlying "Lower Squirrel" sandstone and an abrupt upper contact with the black Excello Shale (Figure 50 and 51).

Figure 49. Isolith Map of "Upper Squirrel" Sandstone. Contour interval equals 5 feet.

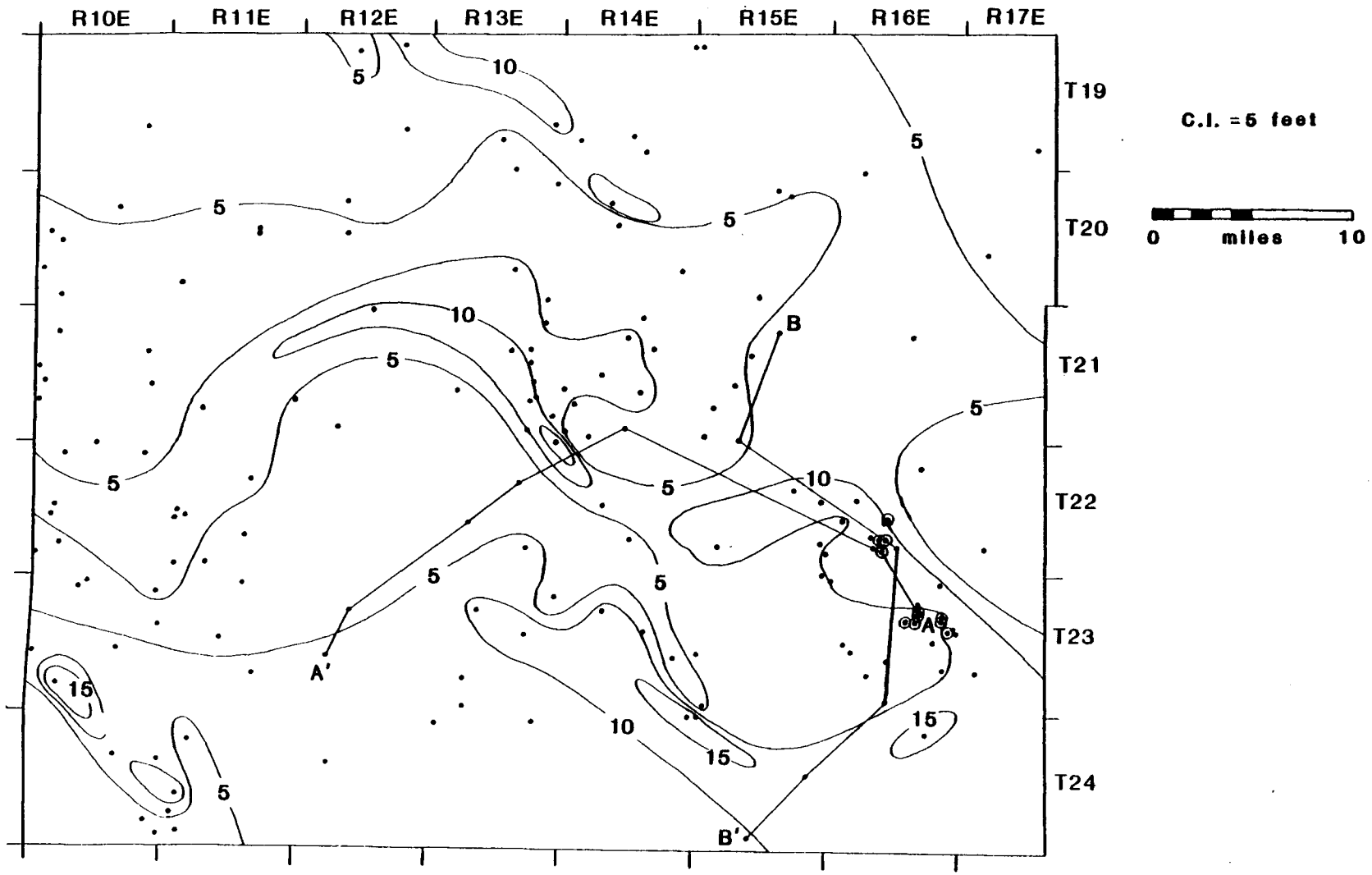
R10E
R11E
R12E
R13E
R14E
R15E
R16E
R17E
T19
T20
T21
T22
T23
T24
C.I. = 5 feet
0
miles
10
A
A'
B
B'
5
10
15

Reinholtz (1982) observed similar log characteristics within this horizon in Anderson County, Kansas. Selley (1976) interprets coarsening-upward log profiles within a delta complex as resulting from the deposition of siliciclastic materials within the distal delta-front or delta slope environment (Figure 43).

In northeast Kansas, the "Upper Squirrel" sand interval represents thick, coarse-grained channel and interchannel materials that were deposited in a terrestrially-influenced environment, and indicates closer proximity to the siliciclastic source area (Nelson, 1984). Preliminary investigations in southeast Kansas and northeast Oklahoma indicate that the "Upper Squirrel" sandstone of east-central Kansas grades laterally into the Breezy Hill Limestone of Oklahoma (Denesen, 1984).

Evidence obtained from well-log signatures and similar investigations of the "Lagonda" interval sandstones suggests that the "Upper Squirrel" sandstone in east-central Kansas represents deposition of siliciclastic material within the distal delta-front or delta slope environment (Figure 52), between well-developed delta plain deposits in northeast Kansas and marine limestone deposits in southeast Kansas and northeast Oklahoma.

The "Upper Squirrel" sandstone of east-central Kansas represents the final phase of sediment deposition within

Figure 50. Cross-section A-A showing laterally continuous "Upper Squirrel" sandstone. Gamma-ray log profiles indicate gradational lower contacts, serrated coarsening-upward profiles with abrupt upper contacts. Datum is base of Excello Shale.

CROSS-SECTION A-A'

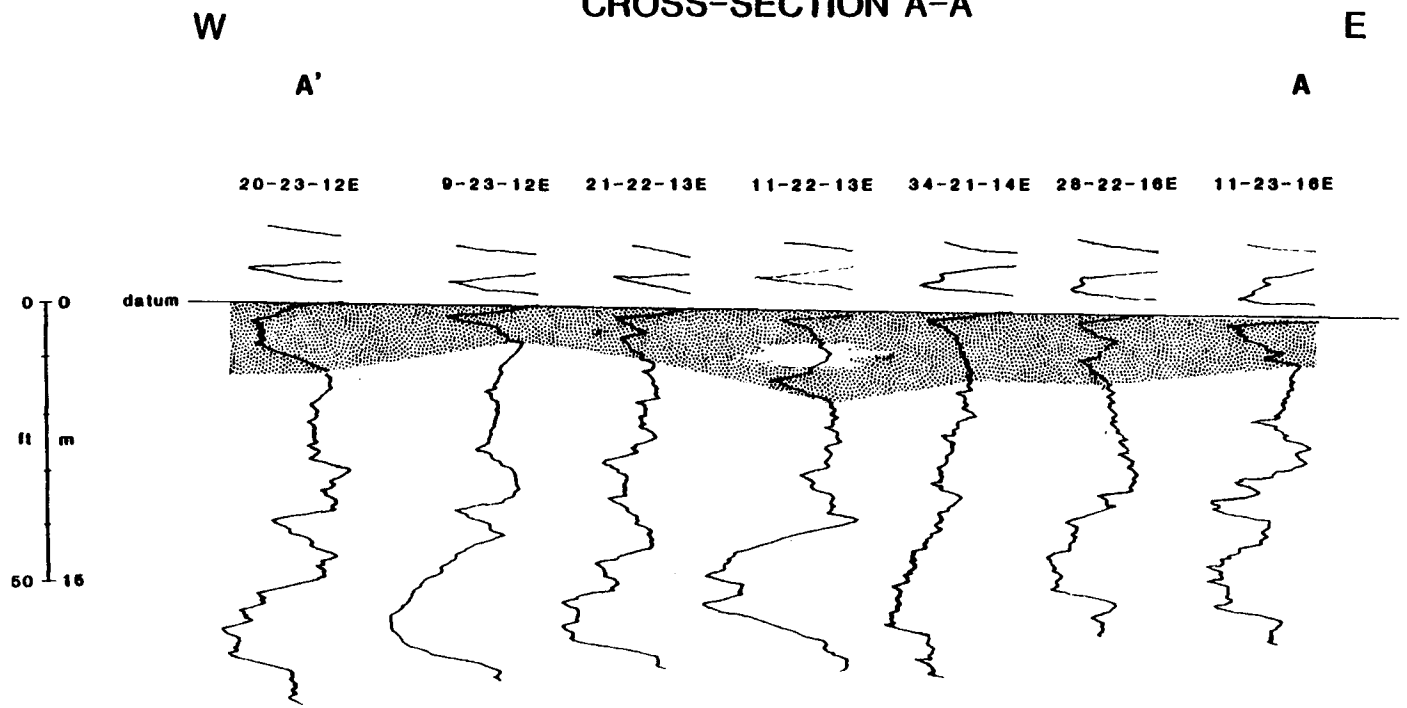

Figure 51. Cross-section B-B showing laterally continuous "Upper Squirrel" sandstone. Gamma-ray signatures indicate gradational lower contacts, serrated coarsening-upward profiles with abrupt upper contacts.

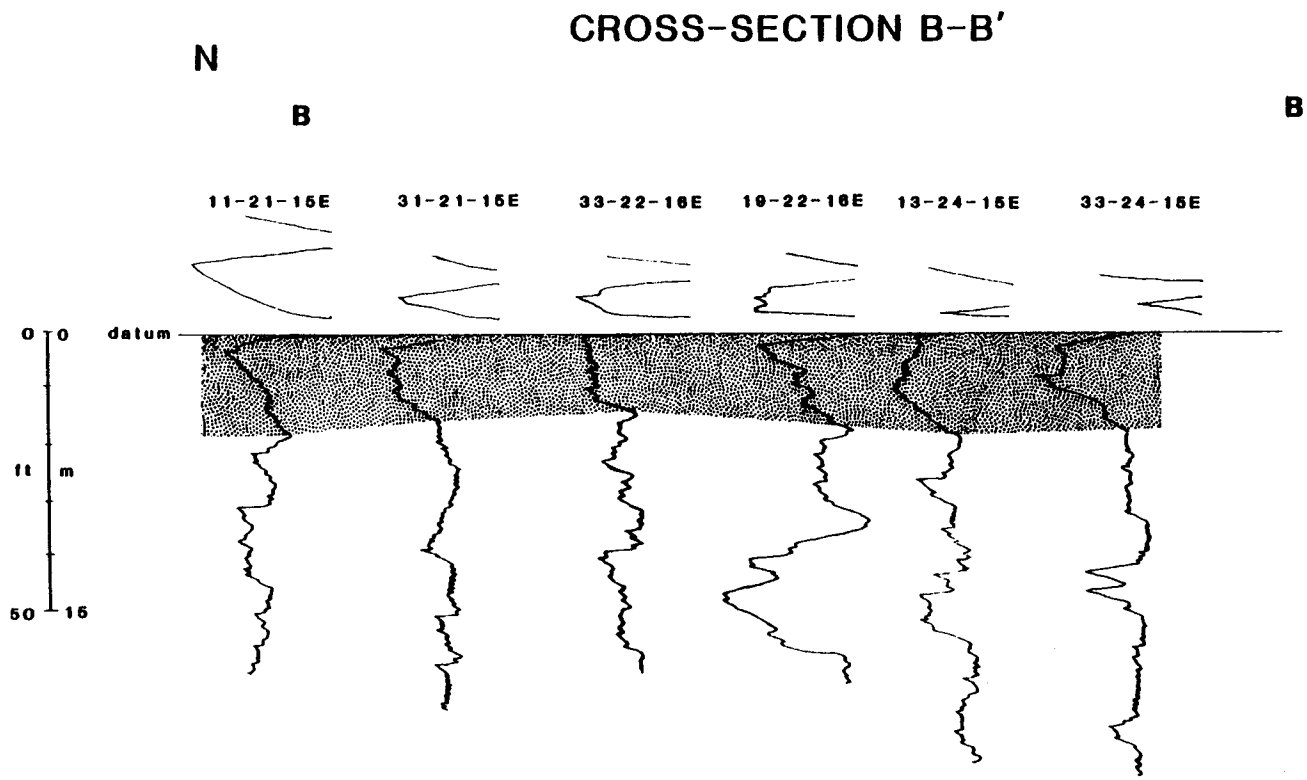
CROSS-SECTION B-B'
N
S
B
B'
11-21-15E
31-21-15E
33-22-16E
19-22-16E
13-24-15E
33-24-15E
0
0
datum
ft
m
50
15

Figure 52. Paleogeographic reconstruction illustrating deposition of the "Upper Squirrel" sandstone. Delta-front sediments in east-central Kansas were derived from well-developed fluvial channels in northeast Kansas studied by Nelson (1984).

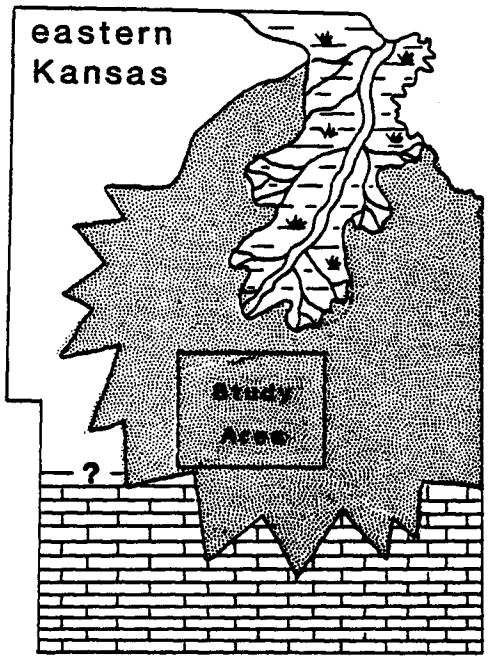

Delta Plain

Delta Front

Marine Shelf

0 miles 100

0 kilometers 60

relatively low sea level stands of the "Lagonda" interval. Maximum marine transgression is recorded by the deposition of the black Excello Shale, which overlies the "Upper Squirrel" sandstone everywhere in the study area and extends into surrounding states.

DIAGENESIS

Diagenesis of Lithofacies B Sandstone

Feldspar Dissolution

Dissolution of feldspar grains is a common diagenetic feature within the "Lower Squirrel" sandstone, contributing up to 70 percent of the total porosity (Table 1). It consists of partially to extensively dissolved grains, forming honey-combed and doughnut-shaped grains (Figure 23), and oversized pore spaces with relict grain boundaries and remnent grain fragments (Figure 24). Secondary porosity in sandstones resulting from feldspar dissolution has been recognized by many workers including Shenhav (1972), Heald and Larese (1973), Schmidt and MacDonald (1979), and Pittman (1979).

Breakdown of feldspar usually occurs early in the burial history and continues through deep burial (Milliken and others, 1981). Boles and Franks (1979) noted that the primary alteration within selected sandstones in the Wilcox Group in Texas was a loss of K-feldspar with increasing depth, occurring between 100 and 120 degrees Celsius. The degree of feldspar dissolution probably reflects the extent of feldspar-grain exposure to pore fluids (Tillman and

Almon, 1979). Where pore fluids had easy access to feldspar grains, extensive dissolution occurs. Feldpspars are relatively fresh where pores are filled with quartz cement. This indicates that feldspar dissolution does reflect exposure to pore fluids and that quartz cementation pre-dates feldspar alteration. Similar relationships were observed in the Cretaceous Frontier Formation sandstones of Wyoming (Tillman and Almon, 1979).

Dissolution of feldspar creates a potential source of aluminum and silica for the formation of authigenic kaolinite within primary and secondary pore spaces. Keller (1970) suggests that feldspar dissolution releases Al and Si cations within a micro-environment, enabling local formation of authigenic clays. Petrographic and SEM examinations reveal a close association between dissolved feldspars and clusters of pore-filling booklets of kaolinite (fig. 53).

Dissolution of feldspars may be a potential source of the silica involved in the formation of secondary quartz overgrowths in adjacent parts of the rock unit (Blatt, 1979).

Formation of Authigenic Silica

Authigenic silica is a ubiquitious cementing agent in the "clean" sandstone of lithofacies B, where it occurs as euhedral to subhedral syntaxial overgrowths.

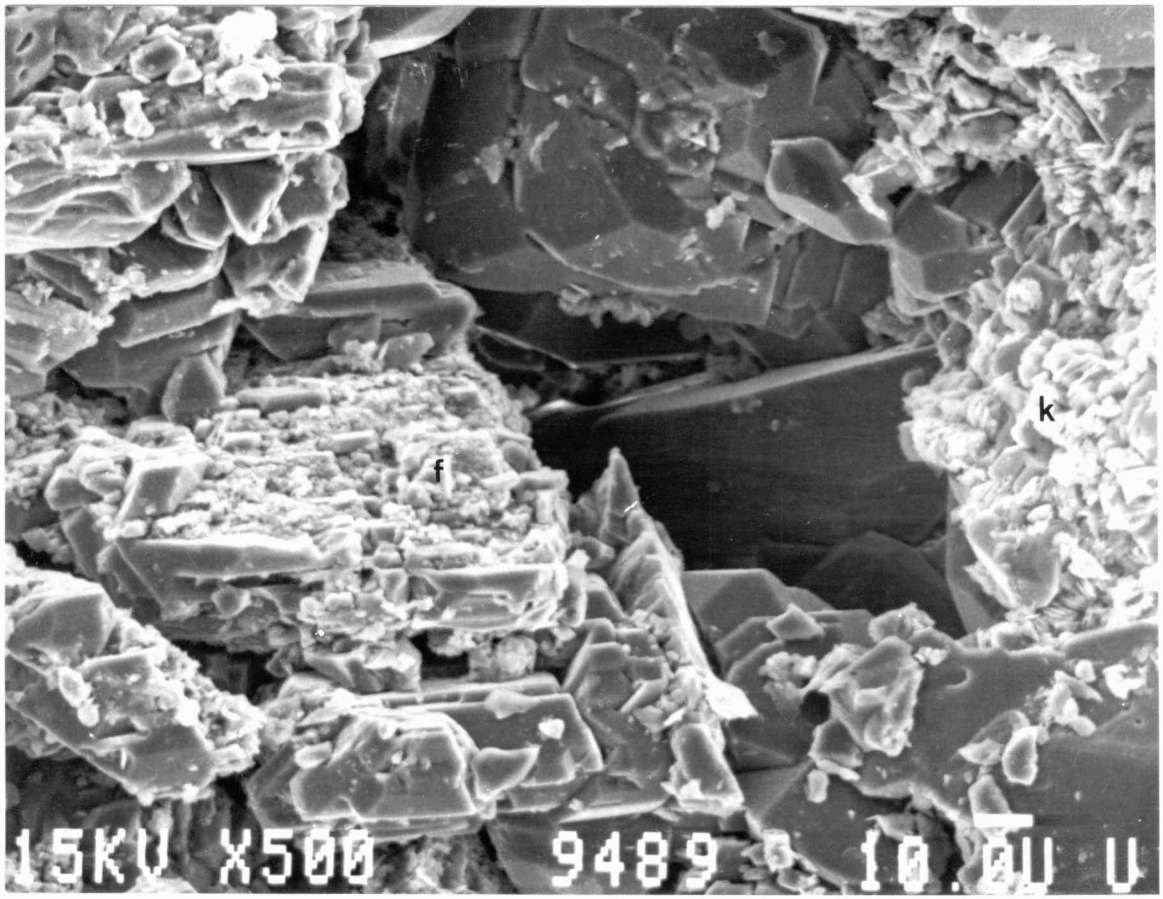

Figure 53. Scanning electron micrograph showing the close association between dissolved feldspar (f) and pore-filling authigenic kaolinite (k). Sample 9680. Bar scale equals 10 microns.

Coarser-grained sandstones with well-developed euhedral silica overgrowths retain numerous large pore spaces and interconnected pore throats (Figure 15), whereas in finer-grained sands, silica cement occurs as interlocking anhedral to subhedral silica overgrowths that significantly reduce porosity and permeability by extensive destruction of pore spaces and throats (Figure 54). Similar trends were recognized by Woody (1983) in selected Cherokee Group sandstones in southeastern Kansas.

Sources of silica precipitated as authigenic cement have been discussed by many workers (e.g., Friedman, 1954; Dapples, 1959; Siever, 1959; Bucke and Mankin, 1971). Many workers, including Waldschmidt (1941), Heald (1959), Thomson (1959) have invoked pressure solution as the principal source of authigenic silica. However, the lack of sutured contacts between detrital quartz grain boundaries suggests that sources of dissolved silica other than pressure solution were responsible for overgrowths in the "Lower Squirrel" sandstone.

Siever (1959) and Dapples (1967) suggest that significant amounts of authigenic silica are derived from ground water. Blatt (1979) suggests that silica released during diagenesis of clay minerals combined with pressure solution, would raise the silica content of subsurface brines from the amount observed in connate water (less than

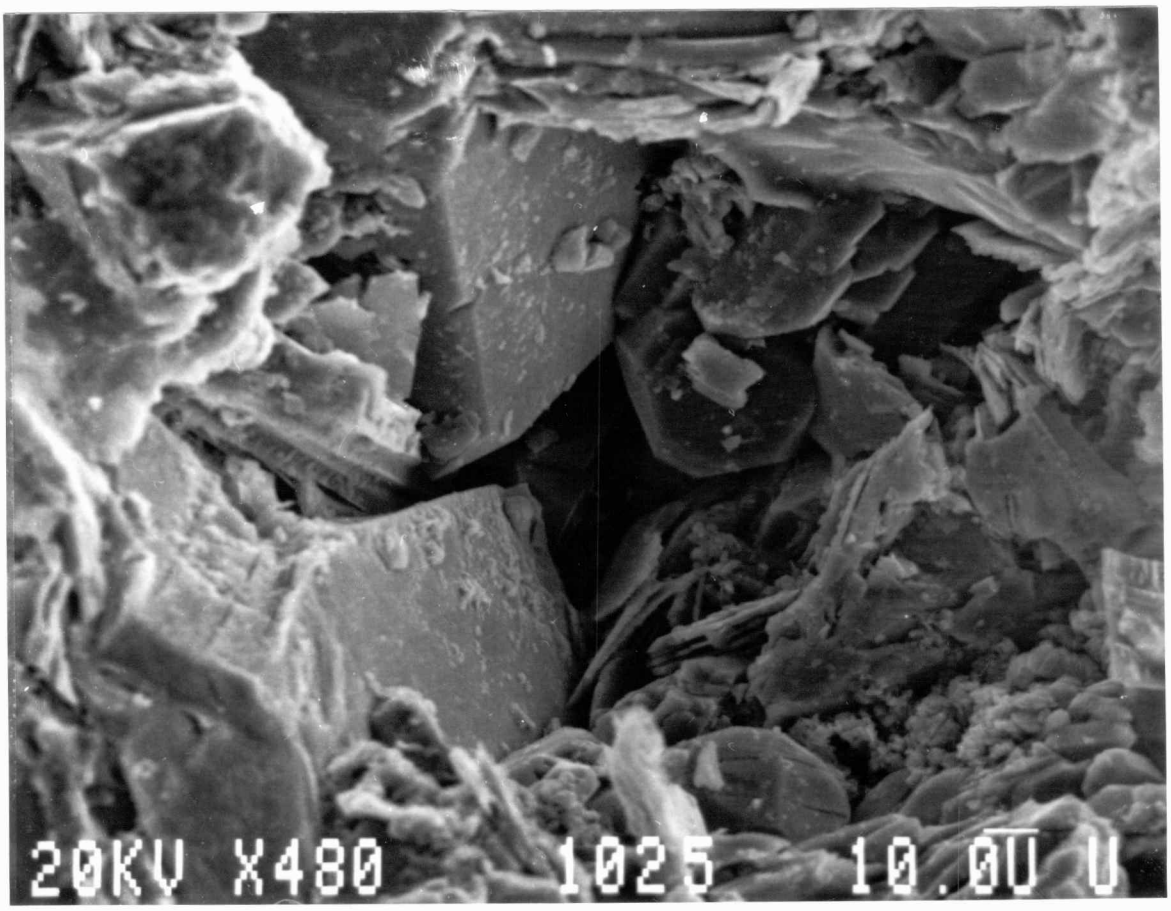

Figure 54. Scanning electron micrograph showing almost total destruction of pore space by silica overgrowths. Sample 1025. Bar scale equals 10 microns.

1 ppm for marine water and 13 ppm for nonmarine water) to the values observed in brine water (up to 100 ppm). Bucke and Mankin (1971) and Boles and Franks (1979) suggest that most of the authigenic silica found in sandstones was derived from the low-temperature illitization of smectite clays in interstratified shales. In the "Lower Squirrel" sandstone, extensive dissolution of feldspar grains could provide additional silica for authigenic overgrowths. In late Carboniferous distributary channel sandstones in England, Hawkins (1978) observed that quartz overgrowths are generally restricted to horizons where kaolinite attains maximum development, suggesting that excess silica released to interstitial waters following the dissolution of feldspar, coupled with the crystallization of kaolinite, was sufficient for precipitation of quartz overgrowths.

SEM analysis reveals that quartz overgrowths often form envelopes around authigenic booklets of kaolinite in the "Lower Squirrel" sandstone, suggesting continued authigenic quartz development during or after the formation of the kaolinite (Figure 55). Similar diagenetic relationships were observed by Hawkins (1978). Lack of well-developed clay rims on detrital quartz grains would provide numerous large surfaces on which authigenic quartz cement could precipitate.

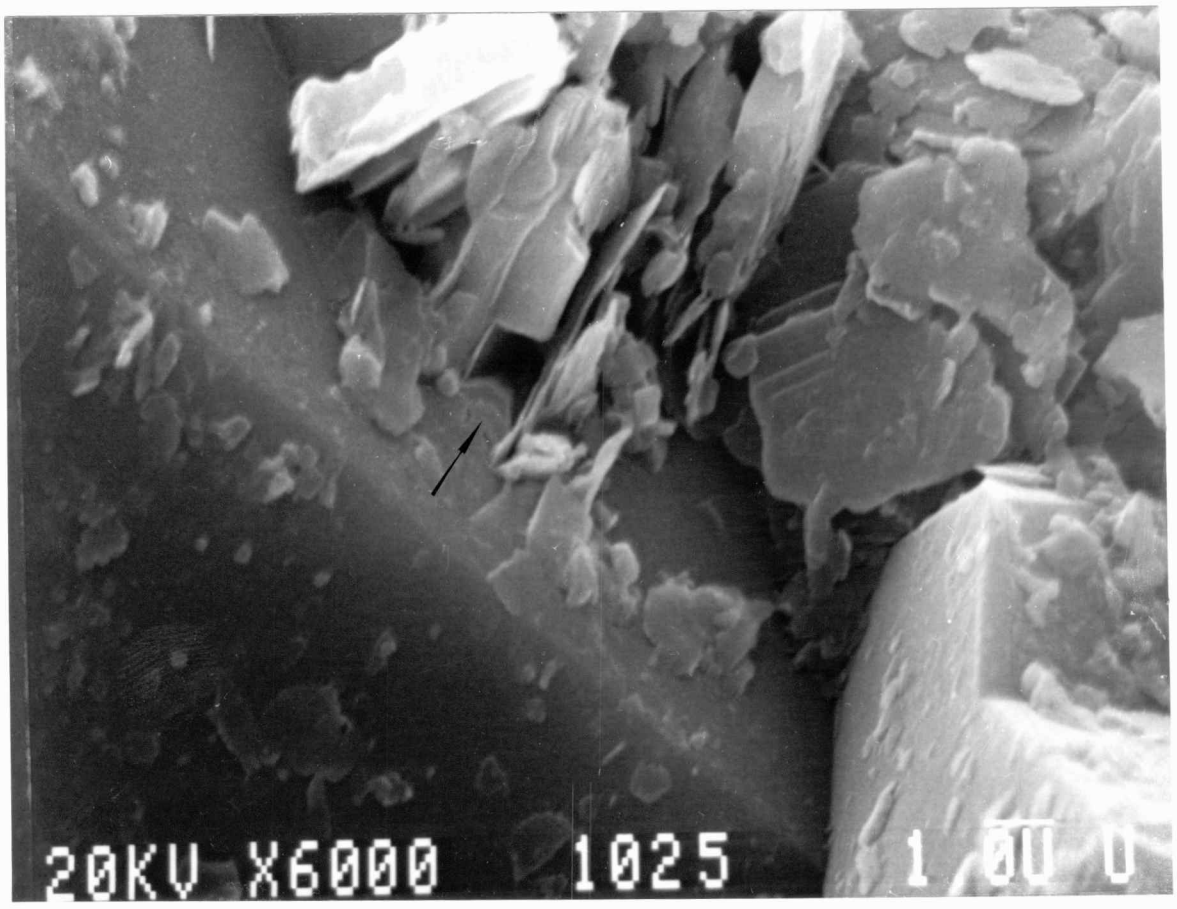

Figure 55. Scanning electron micrograph showing continued authigenic silica development after kaolinite formation(arrow). Authigenic silica often envelopes well-developed kaolinite crystals. Sample 1025. Bar scale equals 10 microns.

Formation of Authigenic Clays

SEM and x-ray analyses reveal that authigenic pore-filling clays within the "Lower Squirrel" sandstone consist of well crystallized kaolinite and minor amounts of stringy, lath-like illite. Primary criteria for recognizing authigenic clays in sandstones are the delicate crystalline structures of clays that could not have survived transport in detrital form (Wilson and Pittman, 1977). Stacked booklets of euhedral kaolinite occur as extensively to irregularly distributed clusters that fill primary intergranular pore spaces, secondary over-sized pores, and secondary pores formed by feldspar dissolution (Figure 56). These characteristics demonstrate an authigenic origin for kaolinite in lithofacies B sandstones. Kaolinite is particularly abundant in the coarser-grained sandstones of lithofacies B. Bucke and Mankin (1971) and Woody (1983) observed similar grain-size/kaolinite-content relationships in Desmoinesian sandstones in Oklahoma and southeastern Kansas. Hawkins (1978) reported that in late Carboniferous distributary channel sands, authigenic kaolinite content is higher in sands with secondary quartz than in similar sands without silica cement. The excess silica released into interstitial water after feldspar dissolution and transformation to kaolinite, was sufficient for the precipitation of quartz overgrowths concomitantly or

penecontemporaneously with kaolinite (Hawkins, 1978). Similar observations were noted in lithofacies B sandstones (Table 1).

Petrographic and SEM analyses of the "Lower Squirrel" sandstones suggest kaolinite forms primarily as a result of feldspar dissolution. Secondary pores created by extensive feldspar dissolution are commonly filled with authigenic kaolinite (Figure 56). Conditions conducive to forming authigenic kaolinite have been discussed by many workers, including Mankin and others (1970), Zeller (1968), and Bucke and Mankin (1971). Bucke and Mankin (1971) recognized four major factors that allowed the formation of significant proportions of authigenic kaolinite in Desmoinesian sandstones in Oklahoma: 1) porosity and permeability, allowing migration of interstitial waters and space for crystal growth; 2) presence of K-feldspar as a source of Al and Si; 3) presence of partially degraded illite as a K+ acceptor that was released during feldpsar dissolution; 4) presence of organic material to maintain a low pH.

All four factors probably contributed to kaolinite formation in the lithofacies B sandstone, as the relatively porous and permeable unit contains abundant partially dissolved K-feldspar grains, degraded illite/smectite clays, and numerous carbonaceous plant detritus.

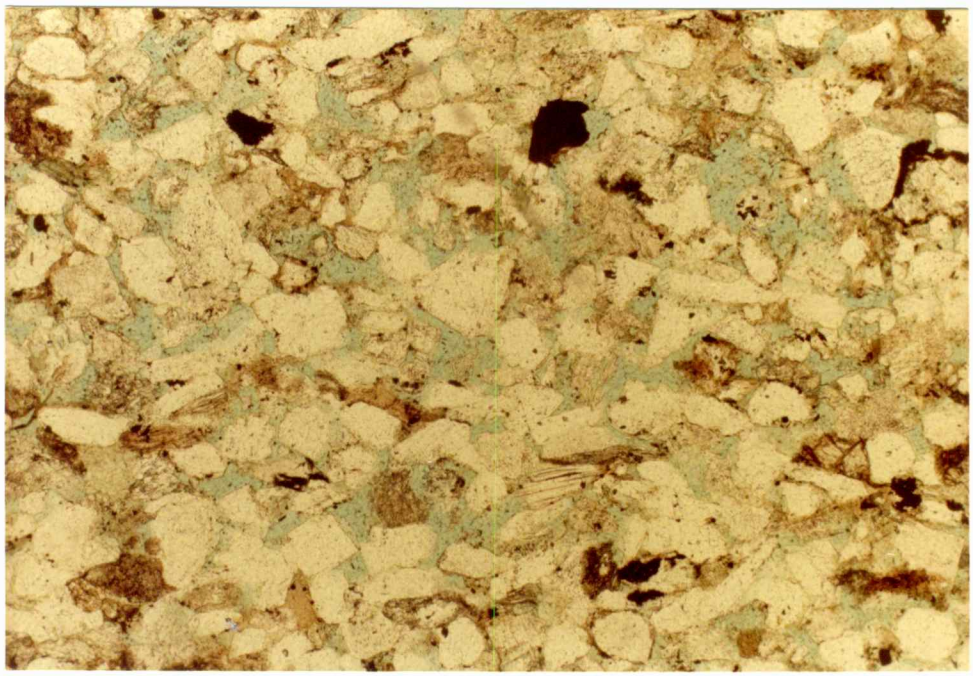

Figure 56. Photomicrograph showing secondary pore space created by feldspar dissolution partially filled by authigenic kaolinite. Plane light. Sample LM-8 956.1. Bar scale equals 0.1mm.

Keller (1970) suggests that irregular distributions of authigenic kaolinite may result from local micro-environmental controls, in that certain local micro-environmental conditions may favor kaolinite formation(i.e. proper Al:Si and [K+]/[H+] ratios), whereas a few millimeters away, conditions may favor the formation of a different mineral. Micro-environmental formation of kaolinite helps explain the patchy distribution of pore-filling, stacked kaolinite booklets in the lithofacies B sandstone.

Petrographic microscope identification of illite was difficult due to its minor occurrence and fine-grain size. Minor amounts of authigenic illite were observed in the lithofacies B sandstone (Figure 31). SEM reveals the delicate crystal morphology of authigenic illite. Aden (1982) found illite to be the major clay constituent within the shales of the Lagonda interval. Bucke and Mankin (1971) identified illite as the major clay-mineral constituent in both sands and shales in Desmoinesian sandstones in Oklahoma, although they considered much of the illite to be detrital in origin.

Sericitization is a common diagenetic feature of the sandstone, as sericite partially to extensively replaces feldspar grains. Replacement of feldspar grains by the K-deficient muscovite occurs along prominant cleavage

planes. Fuchtbauer (1974) suggests that this alteration occurs in late stage diagenesis during deep burial.

Pyrite Formation

Pyrite is a ubiquitous minor constituent of the "Lower Squirrel" sandstone, occurring as small isolated cubes and framboid clusters of tiny crystals within the clay matrix (Figure 57)).

The presence of pyrite indicates reducing conditions, low pH, and high dissolved-sulfur concentrations (Garrels ans Christ, 1980). The concept of micro-environments is used to explain local authigenic minerals proximal to unstable, altering detrital components (Keller, 1970). Keller (1970) suggests that micro-environments result in local high ionic concentrations, and possible precipitation of authigenic minerals. Pyrite crystals are closely associated with plant debris, suggesting that pyrite incorporated sulfur derived from bacterial action accompanying the decomposition of plant debris.

Pyrite is probably an early diagenetic mineral as sulfate-reducing bacteria were probably necessary to metabolize organic matter (Berner, 1981). Petrographic evidence supports early formation of authigenic pyrite. Cubes and clusters of pyrite are occasionally enveloped by authigenic silica, suggesting that pyrite formed prior to silica cementation.

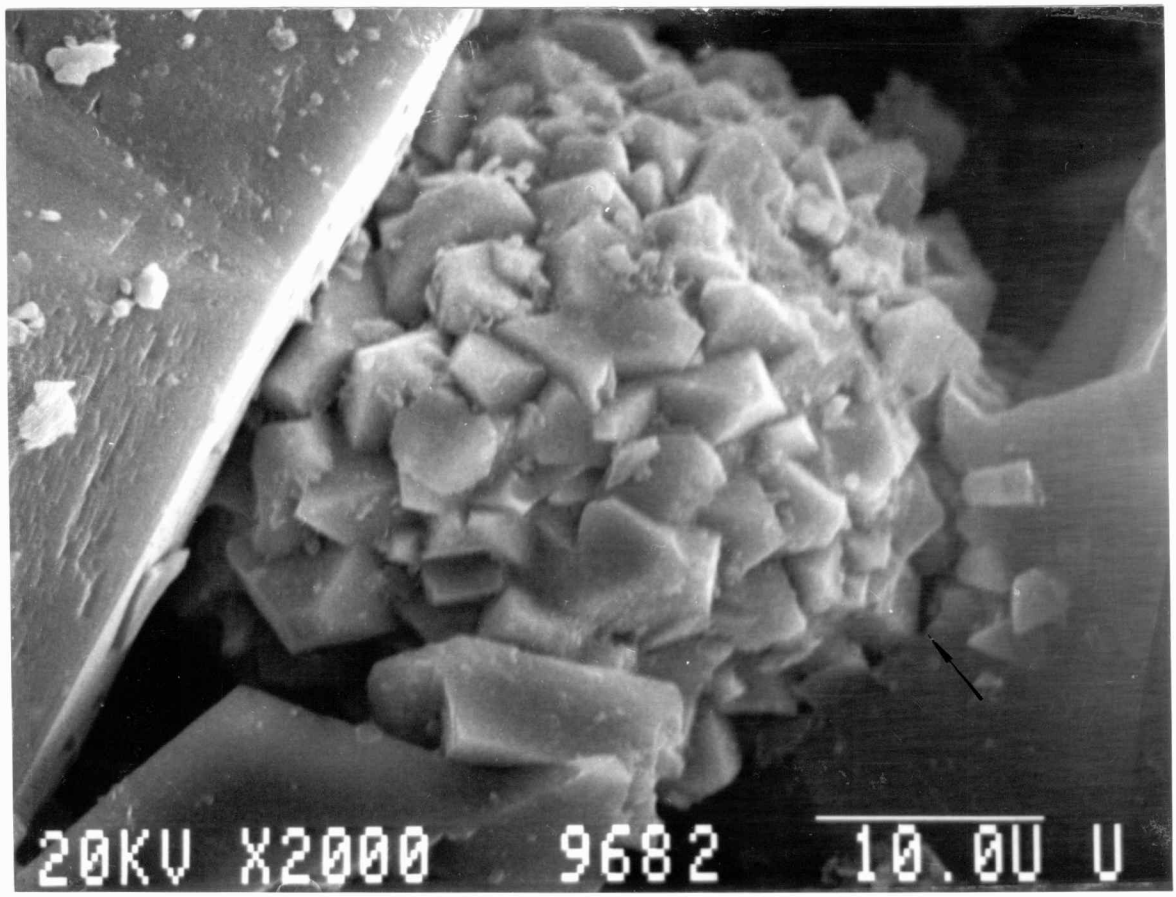

Figure 57. Scanning electron micrograph of pyrite framboid. Note quartz overgrowth after pyrite formation. Sample KB-1-968.2. Bar scale equals 10 microns.

Formation of Fe-Calcite

Minor amounts of Fe-calcite occur as patchy, poikilotopic cement in the "Lower Squirrel" sandstone, and partially replace neighboring feldspar grains and lesser amounts of quartz grains.

Fe-calcite cements post-date quartz overgrowths as indicated by their position in pores surrounding quartz overgrowths and detrital grains (Figure 58).

Precipitation of Fe-calcite depends on the [Ca++][CO --] product of interstitial water (Boles and Franks, 1979). Correns (1950) suggested that the antipathetic relationship between calcite and quartz is related to the inverse relationship of their solubilities with increasing pH. However, Siever (1962) argued that a rise in temperature is a more reasonable method of precipitating calcite than raising the pH to at least 9. Siever (1962) suggested that a temperature increase would promote calcite precipitation and concurrently dissolve silica. In Desmoinesian sandstones in Oklahoma, Bucke and Mankin (1977) proposed that low pH values existed during early diagenesis, followed by an increase in temperature and a rise in the pH to at least 9.

Clay diagenesis within the "Lagonda" interval may also have influenced calcite cementation. During smectite-illite alteration, interlayer Ca++ ions are released as K+ fixation

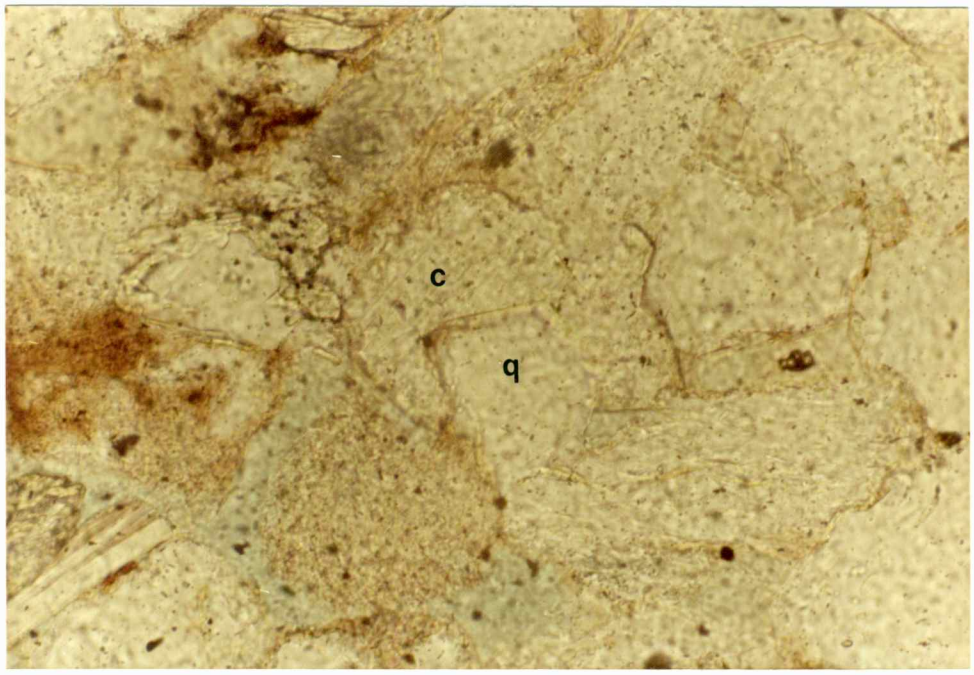

Figure 58. Photomicrograph showing that Fe-calcite cement post-dates syntaxial quartz overgrowths. Sample KB-1 956.7. Plane light. Bar scale equals 0.1mm.

proceeds, and if they combine with CO from organic reactions in shales, they may form calcite cement (Boles and Franks, 1979).

Paragenetic Sequence within Lithofacies B

Pre-diagenetic factors that control the direction and extent of sandstone diagenesis are mineral composition, depositional environment and tectonic setting. These factors influence chemical reactions, fluid-flow rates, and depth and temperature during burial. The "Lower Squirrel" sandstone consists of subarkosic to arkosic sandstones that were deposited upon a stable cratonic shelf within a fluvially-dominated deltaic environment. Maximum burial depth of Cherokee rocks is estimated to have been 1200 meters (Woody, 1983), and the maximum temperature to which the Cherokee Group rocks were subjected probably did not exceed 70 degrees Celsius (Land and Dutton, 1978).

The sequence of alterations in the "Lower Squirrel" sandstone consists of three general stages, although some diagenetic alterations may overlap in time and space (Figure 59). Petrographic and SEM analyses of grain-to-grain, grain-to-cement, and cement-to-cement relationships permit a reasonable interpretation of diagenetic alterations and sequences. The first stage of diagenesis consists of localized pyrite formation as replacement of organic matter.

Pyrite is probably an early diagenetic process and formed at or near the surface as sulfate-reducing bacteria were probably necessary to decay organic matter (Berner, 1980).

Diagenetic alterations in Stage two include several processes that were probably initiated early in the burial history and continued through the later stages of diagenesis. "Dust rims" on detrital quartz grains reflect clay coatings formed prior to extensive silica overgrowths. The well-defined, euhedral crystal faces on quartz grains suggest that silica overgrowths were not inhibited by surrounding grains, and that they developed in primary pore space prior to compaction. Initial authigenic silica formation probably pre-dates pore-filling kaolinite. However, quartz overgrowths often surround pseudohexagonal crystals of kaolinite, suggesting continued authigenic quartz development during and after kaolinite precipitation. Silica overgrowths pre-date both Fe-calcite and hydrocarbon migration.

Stage three is a complex sequence of dissolution, transformation, and precipitation of minerals, in which the precise sequence of alteration is not clear. K-feldspar dissolution is a prerequisite for kaolinite formation. The dissolution of K-feldspar provides the necessary ions for kaolinite formation as well as opening up additional pore space for fluid migration and kaolinite crystal growth.

Figure 59. Primary diagenetic alterations and proposed paragenetic sequence for lithofacies B sandstone. Solid lines indicate extensive development and dashed lines indicate lesser development and probable overlap of authigenic mineral crystallization.

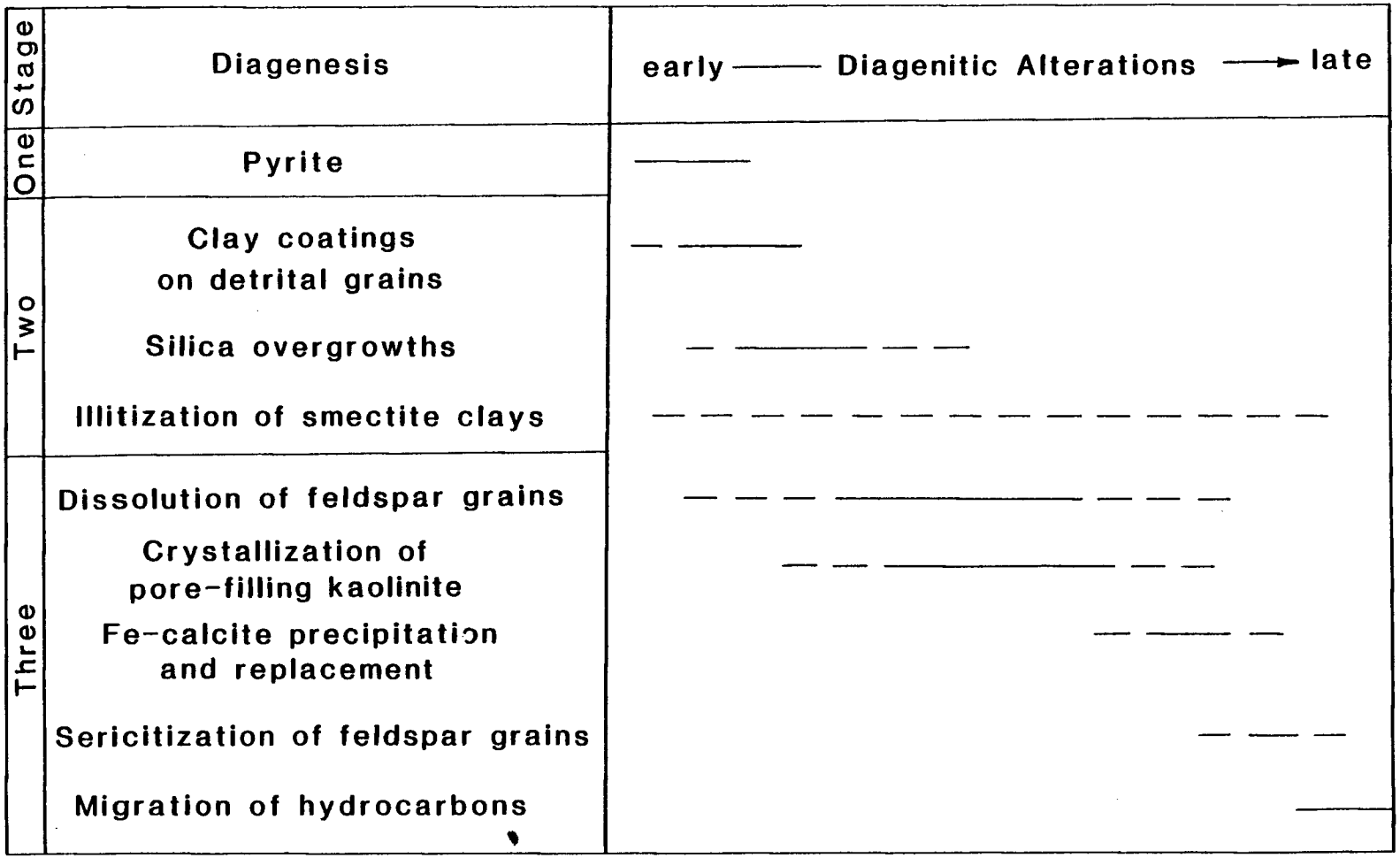
Stage
Diagenesis
early —— Diagenitic Alterations ——→ late
One
Pyrite
Two
Clay coatings on detrital grains
Silica overgrowths
Illitization of smectite clays
Three
Dissolution of feldspar grains
Crystallization of pore-filling kaolinite
Fe-calcite precipitation and replacement
Sericitization of feldspar grains
Migration of hydrocarbons

Partially degraded illite must be availiable as a K+ acceptor during kaolinite precipitation (Bucke and Mankin, 1971). Kaolinitization, and consequently feldspar dissolution, has been interpreted as a near-surface alteration, occurring early in the burial history of sandstones (Loucks and others, 1977). Extensive feldspar dissolution must have occurred after compaction because of the observed fragile nature of the partially dissolved grains. Clear, unaltered feldspar grains enveloped by authigenic silica cement indicate that initial silica cementation took place before feldspar dissolution. Feldspar dissolution and kaolinite precipitation probably continued throughout burial. The limited occurrence of Fe-calcite prohibits the precise relationship of that cement to other authigenic minerals. Petrographic evidence suggests that poikilotopic Fe-calcite post-dates quartz overgrowths (Figure 58). Seritization of feldspar is probably a late-stage alteration. Fuchtbauer (1974) interpreted sericitization of feldspars in other fluvial-deltaic sandstones as a late stage diagenetic process.

Krumbein and Garrels (1952) suggest various sedimentary associations in relation to environmental limitations imposed by oxidation potenital and pH (Figure 60). The authigenic mineral associations observed in lithofacies B

suggest an Eh range of -0.15 to -0.3 and an initial pH of 7.0 to 7.8 to allow the formation of organic matter, pyrite and silica, that later increased to greater than 7.8 to form late-stage calcite cement.

Diagenesis of Lithofacies D Sandstone

The paragenetic sequence for lithofacies D sandstones is similar to the sequence suggested for the sandstone of lithofacies B. However, the significant increase in the amount of calcite cement and decrease in authigenic clay development in lithofacies D suggest alternate diagenetic trends developed as a result of calcite cementation.

Petrographic analyses of the fossiliferous, calcite-cemented sandstone indicate early pyrite formation followed by clay coatings on detrital quartz grains, and development of extensive silica overgrowths prior to calcite cementation. Pressure solution by quartz grains with silica overgrowths along fossil fragment boundaries indicates that silica cementation preceded compaction and that some compaction took place prior to feldspar dissolution and calcite cementation (Figure 61). Feldspar dissolution and kaolinite precipitation probably predate calcite cementation due to the interstitial pore volume required for migration of feldspar-dissolving and kaolinite-precipitating interstitial fluids.

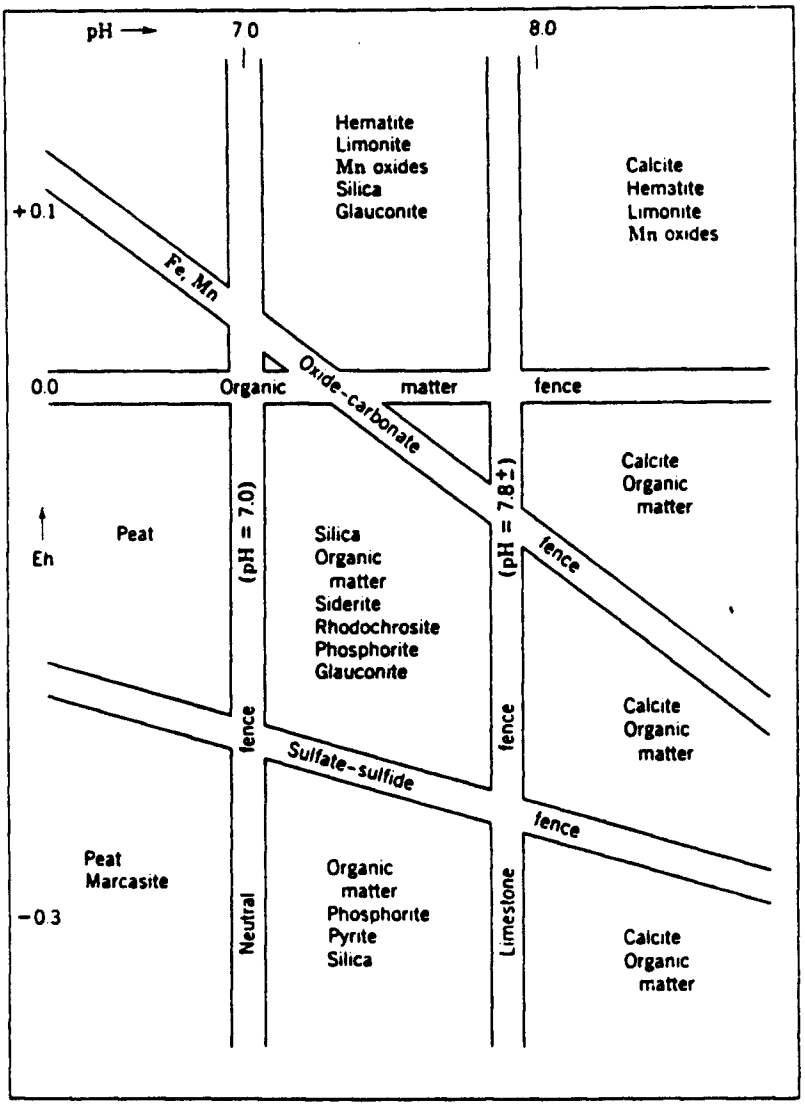

Figure 60. Various sedimentary associations in relation to environmental limitations imposed by oxidation potential and pH (after Krumbein and Garrels, 1952).

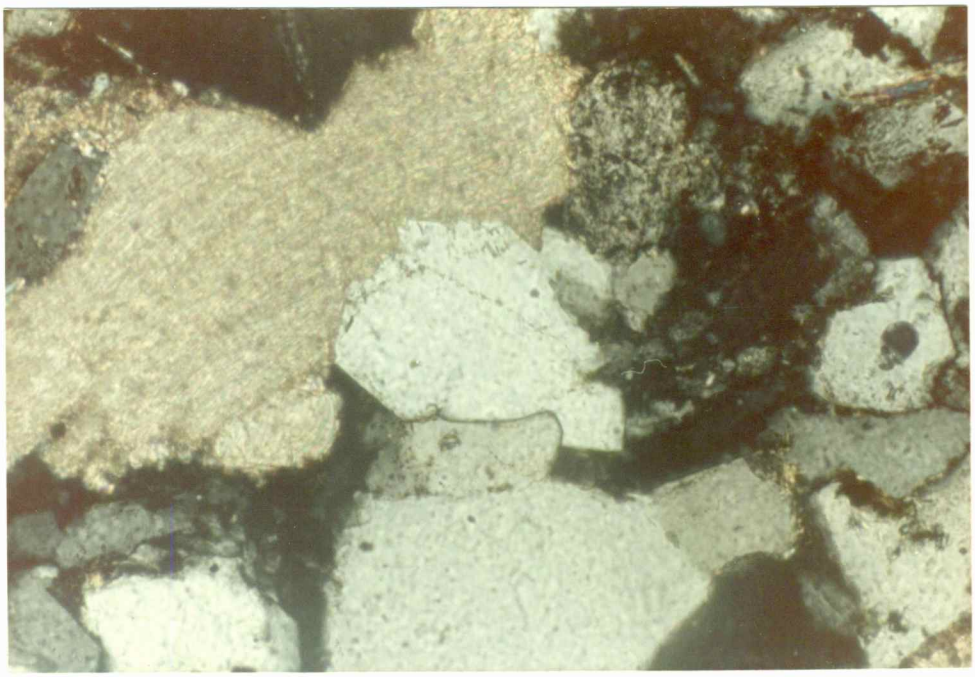

Figure 61. Photomicrograph showing that silica overgrowths precede compaction as euhedral overgrowth is penetrating brachiopod shell. Plane light. Sample KB-1 955.4. Bar scale equals 0.1mm.

Ca for Fe-calcite cementation was probably derived from a combination of smectite-illite clay diagenesis within surrounding shales, and from pressure solution and dissolution of carbonate skeletal grains within the unit. Reprecipitation of dissolved high-Mg calcite as equant sparry low-Mg calcite may occur almost simultaneously with solution (Longman, 1980). Petrographic evidence indicates partial dissolution of high-Mg echinoderm fragments (Figure 39) which is occasionally replaced by sparry calcite.

Formation of authigenic gypsum cement probably occurred after high-Mg calcite dissolution, as gypsum commonly fills secondary pore space within partially dissolved echinoderm fragments (Figure 42). In sedimentary rocks, gypsum is commonly formed by the reaction between sulfuric acid derived from weathering sulfides, and calcium in the sandstones (Deer and others, 1978).

Diagenetic Environment

Heckel (1983) developed a diagenetic model for carbonate rocks in MidContinent Pennsylvanian eustatic cyclothems from which diagenetic patterns may be interpreted. He observed that in MidContinent Pennsylvanian shallow water transgressive calcarenites, carbonate grains are pervasively overpacked, greatly reducing pore space, and the cement is almost entirely composed of blocky, equant

Fe-calcite spar, suggesting late-stage cementation after substancial compaction in deeper-burial, Mg-poor connate zone.

In "Lower Squirrel" sandstones, lithofacies D illustrates pervasive overcompaction as pressure solution and grain welding commonly occur along carbonate skeletal grains (Figure 18). However, the unit consists primarily of siliciclastic grains that would resist pressure solution and grain welding along siliciclastic grain boundaries and prevent significant reduction of pore space by overcompaction. This retention of pore space would allow intersticial pore fluid to circulate through the unit and dissolve unstable feldspar grains (Figure 38), and form authigenic kaolinite within secondary pores prior to Fe-calcite cementation. Fe-calcite formed as oxygen was depleted by organic decomposition, and the resulting reducing conditions permitted sufficient Fe++ in solution to form pore-filling blocky, equant ferroan calcite spar (Heckel, 1983).

The deeper-burial connate diagenetic environment is consistent with the transgressive marine depositional environment suggested for lithofacies D.

SUMMARY AND CONCLUSIONS

Geophysical well-logs enabled subsurface correlation of laterally discontinuous "Lagonda" interval sandstones across the Cherokee basin in east-central Kansas. Laterally continuous black shales within the Cherokee Group were used as marker beds and correlation datum lines. Well-log locations served as control points to plot lithic and stratigraphic data and to illustrate proposed depositional patterns.

Sandstone distribution maps and cross-sections indicate that the "Lower Squirrel" sandstone is elongate, narrow, and laterally discontinuous. Environmental interpretations, based on sandstone geometry, well-log signatures and lithofacies relationships, suggest that the "Lower Squirrel" sandstone and associated sediments were deposited within a fluvially-dominated delta complex that prograded southwestward across the Cherokee shelf. Environments include: 1) distributary channel and mouth-bar deposits; 2) overbank sediments; 3) destructional marine bars; and 4) interdistributary bay-inner shelf deposits. Previous and concurrent investigations suggest that a source area to the north, possibly the Canadian shield, supplied much of the sediment that was deposited upon the shelf.

The "Upper Squirrel" sandstone in east-central Kansas represents deposition of siliciclastic material within a distal delta-front environment between well-developed distributary channel deposits in north-east Kansas, and marine limestones in south-east Kansas and north-east Oklahoma.

Petrographic analyses show that the "Lower Squirrel" lithofacies B sandstone consists predominantly of detrital quartz grains with lesser amounts of feldspar and muscovite fragments. Authigenic cements consist primarily of silica and kaolinite with lesser amounts of Fe-calcite. Pyrite and organic debris are ubiquitious minor constituents fo the sandstone.

The post-depositional history of the "Lower Squirrel" lithofacies B sandstone can be divided into three stages: Stage one consists of localized pyrite formation in association with organic fragments. Stage two consists of silica cementation and rare feldspar overgrowths. In coarser-grained sandstones, euhedral silica overgrowths extend into pore spaces, partially reducing porosity and permeability. In finer-grained sandstones, silica overgrowths form patches of interlocking cement that significantly reduce pore space and pore throats. Stage three is a complex sequence of alteration, dissolution and replacement and has significantly affected porosity and

permeability within the sandstone. Diagenetic alterations include dissolution of aluminosilicate grains, particularly K-feldspar. Dissolution of feldspar grains produced extensive effective secondary porosity. The transformation of feldspar resulted in the precipitation of well crystallized kaolinite that often occludes pore space and interconnected pore throats.

The paragenetic sequence of lithofacies D sandstones is similar to the sequence suggested for the sandstone of lithofacies B. However, the significant increase in the amount of calcite cement coupled with a decrease in authigenic clay development in lithofacies D suggests different cementation emphasis during diagenesis. The type and extent of cementation in lithofacies D compared to lithofacies B probably resulted from marine depositional environmental influences. The source of the calcite cement in lithofacies D was probably through dissolution of carbonate skeletal grains and re-precipitation as pore-filling, poikilotopic Fe-calcite cement.

The overcompacted, fossiliferous, Fe-calcite cemented sandstone of lithofacies D suggests that diagenesis occurred in the deeper-burial connate environment.

REFERENCES

Aden, L. J., 1982, Clay mineralogy and depositional environments of upper Cherokee (Desmoinesian) mudrocks, eastern Kansas, western Missouri and northeastern Oklahoma, unpub. M.S. thesis, Univ. of Iowa, 126 p.

Bass, N. W., 1936, Origin of the Shoestring Sands of Greenwood and Butler counties, Kansas: Kansas Geol. Survey, Bull. 23, 135 p.

Berner, R. A., 1981, A new geochemical classification of sedimentary environments; Jour. Sed. Pet., v. 51, p. 359-365.

Blatt, H., 1979, Diagenetic processes in sandstones, in Scholle, P. A., and Schluger, P. R., eds. Aspects of Diagenesis: SEPM Spec. Pub. No. 26, p. 141-157.

Blatt, H., Middleton, G., and Murray, R., 1972, Origin of sedimentary rocks: Prentice Hall, Inc., Englewood Cliffs, N. J., 634 p.

Boles, J. R., and Franks, S. G., 1979, Clay diagenesis in Wilcox sandstones of southwest Texas: Implications of smectite diagenesis on sandstone cementation: Jour. Sed. Pet., v. 49, p. 55-70.

Brown, L. F., 1979, Deltaic sandstone facies of the Mid-Continent, in Hyne, N.D., ed., Pennsylvanian Sandstones of the Mid-Continent: Tulsa Geological Society Spec. Publ. No. 1., p. 35-63.

Bucke, D. P., and Mankin, C. J., 1971, Clay-mineral diagenesis within interlaminated shales and sandstones: Jour. Sed Pet., v. 41, p. 971-981.

Burggraf, D. R., Jr., White, H. J., and Lindsay, C. G., 1981, Part II : Facies and depositional environments of the Cherokee Group in Webster County, Iowa: Lemish, J., Burggraf, D. R., Jr., and White H. J., (eds.); Cherokee Sandstones and Related Facies of Central Iowa: An examination of Tectonic Setting and Depositional Environments; Iowa Geol. Survey Guidebook Series 5, p. 23-49.

Burst, J. F., 1969, Diagenesis of Gulf Coast clayey sediments and its possible relation to petroleum migration: Am. Assoc. Petr. Geol., v. 53, p. 73-93.

Busch, D. A., 1974, Stratigraphic traps in sandstones-exploration techniques: AAPG Bull., v. 11, p. 1151-1172.

Charles, H. H., 1927, Oil and gas resources of Kansas: Anderson County, Kansas Geological Survey, Bull. No. 6., Part 6., 95 p.

Charles, H. H., 1941, Bush City oil field, Anderson County, Kansas, p. 43-56, in Levorson, A.I., (ed), Stratigraphic Type Oil Fields: Am. Assoc. Petr. Geol., 902 p.

Cleaves, A. W. II, 1975, Upper Desmoinesian-Lower Missourian depositional systems (Pennsylvanian), north-central Texas: Texas Univ., Austin, unbup. Ph.D. dissertation, 256 p.

Coleman, J. M., and Prior, D. B., 1982, Deltaic sediments, in Scholle, P. A., and Spearing, D. eds., Sandstone Depositional Environments: Am. Assoc. Petr. Geol. Pub., p 139-178.

Correns, C. W., 1950, On the geochemistry of diagenesis, in The Behavior of CaCo 3 and SiO 2: Geochim. et Cosmochim. Acta, v.1, p. 49-54.

Dapples, E. C., 1959, The behavior of silica in diagenesis, in Sediments in Sediments, SEPM Spec. Pub. no.7, p. 34-54.

Dapples, E. C., 1967, Silica as an agent in diagenesis, in Larsen, G., and Chilingar, eds., Diagenesis in Sandstones. Developments in Sedimentology 8, Ch. 8, p. 323-342.

Dapples, E. C., 1979, Diagenesis of sandstone, in Larson, G., and Chilingar, G. V., eds., Diagenesis in Sediments and Sedimentary Rocks: Developments in Sedimentology, v. 25A, Elsevier.

Deer, F. R., Howie, R. A., and Zussman, J., 1978, An Introdiction to the Rock-forming Minerals, 11th ed.: John wiley and Sons, Inc., 528 p.

Denesen, S., 1984, The stratigraphy and paleogeography of the Lagonda interval (Middle Pennsylvanian) in southeast Kansas and northeast Oklahoma: Southeastern and North-Central Geol. Soc. Amer., Abstracts with programs, p. 133.

Ebanks, W. J., 1979, Correlation of Cherokee (Desmoinesian) sandstones of the Missouri-Kansas-Oklahoma Tri-state area, in Hyne, N. J., ed., Pennsylvanian Sandstones of the Mid-Continent: Tulsa Geol. Soc. Spec. Pub. No. 1, p. 295-312.

Ebanks, W. J. Jr., James, G. W., and Livingston, N. D., 1977, Evaluation of heavy oil and tar sands in Bourbon, Crawford and Cherokee Counties, Kansas - Final Report: Investigation 77/20, 110 p.

Folk, R. L., 1974, Petrology of Sedimentary Rocks: Hemphill Pub. Co., Austin, Texas, 182 p.

Fothergill, C. A., 1955, The cementation of oil reservoir sands and its origin: Proceedings of the 4th World Petroleum Congress, p. 300-312.

Frank, J. R., 1981, Dedolimitization in the Taum Sauk Limestone (Upper Cambrian) Southeast Missouri, Jour. Sed. Pet., v. 51, p. 7-17.

Friedman, G. M., 1965, Terminology of crystallization textures and fabrics in sedimentary rocks: Jour. Sed. Pet., v. 35, p. 643-655.

Fuchtbauer, H., 1974, Sediments and sedimentary rocks 1, in Engelhardt, W., Fuchtbauer, H. and Muller, G., Sedimentary Petrology, Part II: John Wiley and Sons, Inc. N. Y., 464 p.

Galloway, W. E., 1968, Depositional systems of the lower Wilcox Group, north-central Gulf Coast basin: Trans. Gulf Coast Assoc. Geol. Soc., v. 18, p. 275-289.

Galloway, W. E., and Brown, L. F., Jr., 1972, Depositional systems and shelf-slope relationships in Upper Pennsylvanian rocks, north-central Texas: Texas Univ. Bur. Econ. Rep. Invest., 75, 62 p.

Garrels, R. M., 1960, Mineral equlibria: Harper and Brothers, N. Y., 254 p.

Garrels, R. M., and Howard, P., 1957, Reactions of feldspar and mica with water at low temperature and pressure: Clays and Clay Mineralogy, v. 6, p.68-88.

Garrels, R. M., and Crist, C. H., 1965, Solutions, Minerals and Equlibria: Harper and Row, New York, 450 p.

Hawkins, P. J., 1978, Relationship between diagenesis, porosity reduction, and oil emplacement in late Carboniferous sandstone reservoirs, Bothamsall oilfield, E. Midlands: Geol. Soc. London, v. 135, p. 7-24.

Heald, M. T., 1959, Significance of stylolites in permeable sandstones: Jour. Sed. Pet., v. 29. p. 251-253.

Heald, M. T., and Larese, R. E., 1973, The significance of the solution of feldspars in porosity development: Jour. Sed. Pet., v. 43, p. 458-460.

Heald, M. T., and Larese, R. E., 1974, Influence of coatings on quartz cementation: Jour. Sed. Pet., v. 44, p. 1269-1274.

Heckel, P. H., 1983, diagenetic model for carbonate rocks in Midcontinent Pennsylvanian eustatic cyclothems, Jour. Sed. Pet., v. 53, no. 3, p. 733-759.

Heckel, P. H., Brady, L. L., Ebanks, W. J., Jr., and Pabian, R. K., 1979, Pennsylvanian cyclic platform deposits of Kansas and Nebraska: Kansas Geol. Survey Guidebook Series 4, 79 p.

Howe, W. B., 1956, Stratigraphy of per-Marmaton Desmoinesian (Cherokee) rocks in southeastern Kansas: Kansas Geol. Survey Bull., 123, 132 p.

Hulse, W. J., 1979, Depositional environment of the Bartlesville Sandstone in the Sallyards Field, Greenwood County, Kansas, in Hyne, N.D., ed., Pennsylvanian Sandstones of the Mid-Continent: Tulsa Geological Society Spec. Publ. No. 1. p. 327-336.

Jewett, J. M., 1954, Oil and gas in eastern Kansas: Kansas Geological Survey, Bull. No. 189., 81 p., illus.

Jordan, L., 1957, Subsurface stratigraphic names of Oklahoma: Okla. Geol. Surrvey, Guidebook VI.

Keller, W. D., 1970, Environmental aspects of clay minerals: Jour. Sed. Pet., v. 40, p. 788-813.

Kluth, C. F., and Coney, P. J., 1981, Plate tectonics of the Ancestral Rocky Mountains: Geology, v. 9., p. 10-15.

Land, L. S., and Dutton, S. P., 1978, Cementation of a Pennsylvanian deltaic sandstone: Isotopic data: Jour. Sed. Pet., v. 48, p. 1167-1176.

Land, L. S., and Milliken, K. L., 1981, Feldspar diagenesis in the Frio Formation, Brazoria County, Texas Gulf Coast: Geology, v. 9, p. 314-318.

Lee, W., 1943, The stratigraphy and structural development of the Forest City basin in Kansas, Kansas Geological Survey, Bull. No. 51, 142 p., illus.

Longman, M. W., 1980, Carbonate diagenetic textures from subsurface diagenetic environments: AAPG Bull., v. 64, p. 461-487.

Loucks, R. G., Bebout, D. G., and Galloway, W. E., 1977, Relationship of porosity formation and preservation to sandstone consolidation history-Gulf Coast lower Tertiary Frio Formation: Texas University Bur. Econ. Geol. Circ. 77-5, p. 109-120.

McBride, E. F., 1963, A classifiaction of common sandstones: Jour. Sed. Pet.., v. 33, p. 664-669.

Merriam, D. F., 1963, The geologic history of Kansas: Kansas Geological Survey, Bull. No. 162, 317 p., illus.

Milliken, K. L., Land, L. S., and Loucks, R. G., 1981, History of burial diagenesis determined from Isotopic geochemistry, Frio Formation, Brazoria County, Texas: Am. Assoc. Petr. Geol., v. 65, 1397-1413.

Moore, G. E., 1979, Pennsylvanian paleogeography of the southern Mid-Continent, in Hyne, N.D., ed., Pennsylvanian Sandstones of the Mid-Continent: Tulsa Geol. Soc. Spec. Publ. No. 1, p. 3-9.

Moore, R. C., 1936, Stratigraphic classification of the Pennsylvanian rocks of Kansas: Kansas Geol. Survey Bull. 22, 256 p.

Nelson, M. R., 1984, Coarse channel sequences in the upper Cherokee rocks (middle Pennsylvanian) of north-east Kansas: southeastern and north-central Geol. Soc. Amer., Abstracts with programs, p. 133.

Pettijohn, F. J., Potter, P. E., and Siever, R., 1973, Sands and sandstone: Springer-Verlag, Heidelgerg, Germany, 618 p.

Pittman, E. D. 1979, Porosity, diagenesis and productive capability of sandstone reservoirs, in Scholle, P. A., and Schluger, P. R., eds., Aspects of Diagenesis: SEPM Spec.Pub. No. 26, p. 159-173.

Reinholtz, P. N., 1982, Distribution, petrology and depositional environment of "Bush City Shoestring Sandstone" and "Centerville Lagonda Sandstone" in Cherokee Group (Middle Pennsylvanian), southeastern Kansas: unpub. M.S. thesis, Univ. of Iowa, 180 p.

Rex, R. W., 1966, Authigenic kaolinite and mica as evidence for phase equlibria at low temperatures: Clays and Clay Minerals, v. 13, p. 95-105.

Rich, J. L., 1926, Further observations on shoestring oil pools of eastern Kansas: Am. Assoc. Petr. Geol. Bull., v. 10, p. 568-580.

Schmidt, V., and McDonald, D. A., 1979, The role of secondary porosity in the course of sandstone diagenesis, in Scholle, P. A., and Schluger, P. R.,eds., Aspects of Diagenesis: SEPM Spec. Pub. No. 26, p.175-207.

Scholle, P. A., 1979, A color illustrated guide of constituents, textures, cements, and porosities of sandstones and associated rocks: Am. Assoc. Petr. Geol. Memoir 28.

Searsight, W. V., Howe, W. B., Moore, R. C., Jewett, J. M., Condra, G. E., Oakes, M. C., and Branson, C. C., 1953, Classification of Desmoinesian (Pennsylvanain) of northern Mid Continent: Am. Assoc. Petr. Geol., Bull., v. 37, p. 2747-2749.

Selley, R. C., 1976, Subsurface environmental analysis of North Sea sediments: AAPG Bull., v. 27, p. 244-264.

Shannon, J. P., and Dahl, A. R., 1971, Deltaic stratigraphic traps in West Tuscola field, Taylor County, Texas: Am. Assoc. Petr. Geol., v. 55, p. 1194-1205.

Shenhav, H., 1972, Lower Cretaceous sandstone reservoirs, Israel; Petrology, Porosity, Permeability: Am. Assoc. Petr. Geol. Bull., v. 55, no. 12, p. 2194-2224.

Siever, R., 1959, Petrology and geochemistry of silica cementation in some Pennsylvanian sandstones, in Ireland, H. A., ed., Silica in sediments: SEPM Spec. Pub. No. 7.

Siever , R., 1962, Silica solubility, 0-200 C, and the diagenesis of siliceous sediments: Jour. Geology, v. 70, p. 127-150.

Thomson, A., 1959, Pressure solution and porosity, in Ireland, H. A., ed., Silica in Sediments: Spec. Publ. SEPM, Tulsa no. 7, p. 92-110.

Tillman, R. W., and Almon, W. R., 1979, Diagenesis of Frontier Formation offshore bar sandstones, Spearhead Ranch field, Wyoming: SEPM Spec. Pub., no. 26, p. 337-378.

Visher, G. S., 1968, Depositional framework of the Bluejacket-Bartlesville sandstone, in Visher, G. S., ed., Geology of the Bluejacket-Bartlesville sandstone, Oklahoma: Oklahoma City Geol. Soc. Guidebook, p. 32-44.

Visher, G. S., Saitta, B. S., and Phares, R. S., 1971, Pennsylvanian delta patterns and petroleum occurrences in eastern Oklahoma: Am. Assoc. Petr. Geol. Bull., v. 37, p. 1206-1230.

Waldschmidt, W. A., 1941, Cementing materials in sandstones and their probable influence on migration and accumulation of oil and gas: Am. Assoc. Petr. Geol. Bull. no. 25, p. 1839-79.

Wells, J. S., and Anderson, K. H., 1968, Heavy crude oil in western Missouri: Am. Assoc. Petr. Geol. Bull., v. 52, p. 1720-1731.

Wilson, M. D., and Pittman, E. D., 1977, Authigenic clays in sandstones: recognition and influence on reservoir properties and paleoenvironmental analysis: Jour. Sed. Pet., v. 47, p. 3-31.

Woody, M. D., 1983, Sedimentalogy, diagenesis and petrophysics of selected Cherokee Group (Desmoinesian) sandstones in southeastern Kansas: Shale Shaker, v. 33, no. 9-10, p. 91-122.

Zeller, D. E. (ed), 1968, The stratigraphic succession in Kansas: Kansas Geological Survey, Bull. No. 189, 81 p.